

**FORMATION, DISTRIBUTION,
AND PATHOPHYSIOLOGICAL RELEVANCE
OF THE 'ADVANCED GLYCATION END-PRODUCT'
N^ε-(CARBOXYMETHYL)-LYSINE
IN TARGET TISSUES OF DIABETIC ORGAN DAMAGE
AND IN DEGENERATIVE AND CHRONIC
INFLAMMATORY TISSUE LESIONS**

**BILDUNG, VERTEILUNG AND PATHOPHYSIOLOGISCHE
BEDEUTUNG VON
N(EPHILON)-CARBOXYMETHYLLYSIN
BEI DIABETISCHER ORGANSCHÄDIGUNG UND IN CHRONISCH
DEGENERATIVEN UND CHRONISCH ENTZÜNDLICHEN
GEWEBELÄSIONEN**

DISSERTATION

der Fakultät für Chemie und Pharmazie
der Eberhard-Karls-Universität Tübingen
zur Erlangung des Grades eines Doktors
der Naturwissenschaften

2004

vorgelegt von
Ulrich Friess

Tag der mündlichen Prüfung: 20.07.2004

Dekan: Prof. Dr. Hans-Georg Probst

1. Berichterstatter: Prof. Dr. Dr. h.c.mult. Wolfgang Voelter

2. Berichterstatter: Prof. Dr. Michael Duszenko

Die vorliegende Arbeit wurde von April 2000 bis Juni 2003 unter der Leitung von Herrn Prof. Dr. Dr. h.c.mult. Wolfgang Voelter und Herrn Prof. Dr. Erwin Schleicher am Institut für Physiologische Chemie und im Zentrallaboratorium der Medizinischen Klinik der Universität Tübingen (Abteilung Innere Medizin IV, Ärztlicher Direktor Prof. Dr. Hans-Ulrich Häring) angefertigt.

Teile dieser Arbeit wurden bereits veröffentlicht oder präsentiert:

Publikationen:

1. Schleicher E, Nerlich A, Haslbeck M, Heuss D, Kasper M, Bierhaus A, Nawroth PP, Haering HU, **Friess U**: Formation of N^ε-(carboxymethyl)lysine in inflammatory and non-inflammatory conditions of nerve and muscle and in inflammatory cells *in vitro*. *Proceedings of the 7th International Symposium on the Maillard Reaction, Kumamoto, 2001*, Elsevier International Congress Series (2002) 1245:53-59.
2. **Friess U**, Waldner M, Wahl HG, Lehmann R, Haering HU, Voelter W, Schleicher E: Liquid chromatography-based determination of urinary free and total N(epsilon)-(carboxymethyl)lysine excretion in normal and diabetic subjects. *J Chromatogr B Analyt Technol Biomed Life Sci* (2003) 794:273-280.

3. Haslbeck KM, Schleicher ED, **Friess U**, Kirchner A, Neundörfer B, Heuss D: N^ε-Carboxymethyllysine in diabetic and non-diabetic polyneuropathies. *Acta Neuropathol* (2002) 104:42-52.
4. Schwab W, **Friess U**, Hempel U, Schulze E, Makita Z, Kasper M, Simank HG: Immunohistochemical demonstration of N^ε-(carboxymethyl)lysine protein adducts in normal and osteoarthritic cartilage. *Histochem Cell Biol* (2002) 117:541-546.

Posterpräsentationen:

5. **Friess U** et al.: Urinary excretion of free and bound N^ε-(carboxymethyl)lysine in nonproteinuric diabetics (Kongress Labormedizin der DGKC/DGLM, Rostock 9/2001).
6. **Friess U**, Bierhaus A, Haslbeck M, Waldner M, Nawroth PP, Haering HU, Schleicher ED. Accumulation and distribution of N(ε)-(carboxymethyl)lysine in tissues and leukocytes in Diabetes Mellitus and colocalisation with the receptor for advanced glycation end-products and the transcription factor NFκB. *Diabetes und Stoffwechsel* 11, Suppl.1 (2002), (Jahrestagung Deut. Diabetes Ges., Dresden 5/2002).
7. **Friess U**, Waldner M, Weigert C, Griendling K, Haering HU and Schleicher E: Intracellular N^ε-(carboxymethyl)lysine formation in monocytic and neuroglial cell lines. *Second Symposium for advanced glycation end-products, Jena 2003*.

Danksagung

Herzlich danken möchte ich

Herrn Prof. Dr. Dr. h.c. Voelter für die Annahme als Doktorand und die freundliche Unterstützung bei der Realisierung dieser Promotion.

Herrn Prof. Dr. E. Schleicher für die Überlassung des Themas und die intensive Betreuung beim Verfassen der Veröffentlichungen.

Herrn Prof. H.-U. Häring für das stete Interesse an meiner Arbeit.

Michaela Waldner für die sorgfältige und tatkräftige Mitarbeit im Labor.

Cora Weigert, Rainer Lehmann, Alexander Beck und Klaus Möschel für viele Tips und die gesamte Unterstützung in den letzten drei Jahren.

CONTENTS

1	INTRODUCTION	1
1.1	Maillard Reaction and ,advanced glycation end-products (AGEs)'	1
1.2	,Early glycation products' and ,advanced glycation end-products' are also observed <i>in vivo</i>	4
1.3	Classification of AGEs	5
1.4	Mechanisms of the <i>in vivo</i> formation of AGEs	6
1.5	Intracellular AGE formation	8
1.6	N ^ε -(carboxymethyl)-lysine (CML)	9
1.7	Pathogenesis of diabetic organ damage	11
1.8	Oxidative stress – a key feature of diabetes mellitus and of tissue lesion in other diseases	13
1.9	Oxidative stress	16
1.10	Why could CML represent a potential biomarker for oxidative stress?	18
1.10.1	<i>In vitro</i> , formation of CML involves oxidative chemistry	18
1.10.2	CML is formed in a wide variety of diseases where oxidative stress has been implicated in the pathogenesis	21
1.10.3	In experimental settings, CML is involved in a variety of pathomechanisms	21
1.10.4	CML is a ligand for the receptor for AGEs (RAGE) and colocalises with RAGE in tissue lesions. Experimental data show a possible pathophysiological role of CML/RAGE interaction in chronic inflammatory and degenerative diseases	22
1.10.5	When present, CML depositions are often found within or in close proximity to infiltrating inflammatory cells and activated resident cells	23
1.10.6	From cell culture experiments there is evidence for <i>de novo</i> intracellular CML formation	24
1.10.7	CML formation on cellular proteins has also been described <i>in vivo</i> in circulating blood cells	25

1.10.8	Many of the CML-forming cell types possess enzymatic systems to generate oxidative stress.	25
2	AIM OF THIS STUDY	27
3	MATERIAL AND METHODS	28
3.1	Chemicals	28
3.2	Tests, kits and other materials	31
3.2.1	Isolation of leucocyte subclasses	32
3.2.2	Immunoprecipitation	32
3.2.3	2-D Elpho	32
3.3	Cell culture media and additives	33
3.4	Cell lines	33
3.5	Cell culture conditions and experimental conditions in cell culture experiments	34
3.5.1	Mono Mac 6, PLB 985 and PLB 985gp91 Δ 488-497 monocytic cells	34
3.5.2	N11 and N11/6 murine microglial cells	35
3.6	Equipment	38
3.7	<i>In vitro</i> chemical carboxymethylation of proteins	39
3.8	Determination of CML content by amino acid analysis	41
3.9	<i>In vitro</i> lipid peroxidation of RNAse	42
3.10	Synthesis of CML standard	43
3.11	Preparation of cell lysates and protein extracts	48
3.12	Western blots / dot blots	50
3.13	Antibodies	53
3.14	HPLC determination of urinary CML excretion	56
3.14.1	Study group and sample collection	56
3.14.2	Preparation of the urine samples	58
3.14.3	Sample derivatisation and HPLC analysis	58
3.15	Immunohistochemistry and Western-blotting in muscle and nerve tissue	59
3.16	Immunohistochemistry and Western-blotting of CML-modified proteins in cartilage	60
3.17	Density gradient preparation of granulocytes	61
3.18	Preparation of leukocyte subclasses	63
3.19	Luminol and lucigenin chemiluminescence assay for granulocytes	65

3.20	Lucigenin chemiluminescence assay for cell culture cells	65
3.21	Statistical analysis	69
4	RESULTS	70
4.1	Chemical carboxymethylation of model proteins and characterisation of the used anti-CML antibodies	70
4.2	CML excretion is increased in urine in diabetic subjects and CML formation can be demonstrated <i>in vivo</i> in tissues and in circulating leukocytes	79
4.2.1	Increased <i>in vivo</i> formation and excretion of protein-bound CML in diabetic subjects	79
4.2.1.1	Validation of the HPLC method	79
4.2.1.2	Urinary CML excretion in diabetic and non-diabetic subjects	83
4.2.2	Demonstration of increased <i>in vivo</i> accumulation of CML in nerve, muscle and vascular tissues in diabetes mellitus and in chronic inflammatory and chronic degenerative diseases	86
4.2.2.1	CML in noninflammatory and inflammatory peripheral polyneuropathies	86
4.2.2.2	CML in noninflammatory and inflammatory myopathies	89
4.2.2.3	CML accumulation in osteoarthritis	93
4.2.3	CML accumulation in circulating granulocytes	96
4.3	Mechanism of CML formation in inflammation-associated cells	98
4.3.1	Lipid peroxidation leads to carboxymethylation of proteins <i>in vitro</i>	98
4.3.2	The 'oxidative burst' of granulocytes leads to the carboxymethylation of serum proteins	100
4.3.3	In pre-differentiated monocytic cell lines, stimulation of ROS-generating mechanisms leads to CML modification of distinct cellular proteins	102
4.3.3.1	Experiments with pre-differentiated Mono Mac 6 cells	102
4.3.3.2	Experiments with pre-differentiated PLB 985 and PLB 985 gp91 Δ 488-497 (NADPH oxidase knock out) monocytic cells	115

4.3.4	CML formation in stimulated N11 and N11/6 (NADPH oxidase deficient) microglia cells	117
4.3.5	Do inhibitors of the respiratory chain influence CML formation?	119
4.3.6	Identification of CML-modified proteins	124
5	DISCUSSION	125
5.1	CML excretion in urine	125
5.2	Pathophysiological significance of CML accumulation in diabetes and in chronic inflammatory or chronic degenerative diseases	128
5.2.1	Over a life time the amount of protein glycation in tissues remains almost constant but the CML content increases in an age-dependent fashion	128
5.2.2	CML accumulation in extracellular matrix proceeds slowly as an inevitable process over months to years and is increased by hyperglycemia	129
5.2.3	Under oxidative conditions, CML formation proceeds within hours to days, especially in lesioned tissue and intracellularly	129
5.2.3.1	CML accumulation in diabetic organ damage	130
5.2.3.2	CML accumulation in atherosclerosis and vascular disease	135
5.2.3.3	CML formation in Alzheimer's disease and other neurodegenerative conditions	138
5.2.3.4	CML formation in degenerative conditions as osteoarthritis	139
5.2.3.5	CML formation in inflammatory conditions	141
5.2.4	Is intracellular CML actually formed within the cell?	144
5.3	Which cellular source of ROS production is involved in CML formation?	147
5.3.1	Is NADPH oxidase implicated in CML formation?	147
5.3.2	Is the cellular NADPH oxidase activity crucial for CML formation?	150
5.3.3	Is ROS production from the mitochondrial respiratory chain involved in CML formation?	151

6 ZUSAMMENFASSUNG (DEUTSCH)	153
7 SUMMARY (ENGLISH)	158
8 REFERENCES	162
9 APPENDIX	193

ABBREVIATIONS

3-DG	3-Deoxyglucosone
4-OHCA	α -Cyano-4-hydroxycinnamic acid
AA	Amino acid
Ab	Antibody
AD	Alzheimer's disease
AGE	Advanced glycation end-product
APS	Ammonium persulfate
ASA	Amino acid analysis
au	Arbitrary unit
BMI	Body mass index
BSA	Bovine serum albumin
CCCP	Carbonyl cyanide 3-chlorophenylhydrazone
CD	Cluster of differentiation
CEL	N ^ε -(carboxyethyl)-lysine
CIDP	Chronic inflammatory demyelating polyneuropathy
CML	N ^ε -(carboxymethyl)-lysine
CMT I	Charcot-Marie-Tooth-disease type I
COMP	Cartilage oligomeric matrix component
CPEO syndrome	Chronic progressive external ophthalmoplegia syndrome
CPR	Cytochrome P450 reductase
CV	Coefficient of variation
DAG	Diacyl glycerole
DHAP	Dihydroxyacetone phosphate
Dil.	Dilution
DM	Diabetes mellitus
DMEM	Dulbecco's modified Eagle's medium

D-Myo	Dermatomyositis
DOLD	3-Deoxyglucosone-derived lysine dimer
DPI	Diphenyleneiodonium chloride
DTT	Dithiothreitol
ECL	Enhanced luminol chemiluminescence
ECM	Extracellular matrix
EDTA	Ethylendiamintetraacetate
ESRD	End stage renal disease
FCS	Fetal calf serum
fMLF	N-formyl-met-leu-phe
GAPDH	Glyceraldehyde-3-phosphate dehydrogenase
GC-MS	Gas chromatography - mass spectrometry
GOLD	Glyoxal-derived lysine dimer
GSH	Reduced glutathione
HbA1c	Hemoglobin A1c
HEPES	N-(2-hydroxyethyl)piperazine-N'-2-ethanesulfonic acid
HMAP	4'-Hydroxy-3'-methoxyacetophenone (apocynine, acetovanillone)
HMSN I	Hereditary motorsensoric neuropathy type I
HRP	Horse radish peroxidase
HSA	Human serum albumin
HSS	Hanks' salt solution
IHC	Immunohistochemistry
IP	Immunoprecipitation
kD	Kilo Dalton
LC-MS	Liquid chromatography – mass spectrometry
LDL	Low density lipoprotein
LGD	Limb-girdle-dystrophy

L-NAME	Nitro-L-arginine methyl ester hydrochloride
LPS	Lipopolysaccharide
Mab	Monoclonal antibody
MDA	Malondialdehyde
MELAS syndrome	Mitochondrial encephalopathy, lactic acidosis and stroke like episodes syndrome
MGO	Methyl glyoxal
MNR	Magnetic nuclear resonance (spectrometry)
MOLD	Methylglyoxal-derived lysine dimer
MPA	3-Mercaptopropionic acid
MPO	Myeloperoxidase
MSR	Macrophage scavenger receptor
MW	Molecular weight
NDG	Nordihydroguaiaretic acid
NEAA	Non essential amino acids
NET-G	NET-G buffer
NF κ B	Nuclear factor kappa B
NP	Neuropathy
OA	Osteoarthritis
OPA	o-Phtaldialdehyde
OPI	Oxalacetate, pyruvate, insulin
PAGE	Polyacrylamide gel electrophoresis
PBMC	Peripheral bone mononuclear cells
PBS	Phosphate buffered saline
PHOX	Phagocytic NADPH oxidase
PKC	Protein kinase C
PMA	Phorbol-12-myristat-13-acetat
P-Myo	Polymyositis

PN	Polyneuropathy
RA	Rheumatoid arthritis
RAGE	Receptor for AGEs
RP-HPLC	Reversed phase high pressure chromatography
RT	Retention time
SD	Standard deviation
SDS	Sodium dodecylsulfate
SELDI-MS	Surface enhanced laser desorption/ionisation mass spectrometry
SIM-GC-MS	Single ion monitoring GC-MS
SMC	Smooth muscle cells
TEMED	N,N,N',N'-tetramethylethylenediamine
TFA	Trifluoroacetic acid
TNF α	Tumor necrosis factor alpha
TRIS	Tris[hydroxymethyl]aminomethane
TTFA	2-Thenoyltrifluoroacetone
TLC	Thin layer chromatography
WB	Western blot

1 INTRODUCTION

1.1 Maillard Reaction and ,advanced glycation end-products (AGEs)'

The process of 'non-enzymatic browning' has been known in food chemistry for almost a century. In this series of reactions, the amino groups of amino acids, peptides or proteins react with glucose or other reducing sugars and produce a heterogeneous group of colourless or yellow-brown products in a complex series of reactions. These products sometimes show fluorescence and/or form crosslinks between proteins or other macromolecules. This process was described for the first time by the French Chemist L.C. Maillard [1] and is called the Maillard reaction or "non-enzymatic glycation". The products of this process have been named 'Maillard Products' or ,advanced glycation end-products' (AGEs), and give bread crusts and roasted or fried food their characteristic taste and color.

The Maillard reaction does not describe a specific reaction, but is instead the general term for a series of heterogeneous reactions [2; 3]. The process in its entirety is illustrated schematically in **Figure 1-1**. It consists of the early phase of protein glycation producing the "early glycation products", which is then followed by a number of subsequent reactions. The mechanism of the early phase has been identified and is described in **Figure 1-2**. It consists of a reaction between glucose and a protein-bound lysine side chain. In the first step, the nucleophile ϵ -amino group of the lysine side chain interacts with the carbonyl carbon atom of the reducing sugar. A Schiff's base is produced in an addition and condensation reaction. This step is fast and reversible.

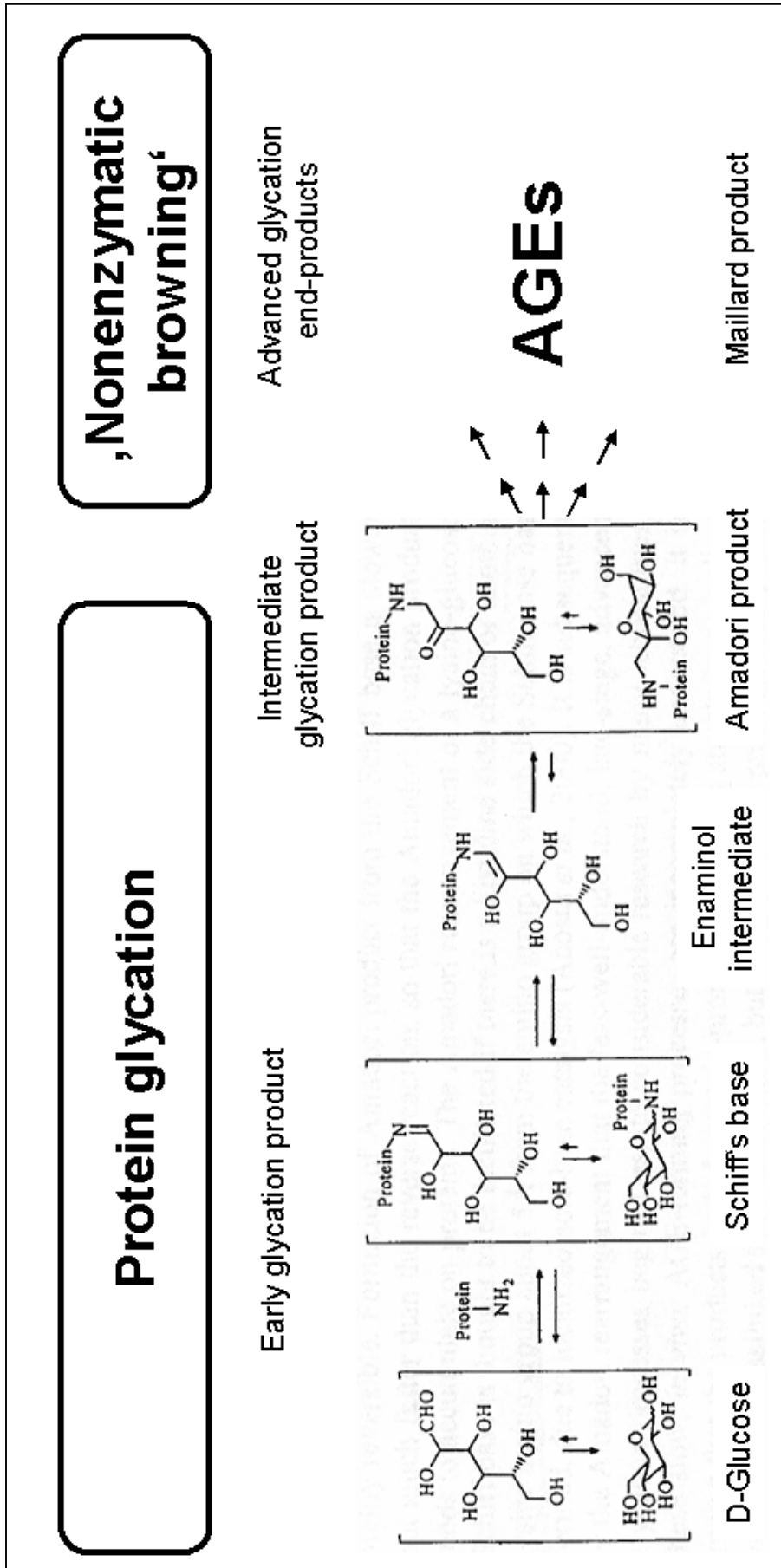


Figure 1-1. Overview on the early and late stage of the Maillard reaction.

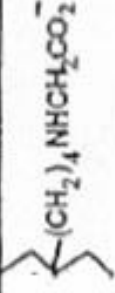
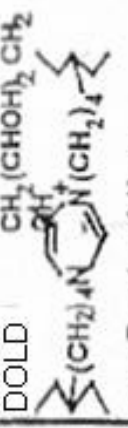
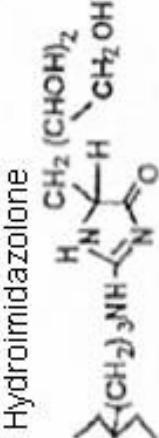
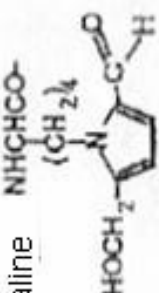
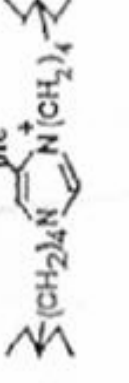


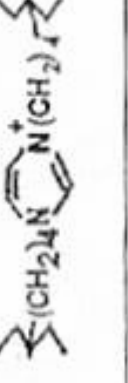
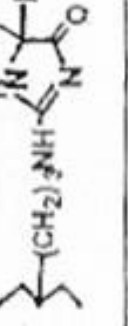
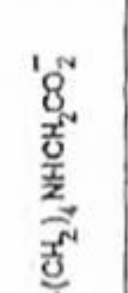
Glycating agent	Crosslinks	Receptor recognition factors	Others
Glucose	Pentosidine Others	3-DG-derived hydroimidazolone	CML 
3-DG	DOLD  >>>Pentosidine	Hydroimidazolone 	Pyrraline 
Methylglyoxal	MOLD 	Hydroimidazolone 	CEL 
Glyoxal	GOLD 	Hydroimidazolone 	CML 

Figure 1-2. Functional classification of advanced glycation end-products derived from glucose, 3-deoxyglucosone (3-DG), methylglyoxal and glyoxal. Abbreviations: CML: N^ε-(carboxymethyl)-lysine; CEL: N^ε-(carboxyethyl)-lysine; GOLD, MOLD and DOLD: glyoxal-, methylglyoxal- and 3-DG-derived imidazolium lysine dimer (from [18]).

In the subsequent Amadori reaction, a relatively stable keto-amine (fructosamine) is formed by an intermediate open-chain enol step. The equilibrium of this rearrangement is shifted towards the keto-amine side, and this step determines the speed of the protein glycation. The resulting fructosamine structure is instable and reacts in a number of complex follow-up reactions to form several intermediate products. Even though a large number of AGEs have been isolated in tissues and reaction mixtures, the intermediate steps of these reactions are only partly known, and it is still not possible to describe the complete chain of reactions of the late phase for the Maillard reaction. To date, the AGEs known are mostly stable metabolites that are not changed during the isolation and purification process and do not react further.

1.2 ‘Early glycation products’ and ‘advanced glycation end-products’ are also observed *in vivo*

Within the last 30 years it became evident that the Maillard reaction does not only occur in reaction mixtures, but also within the human body and that it plays an important role in the processes of aging, degenerative diseases and in the development of diabetic endorgan damage [4-7]. Early glycation products and AGE precursors were first discovered *in vivo* in hemoglobin [8; 9] and the measurement of glycated hemoglobin (HbA1c) is used widely to assess the degree of long term hyperglycemia in diabetic patients [10].

Besides hemoglobin and serum proteins, the long-lived proteins of the extracellular matrix, such as collagens, become glycated. Glycation has been demonstrated in the proteins of tendons, bone, skin and connective tissue, aorta and the glomerular

basement membrane and, further, the rate of glycation has been found to correlate with the degree of hyperglycemia [11-13].

However, there is little convincing evidence that glycation itself is a dangerous process [14]. Because of protein turnover and the abundance of most enzymes and proteins in the body, it is unlikely that glycation itself is significant in the pathogenesis of diseases [14; 15]. The rate of formation of AGEs exceeds that predicted by first order kinetics in protein glycation [10]. This implies that over time even modest hyperglycemia can result in significant accumulation of AGEs on long-lived proteins. This is well illustrated in certain long-lived proteins such as lens crystallins or tissue collagens. Because of the long biological half-life, these proteins have been used most frequently to assess the progress of the Maillard reaction *in vivo* and now, attention is focused on the permanent, irreversible AGEs [14; 16].

1.3 Classification of AGEs

A number of AGEs have also been found *in vivo* in tissues and extracellular fluids. As shown in **Figure 1-2**, this group of compounds is very heterogeneous. The most commonly used classification of AGEs is based on putative pathophysiological relevance [17; 18], since modification of a macromolecule by AGEs very often results in changed or impaired function. Often, AGE modification leads to molecular crosslinking or to changes in charge or conformation. AGE-modified proteins can show changed enzymatic activity, changed rates of catabolism or abnormal receptor binding properties. AGEs can act as ligands of pathophysiologically active effector systems such as the receptor for advanced glycation end products (RAGE) or the NF κ B system

[19]. **Figure 1-2** shows the structure and classification of the most important AGES which have been characterized according to their potential or observed pathophysiological activities.

1.4 Mechanisms of the *in vivo* formation of AGEs

Throughout the last 30 years, a large body of evidence has accumulated indicating that AGEs are formed *in vivo* from glycation during cell metabolism, i.e. from the reaction of reducing sugars (e.g. glucose, fructose, ribose, trioses or others), sugar phosphates or of related compounds such as ascorbic acid with amino groups in proteins, lipids and nucleic acids [20]. Glucose has the slowest glycation rate whereas intracellular sugars, such as glucose-6-phosphate or fructose, form AGEs at a much faster rate. The order of the rate of glycation of different intermediates in metabolism is glycolaldehyde > glyceraldehyde > glucose-6-phosphate > xylose > fructose > glucose [21; 22].

If oxidation accompanies glycation, then the products formed are known as glycoxidation products. The AGEs N^ε-(carboxymethyl)lysine and pentosidine are such examples. A current scheme for the *in vivo* formation of AGEs is given in **Figure 1-3**. Of importance in the Maillard reaction is the formation of reactive intermediate products during the Amadori rearrangement. These compounds are known as α -dicarbonyls or oxoaldehydes and include such products as glyoxal, methylglyoxal (MGO) and 3-deoxyglucosone (3-DG) [23]. The 3-DG is formed by rearrangement and hydrolysis of Amadori adducts and from fructose-3-phosphate, a product of the polyol pathway. MGO is formed during glycolysis and also from the oxidative decomposition of poly-unsaturated fatty acids (lipid peroxidation).

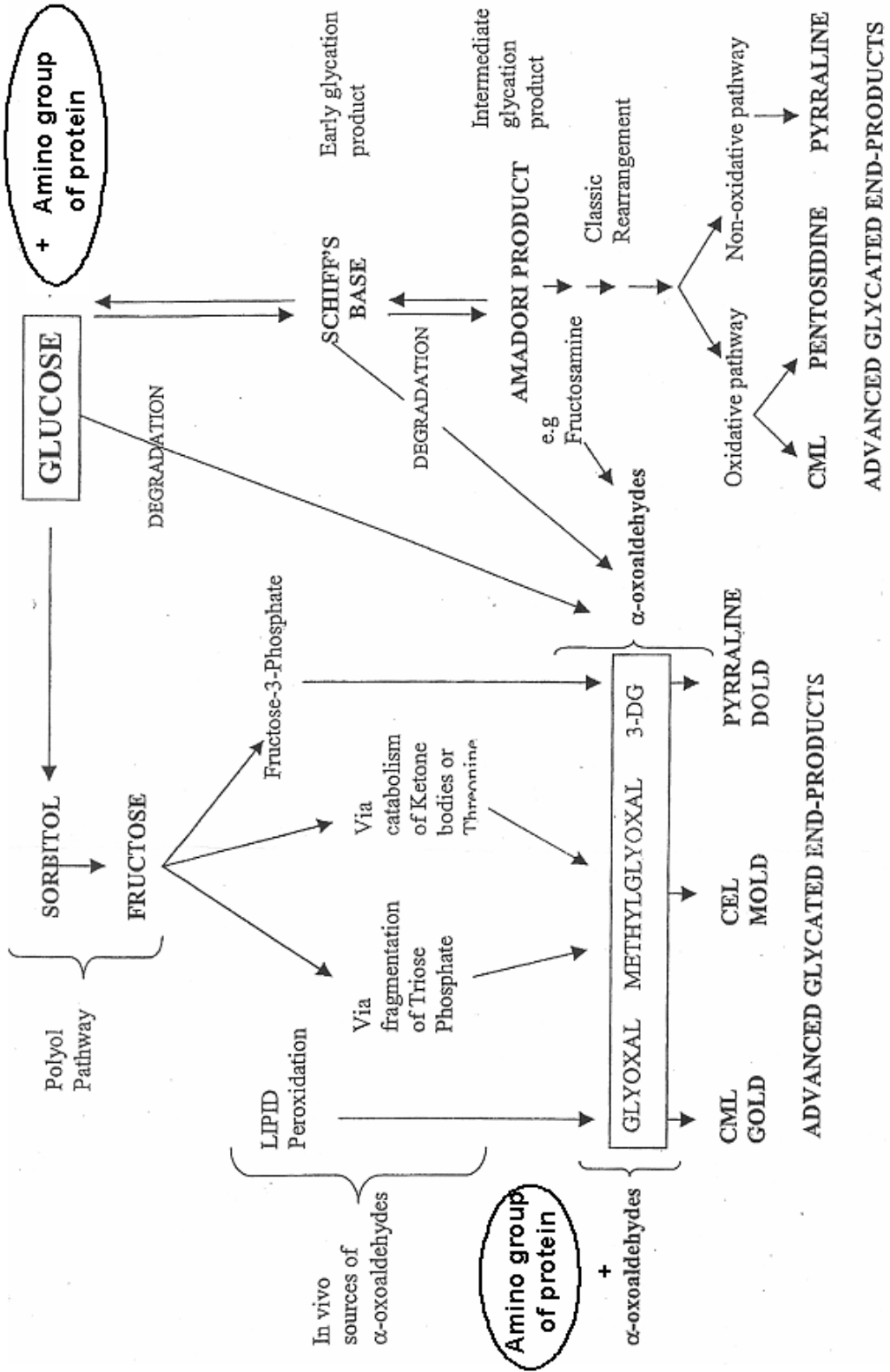


Figure 1-3. *In vivo* AGE formation pathways. For details see text (adapted from [20]).

In addition, MGO can be derived from fructose by fragmentation of triose phosphates or from the catabolism of ketone bodies and threonine [24]. MGO, 3-DG and glyoxal have recently been proposed to be formed from all stages of the glycation process by degradation of glucose or Schiff's bases in early glycation or from Amadori products such as fructosamine in the intermediate stages of glycation. The accumulation of reactive dicarbonyls from glycooxidation or from lipoxidation or from both is termed carbonyl stress [25; 26]. These dicarbonyl precursors can go on to form oxidative AGEs such as N^ε-(carboxymethyl)-lysine (CML) and pentosidine or non-oxidative AGEs derived from 3-DG [deoxyglucosone-lysine dimer (DOLD)] or MGO [Methyl glyoxal lysine dimer (MOLD)]. This recently described phenomenon of carbonyl stress has been observed in both, diabetes and uremia [27-29] and has been implicated in the accelerated vascular damage observed in both conditions.

1.5 Intracellular AGE formation

Originally, the formation of AGEs was thought to arise exclusively from the non-enzymatic reactions between extracellular proteins and glucose. However, the rate of AGE formation from glucose is orders of magnitude slower than the rate of AGE formation from dicarbonyl precursors generated intracellularly. Recently it has been recognised that AGEs can also form rapidly on cytoplasmatic proteins and other intracellular components such as lipids and nucleic acids [30; 31]. It now seems likely that intracellular hyperglycemia and/or oxidative stress is the primary initiating event in the formation of both intracellular and extracellular AGEs [30; 31].

As shown in **Figure 1-3**, AGEs can arise from intracellular autoxidation of glucose to glyoxal, decomposition of the Amadori product to 3-DG, and fragmentation of trioses as glyceraldehyde-3-phosphate and dihydroxyacetone phosphate to MGO. These reactive intracellular dicarbonyls –glyoxal, MGO and 3-DG- can then react with the amino groups of intracellular proteins to form AGEs. Indeed, it has been demonstrated that intracellular AGEs may form at a rate of up to 14-fold higher in high (30mM) glucose conditions [31]. MGO is detoxified by the glyoxalase system [32; 33]. All three AGE precursors are also substrates for other reductases.

Overall, the reactions leading to AGE formation *in vivo* are complex and not fully understood. The best characterised metabolic pathways are the reactions leading to N^ε-(carboxymethyl)-lysine (CML), where multiple steps require oxidative chemistry. CML has therefore gained interest as a potential biomarker for oxidative stress [34-36].

1.6 N^ε-(carboxymethyl)-lysine (CML)

The most abundant and best characterised AGE is N^ε-(carboxymethyl)-lysine (CML) [37; 38]. Originally, CML was described as an AGE resulting from a Maillard type reaction of glucose with lysine residues [39]. The authors made the interesting observation, that under anaerobic conditions, CML formation was abolished *in vitro*. Subsequently, CML was found to be the most abundant AGE to be formed in a variety of oxidative conditions [40]. In contrast to other AGEs, which also form under nonoxidative conditions, CML is now considered to be an advanced *glycoxidation* end-product. CML has become a key

marker of protein modification in response to glyoxidative, lipoxidative and carbonyl stress *in vitro* and it has been suggested that CML could also represent a biomarker for systemic or local oxidative stress in tissue lesions *in vivo* [34-36]. CML is the most abundant AGE in tissues and body fluids. It is an irreversible protein modification which is stable to acid hydrolysis and can be quantified from protein hydrolysates. Although CML is the smallest one of the AGE modifications, it might be functionally relevant. It leads to a change in charge since, after modification, the former positively charged lysine residues carry a negatively charged carboxylic group. Therefore, a zwitter ion results which may in turn exert different biological properties.

The occurrence and distribution of CML in tissues has been studied extensively using specific antibodies. Immunolocalisation of CML has been demonstrated in skin, lung, heart, kidney, intestine, intervertebral discs and particularly in arteries (as reviewed in [35; 41] and in the discussion section). The content of CML increases with the chronological age of proteins [42-44]. CML accumulation has been demonstrated in all tissues associated with diabetic organ damage. In diabetes, the rate of CML is accelerated as compared to that seen in aging and in some studies, the age-adjusted concentration of CML has been found to correlate with the severity of diabetic complications [14; 45]. Furthermore, high levels of CML have been observed within atherosclerotic plaques, in foam cells [34; 41; 46] and in a variety of chronic degenerative and chronic inflammatory diseases, as discussed below.

1.7 Pathogenesis of diabetic organ damage

Diabetic organ damage affects very different organs such as the kidney, eye, peripheral nerves, skin, heart, and the brain. Vascular changes can be found in all the different types of late stage deterioration of organ function and damage can be microvascular (e.g. kidney, retina, nerves) or macrovascular (e.g. brain, carotic artery). In Germany in the year 2000, the number of newly diagnosed cases of diabetic retinopathy was 56,000 (including 2300 cases of blindness) and the number of diabetic kidney disease was 4000. The annual costs for dialysis are in excess of 180 Million Euro. Due to diabetic alterations of the blood vessels, 28,000 limb amputations and 35,000 myocardial infarctions were counted in the year 2000 (Bretzel, RG 2000). The medical costs of diabetic complications are of economic importance and are an estimated one billion Euro per year, which is as high as the primary costs of diagnosis and treatment of diabetes mellitus.

Strict control of blood sugar levels slow the development of diabetic damage considerably, and several research studies have suggested that hyperglycemia contributes directly or indirectly to the pathogenesis of diabetic late stage tissue/organ damage [30; 47] through five different mechanisms. These mechanisms can interact and are shown schematically in **Figure 1-4**.

Hyperglycemia can lead to

- a. increased intracellular and extracellular formation of AGEs [49; 50]
- b. activation of protein kinase C, followed by an activation of NADPH-dependent oxidase [51]

- c. activation of the polyol metabolism that results in an accumulation of sorbitol [52]
- d. activation of the hexosamine pathway [53]
- e. increased production of superoxide anions and other reactive oxygen species from the mitochondrial respiratory chain [54].

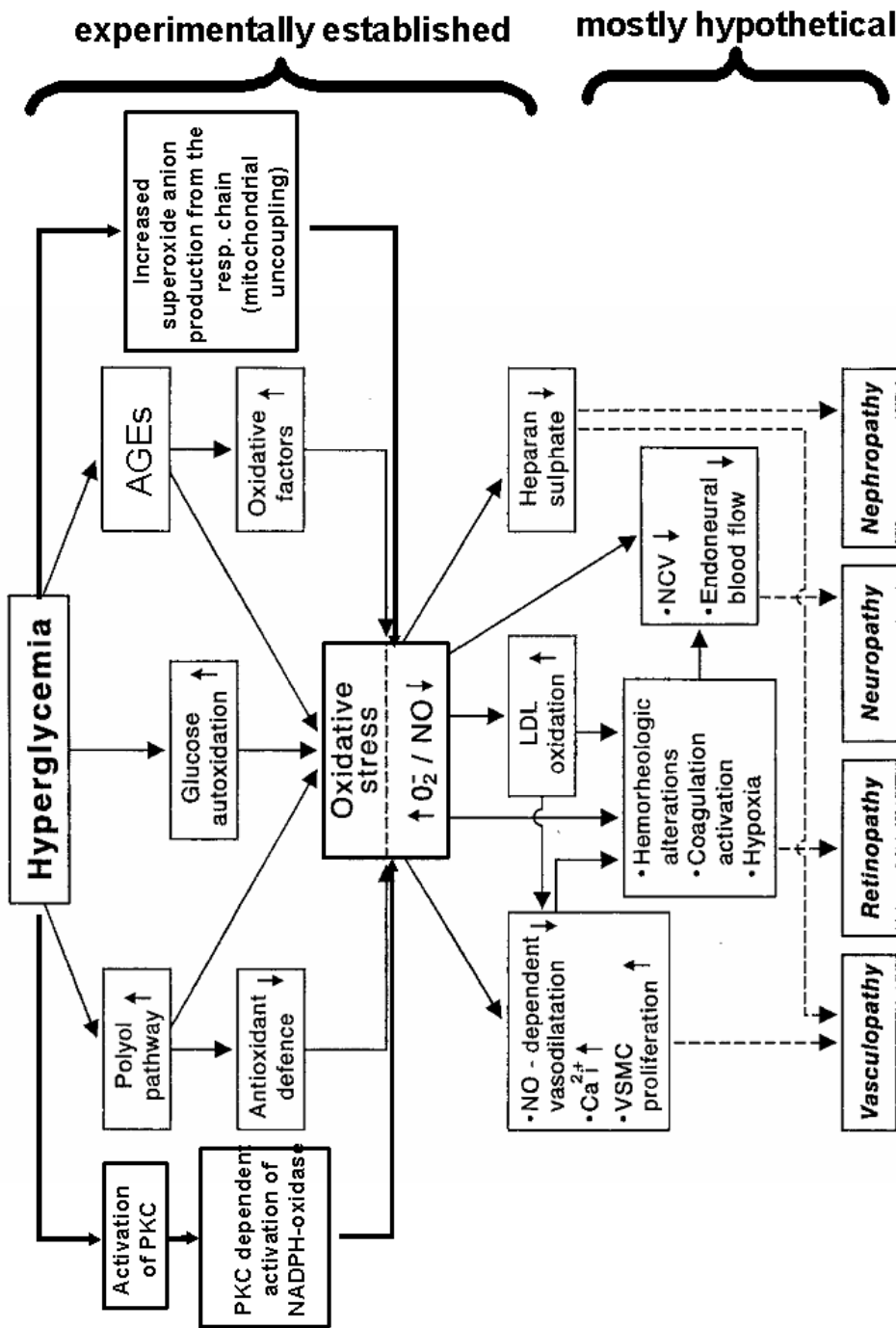


Figure 1-4. Pathophysiological mechanisms involved in the development of diabetic organ damage (from [48], modified).

A possible final endpoint of all cellular changes induced by hyperglycemia appears to be the production of cellular oxidative stress [47; 55-57].

1.8 Oxidative stress – a key feature of diabetes mellitus and of tissue lesion in other diseases

Accumulating data support the hypothesis that oxidative stress might play an important role in the pathogenesis of late diabetic complications [47; 48; 56; 58]. Several studies have shown that increased production of ROS and/or antioxidant depletion occurs in patients with diabetes mellitus [59-64]. Several pathways are supposed to contribute to the oxidative stress associated with acute or chronic hyperglycemia, most importantly increased ROS production from the mitochondrial respiratory chain [65] or from activated ROS-generating enzymes and glucose autoxidation. [40; 66; 67]. A close relationship of oxidative stress and glycemic control has been described by showing a positive correlation between malondialdehyde (MDA) and both, fasting blood sugar and glycated hemoglobin [68]. Moreover, the hypothesis that free radicals and subsequent oxidative stress might mediate the effects of hyperglycemia is supported by the observation that antioxidants counteract many of the injurious effects of hyperglycemia [69-71]. Besides production of oxygen free radicals, depletion of antioxidative capacities may also play an important role in diabetic tissue damage [72-74]. In a recent study, Nourooz-Zadeh and colleagues described a relationship between the quality of glycemic control and the presence of free radicals and thereby demonstrated oxidative stress occurring prior to the manifestations of late diabetic complications [75].

An important mechanism by which hyperglycemia increases intracellular stress was recently described by Brownlee and Nishikawa [30; 55]. As shown in **Figure 1-5**, these authors propose that hyperglycemia-induced mitochondrial superoxide production (e) activates all of the first four mechanisms (a-d) mentioned above. From experimental data it was suggested that excess superoxide partially inhibits the glycolytic enzyme GAPDH, thereby diverting upstream metabolites from glycolysis into the pathways of glucose overutilisation. This results in an increased flux of dihydroxyacetone phosphate (DHAP) to DAG, an activator of PKC, and of trioses to MGO, the main intracellular AGE precursor. The increased flux of fructose-6-phosphate to UDP-N-acetylglucosamine increases modifications of proteins by O-linked N-acetylglucosamine (GlcNAc). Furthermore, the increased glucose flux through the polyol pathway consumes NADPH and depletes GSH, thereby diminishing the intracellular antioxidative capacity.

In diabetics, there is not only evidence of increased oxidative stress in body fluids or locally in the tissues, but additionally, it is possible to show the effect of oxidative stress on potential target cells. The activation of the redox sensitive transcription factor NF κ B has been found in the immuno-histological analysis of blood vessels and kidney samples and in peripheral mononuclear blood cells of patients with diabetes mellitus [76]. Furthermore, antioxidants such as vitamin E and thioct acid (α -lipoic acid) were able to reduce oxidative stress and NF κ B-activation [77].

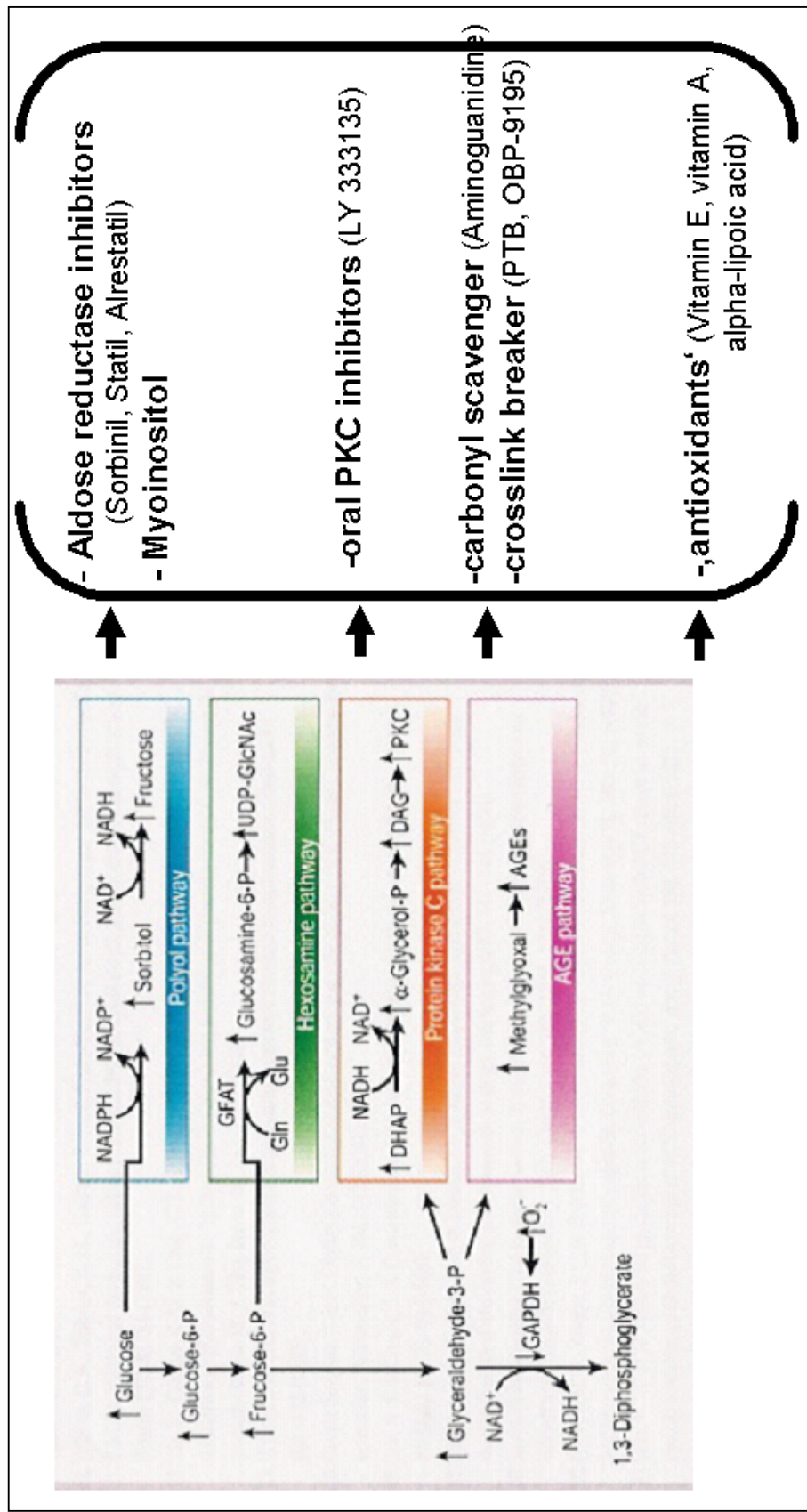


Figure 1-5. Brownlee-hypothesis for the development of hyperglycemia-induced tissue damage. Hyperglycemia-induced mitochondrial superoxide production activates four pathways of hyperglycemic damage (left). Several pharmacological interventions were shown to interfere effectively and to reduce diabetic complications in animal models or in early clinical trial (right). (from [30]).

1.9 Oxidative stress

The term oxidative stress describes the increased occurrence of reactive oxygen species (ROS) in the extracellular and intracellular environment [78]. The term ROS includes radicals and reactive non-radical components as listed in **Figure 1-6**, which can induce oxidative damage in biological systems [78-80]. In essence, oxidative stress results from an imbalance between the production of reactive oxygen species and antioxidative defence [79]. The most relevant exogenous or endogenous sources for ROS are depicted in **Figure 1-7**.

A number of different antioxidative mechanisms protect cells under physiological conditions from damage by ROS [81; 82]. Superoxide dismutases and peroxidases are anti-oxidating enzymes that catalyse the reduction of peroxides and thereby neutralize endogenously produced ROS. A second line of defence is formed by molecules that react with free radicals. Such scavengers include vitamin E, vitamin C, α -lipoic acid, β -carotene, coenzyme Q, uric acid, bilirubine und albumin [69; 82; 83].

Radicals	Non-radicals
Superoxide, $O_2^{\bullet-}$	Hydrogen peroxide, H_2O_2
Hydroxyl, OH^{\bullet}	Hypochlorous acid, $HOCl^a$
Peroxyl, RO_2^{\bullet}	Ozone, O_3
Alkoxy, RO^{\bullet}	Singlet oxygen $^1\Delta_g$
Hydroperoxyl, HO_2^{\bullet}	Peroxynitrite, $ONOO^{-b}$

^aCould equally well be called a 'reactive chlorinating species'. Discussed in Section 2.5.2.

^bDiscussed in Section 2.5.4. Could equally well be called a 'reactive nitrogen species'.

Figure 1-6. Physiologically important reactive oxygen species (taken from [80]).

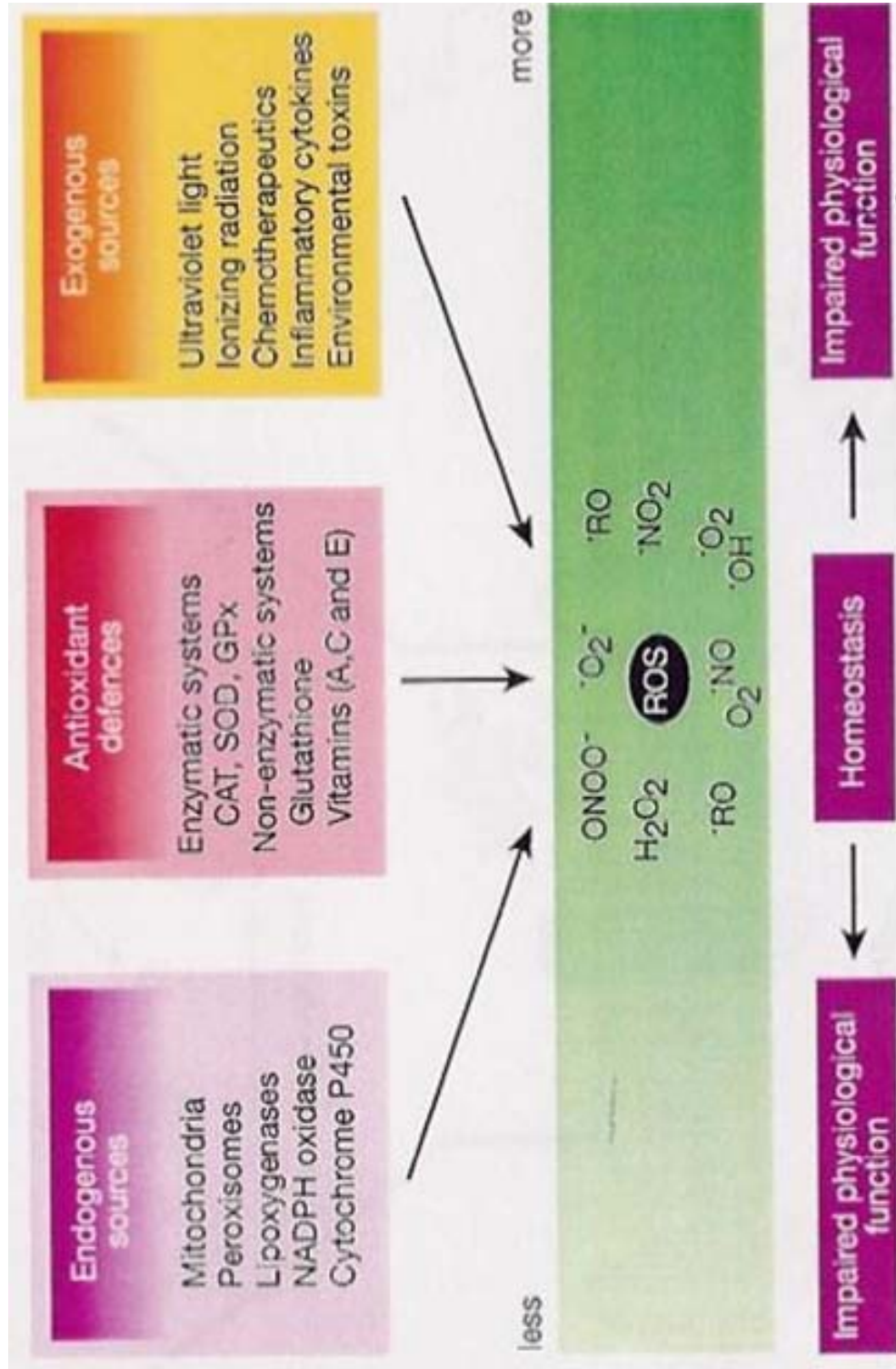


Figure 1-7. Endogenous and exogenous sources for intracellular oxidative stress (from [79]).

1.10 Why could CML represent a potential biomarker for oxidative stress?

1.10.1 *In vitro*, formation of CML involves oxidative chemistry

Originally, the Amadori adduct was considered the common precursor of all AGEs [35]. The CML formation from the Amadori adduct (right pathway in **Figure 1-8**) requires oxidative cleavage of the six carbon backbone of the sugar, a reaction which is essentially irreversible. Therefore, oxidation chemistry had been proposed as a rate limiting step in this mechanism of CML formation.

However, in the late 1980s, Wolff [84] proposed an alternative pathway, *autoxidative glycation*, in which reducing sugars were first fragmented oxidatively to yield smaller, more reactive, carbonyl intermediates, such as glyoxal, then proceeding to react with protein to form AGEs. In studies on autoxidative glycation it was found by Wells-Knecht et al. [85] that glyoxal and arabinose were the major products of autooxidation of glucose and that CML was formed during the reaction of glyoxal with proteins (left pathway in **Figure 1-8**). Additionally, ascorbate, which oxidises in the presence of free metals into the highly labile dehydroascorbate, undergoes further decomposition to form pentoses and tetroses which contribute to CML formation by subsequent reactions [86].

It is now known that CML can be formed by a maze of alternative pathways involving oxidative chemistry and reactive carbonyl intermediates. It may be formed during autoxidation of carbohydrates, including aldoses and ketoses [87], 3-deoxyglucosone [88] and ascorbate, from Schiff's base and

Amadori adducts [89], by autoxidation of fatty acids and amino acids such as serine [90] and from phosphorylated intermediates in carbohydrate metabolism [91]. In addition, Knecht et al. [85] described that CML could be formed independently from glucose autoxidation by an intramolecular Cannizzaro reaction from the precursors glyoxal and glycolaldehyde. Additionally, it may be formed from products of the polyol pathway [91].

Metal-catalysed autoxidation of glucose in the presence or absence of proteins is paralleled by the generation of ROS, such as hydroxyl radicals or superoxide radicals [92-96], that can undergo dismutation to hydrogen peroxides. Incubation of proteins, low density lipoproteins (LDL) or phosphatidylcholine liposomes with glucose under oxidising conditions in the presence of transition metals (e.g. copper) [97] also results in increased carbohydrate incorporation/fragmentation and formation of CML and thiobarbituric acid-reactive components. In the transition metal-mediated "Fenton reaction", hydrogen peroxide can produce highly reactive hydroxyl radicals. Additionally, the reactive oxygen/reactive nitrogen species peroxynitrite induces the formation of CML on proteins [98].

Thus, not only glycation, but also oxidative damage of macromolecules accounts for the formation of CML and other AGEs. Therefore, it has been supposed [36; 99] that formation of glycoxidation products *in vivo* does not only depend on the relative glucose concentrations, but also on the local oxidative environment.

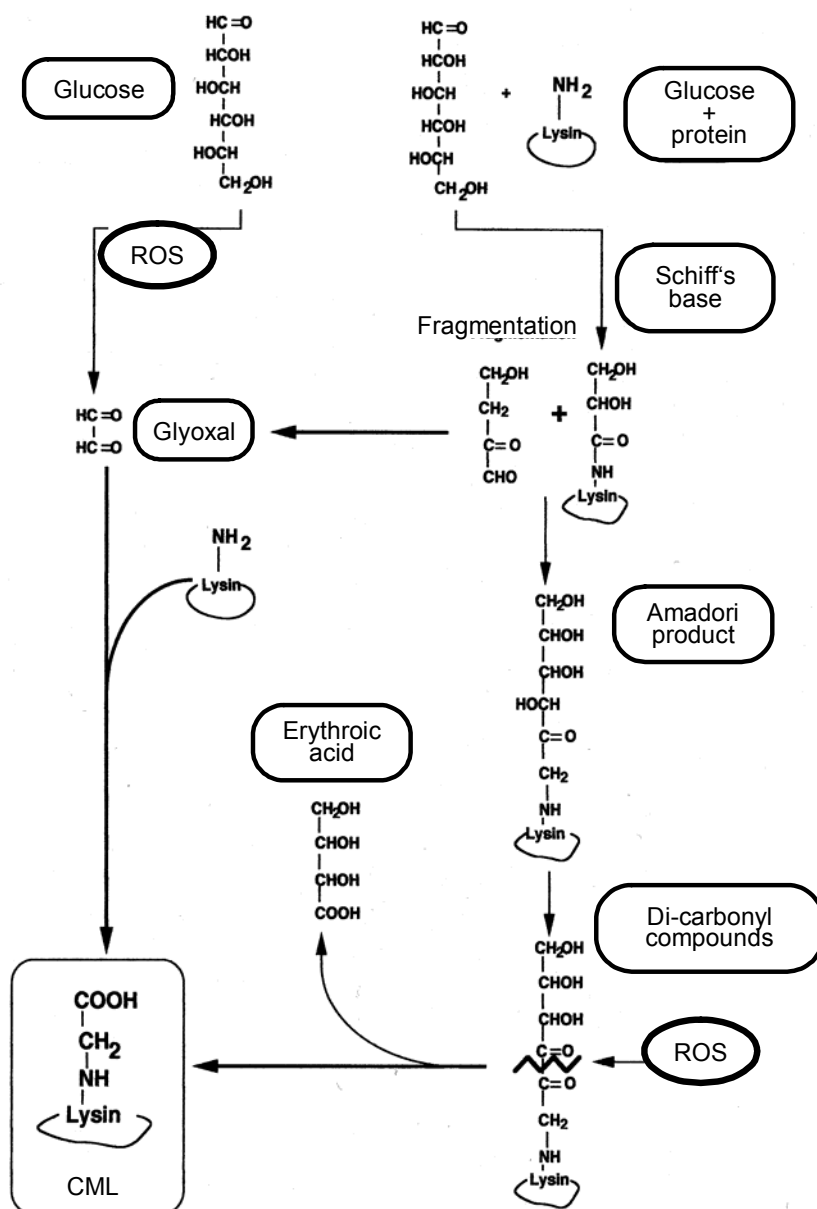


Figure 1-8. Formation of N(epsilon)-(carboxymethyl)lysine (CML). CML can be formed directly from glucose in the process of autoxidative glycation (left pathway) or from the Maillard reaction of glucose and proteins (right pathway). During the initial step of autoxidative glycation, glucose is fragmented by reactive oxygen species (ROS) to form glyoxal which reacts further to form CML on lysine residues of proteins. The formation of CML from intermediates of the Maillard reaction, such as the Schiff's base or the Amadori product, requires oxidative cleavage of the carbon backbone by ROS. Therefore, the presence of ROS has been proposed as a rate limiting step in CML formation.

1.10.2 CML is formed in a wide variety of diseases where oxidative stress has been implicated in the pathogenesis

There is the notion that histological depositions of CML were observed in a wide variety of pathological conditions where oxidative stress has been implicated in the pathomechanism [6]. Apart from diabetic organ damage and diabetic microvascular disease [100], CML formation has been found in an array of chronic inflammatory and degenerative diseases. CML depositions have been found in seemingly disparate pathologies, such as connective tissue disease (particularly rheumatoid arthritis) [101], in degenerative neurological diseases such as M. Alzheimer [102-104] or in end-stage renal disease (ESRD) [105; 106]. *In vitro* work has mostly shown CML and other AGEs to be part of the complex interactions of oxidative stress and vascular damage, particularly in atherosclerosis [34] and in the accelerated vascular damage in ESRD [107] or diabetes.

1.10.3 In experimental settings, CML is involved in a variety of pathomechanisms

At present, it is unknown whether CML may serve solely as a biomarker for oxidative stress or whether it has biological functions in perpetuating chronic inflammation and other pathological processes. Nevertheless, there is evidence that CML and other AGEs play a key role in a wide variety of pathophysiological mechanisms, be it as an indicator or as a stimulus sustaining chronic inflammation and tissue damage. On the one hand, the CML/AGE modification alters the structure, function and turnover rate of proteins. On the other hand, it has been shown that physiologically relevant quantities of CML-modified proteins are effective ligands for the receptor for AGEs

(RAGE) [108] as discussed in the following paragraph. CML and AGEs have been shown to induce or to be associated with the ras/raf/MAP-kinase pathway [109; 110] and also with differential gene expression [111]. CML has been shown to induce RAGE-mediated intracellular ROS generation by activation of cellular NADPH oxidase [112]. Further evidence for the involvement of CML in the pathogenesis of diabetic late complications comes from the observation that structurally different inhibitors of CML formation also ameliorate diabetic tissue damage in animal models [113; 114].

1.10.4 CML is a ligand for the receptor for AGEs (RAGE) and colocalises with RAGE in tissue lesions. Experimental data show a possible pathophysiological role of CML/RAGE interaction in chronic inflammatory and degenerative diseases

RAGE is a 35 kD protein which is expressed on endothelial cells, monocytes/macrophages, T-lymphocytes, smooth muscle cells, mesangial cells, neurones and microglial cells [115; 116]. *In vitro* and *in vivo* studies have shown that CML/AGE-RAGE binding on macrophages, endothelial and microglia cells leads to intracellular oxidative stress and activation of the redoxsensitive transcription factor NF κ B [67; 108; 117]. An actual hypothesis [118] links CML/RAGE-mediated activation of NF κ B to the perpetuation of pathological processes such as chronic inflammation, atherosclerosis and diabetic organ damage.

The colocalisation of CML and RAGE has been described in various organs susceptible to diabetic late complications and to microvascular injury, including kidney [119], retina [120], nerve and other organs [121]. There is ongoing debate as to whether

this colocalisation reflects a receptor-mediated clearance mechanism or a functionally relevant receptor-triggered pathomechanism of tissue damage [67; 122; 123].

1.10.5 When present, CML depositions are often found within or in close proximity to infiltrating inflammatory cells and activated resident cells

There are numerous observations from immunohistochemical studies, using CML-specific antibodies, that CML-immunoreactivity is localised within invading inflammatory or activated resident cells, suggesting that these cell types are involved in CML formation. This has been observed in atherosclerosis (as shown in **Figure 1-9**), in Alzheimer's disease (as shown in **Figure 1-10**) and in other conditions such as macular retina degeneration [41; 102; 124]. Thus, it is possible that accumulated CML at the sites of tissue injury might originate, in part, from infiltrating inflammatory cells or from activated resident cells involved in tissue injury or repair.

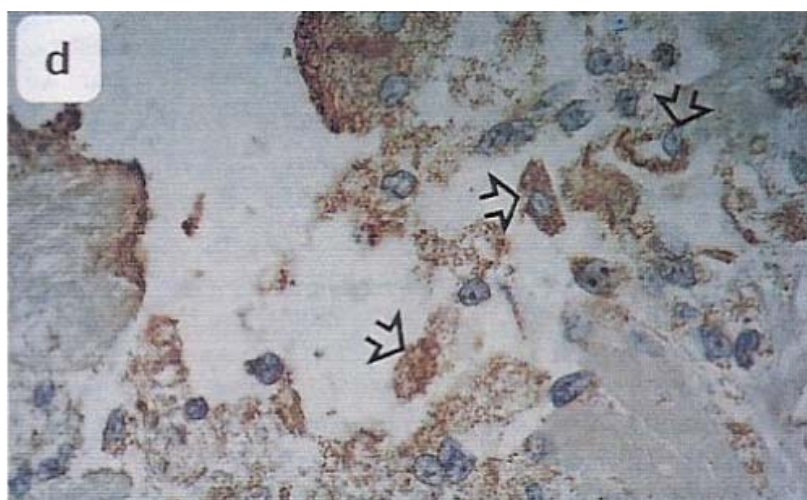


Figure 1-9. Intracellular CML accumulation in macrophages in atherosclerosis. Immunohistochemical staining of an atherectomy specimen from a 58-year subject shows strongly positive CML staining in multiple foam cells (arrows) at the margins of the atheroma (from [41]).

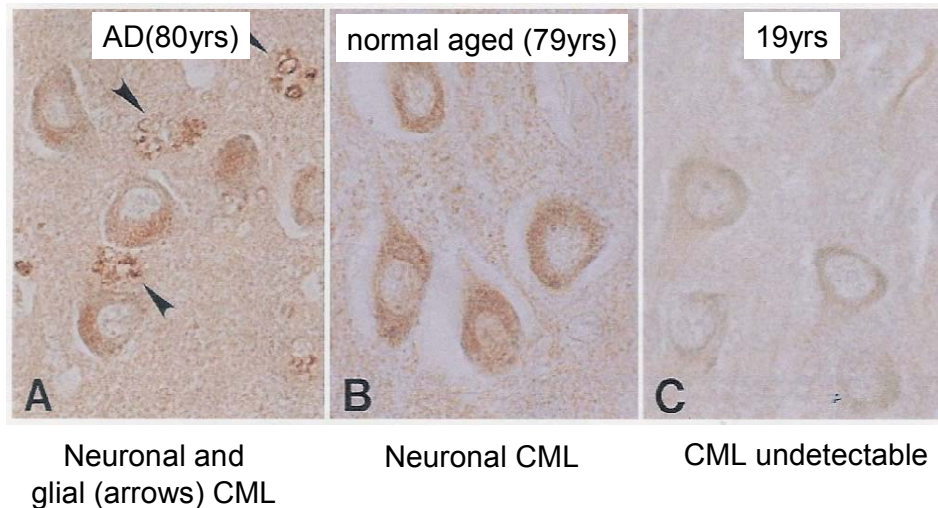


Figure 1-10. CML in Alzheimer's disease. In Alzheimer's disease (AD, left), CML preferentially accumulates in neuroglia cells as compared to age-matched controls (middle). In brain biopsy specimen of young subjects (left) CML is not detectable (from [102]).

1.10.6 From cell culture experiments there is evidence for *de novo* intracellular CML formation

In numerous immunohistochemical studies, intracellular CML depositions have been described at the sites of tissue damage. However, in these studies it was not clear whether the CML positive material was actually formed within the cell or was rather taken up by phagocytic processes and stored subsequently in the endocytic vesicles or lysosomes.

From cell culture models, it eventually became clear that the *de novo* CML/AGEs formation can occur intracellularly and can result in the CML modification of intracellular proteins. Inside the cell, carboxymethylation of proteins proceeds at a much greater rate than in the extracellular compartment [4; 31] since the cellular sugar phosphates and carbonyl intermediates, such as glucose-6-phosphate, fructose, glyceraldehyde, glycolaldehyde or glyoxal, are much more reactive towards lysine residues than glucose.

Evidence for intracellular CML formation comes now from a variety of cell types such as aortic endothelial cells, lung epithelial cells or cultured cortical neurons [31; 125-127]. Giardino et al. [31] observed a 13.8-fold higher rate in intracellular CML formation in cultured endothelial cell when they were cultured in high glucose (30mM) conditions as compared to normal glucose. Furthermore, cells which were deficient in glyoxalase I showed an even higher increase in CML modification. The overexpression of glyoxalase I completely prevented the high glucose-induced AGE formation [32].

1.10.7 CML formation on cellular proteins has also been described *in vivo* in circulating blood cells

Evidence for the carboxymethylation of intracellular proteins comes not only from cell culture studies, but also from *ex vivo*-isolated circulating blood cells. Hammes et al. [45] detected increased levels of CML in circulating long-lived T-lymphocytes and Schiekofer et al. described intracellular CML modification of proteins in circulating peripheral blood monocyctic cells (PBMC) under short term (2 h) hyperglycemia [109]. Pamplona et al [128; 129] detected a number of carboxymethylated intracellular proteins, including mitochondrial proteins, by Western-blotting analysis and Baynes et al (personal communication) detected CML in liver and muscle proteins at levels comparable to concentrations found in extracellular matrix.

1.10.8 Many of the CML-forming cell types possess enzymatic systems to generate oxidative stress.

Cellular oxidative stress is formed by processes like oxidative phosphorylation or by cellular enzymes such as myeloperoxidase or NADPH oxidase. Furthermore, it is known that cellular

oxidative stress promotes formation of CML and other AGEs. This has been demonstrated in granulocytes [130] and monocytic cells [131], as well as in cell lines of epithelial [126], endothelial [31] and neuronal [88; 127] origin. In these studies, oxidative stress was generated either by ROS-generating enzymes [130] or by diminishing the antioxidative defense, e.g by GSH depletion through menadione [45]. The ROS-mediated CML formation was most obvious in granulocytes, where stimulation with the phorbol ester PMA resulted in an “oxidative burst” from myeloperoxidase and NADPH oxidase leading to rapid carboxymethylation of model proteins [130].

Many of the cell types in which intracellular CML formation has been described so far, contain enzymes to exert oxidative stress, namely NADPH oxidase. Cellular NADPH oxidase has been described so far in granulocytes and macrophages and in endothelial cells, chondrocytes, osteoclasts, neurons and other nonphagocytic cells (reviewed in [132]). Remarkably, in most of these cell types, CML formation has been demonstrated in immunohistochemical studies, and a primary aim of the present study is to prove or disprove the involvement of NADPH oxidase and NADPH oxidase-generated superoxide anions in CML formation.

2 AIM OF THIS STUDY

In the present study, the hypothesis will be tested that the advanced glycation end product (AGE) N^ε-(carboxymethyl)-lysine (CML) is

- (a) produced intracellularly in macrophages and granulocytes,
- (b) a product of lipid-peroxidation,
- (c) formed under the influence of reactive oxygen species (ROS), especially of superoxide anions which are produced by cellular NADPH oxidase.

Furthermore, this study will examine, whether

- (d) the analysis and measurement of CML in tissues and body fluids and the identification of specific CML-modified proteins may add to the understanding of the pathophysiological processes in chronic inflammatory and degenerative diseases.

3 MATERIAL AND METHODS

3.1 Chemicals

All solvents were of HPLC grade. All reagents and buffer salts were p. A. or of the highest grade obtainable. The following chemicals were used:

Arachidonic acid	Sigma, Deisenhofen, A9673
3-Mercaptopropionic acid (MPA)	Sigma, Deisenhofen
Acetic acid	Merck, Darmstadt
Acetone	Merck, Darmstadt
Acetonitrile	Merck, Darmstadt
Acrylamide(30%)/bis (N,N'methylenbisacrylamide)(0.8%)	Roth, Karlsruhe
Albumin, bovine serum (BSA), fraction V, low endotoxin	Sigma, Deisenhofen, A8806
Albumin, human serum (HSA), low endotoxin	Sigma, Deisenhofen, A5843
Aminoguanidine	Sigma, Deisenhofen, A8835
Ammonium bicarbonate	Merck, Darmstadt
Ammonium persulfate	Serva, Heidelberg
Aprotinin (Trasylol)	Bayer, Leverkusen
Boc-Lys-OH [N- α -t.-Boc-L-lysine]	Calbiochem, Laufelingen, CH
Calcium chloride	Serva, Heidelberg
Carboxyethyl-lysine	Prof. Hammes, Mannheim
Carboxymethyl-lysine	U. Friess, Tuebingen M. Lederer, Stuttgart H. Echner, Tuebingen

CM-H ₂ DCFDA	Molecular Probes, Göttingen
Coomassie brilliant blue R-250	Serva, Heidelberg
Digitonin	Sigma, Deisenhofen, D5628
Dimethyl sulfoxide (DMSO)	Roth, Karlsruhe
Di-potassium hydrogen phosphate	Merck, Darmstadt
D-mannitol	Sigma, Deisenhofen, M8429
DTT (dithiothreitol)	Sigma, Deisenhofen
EDTA (ethylenediaminetetraacetate)	Merck, Darmstadt
Ethanol (95%, 70%)	Merck, Darmstadt
Ferritin, cationized	Sigma, Deisenhofen, F7879
Glycerol	Serva, Heidelberg
Glyoxylic acid, sodium salt	Fluka, Buchs, CH
Hemoglobin A ₀	Sigma, Heidelberg, H0267
HEPES (N-(2-hydroxyethyl)piperazine- N'-2-ethanesulfonic acid)	Serva, Heidelberg
Histopaque-1119/-1077	Sigma, Deisenhofen
Hydrochloric acid (>36.5% w/w))	Sigma, Deisenhofen
Hypoxanthine	Sigma, Deisenhofen, H9377
L-glutamine	Sigma, Deisenhofen, G7029
Linoleic acid	Sigma, Deisenhofen, L1376
Lipopolysaccharide (LPS) from E. coli 026:B6	Sigma, Deisenhofen, L8274

Lucigenin (bis-N-methylacridiniumnitrate)	Sigma, Deisenhofen
Luminol (3-aminophthalhydrazide)	Fluka, Neu-Ulm
Lysozyme	Seikagaku, Japan
Methanol	Merck, Darmstadt
N,N,N',N'-tetramethyldiamine (TEMED)	Serva, Heidelberg
NADPH	Sigma, Deisenhofen, N6505
Oleic acid	Sigma, Deisenhofen, O1383
o-Phtaldialdehyde (OPA)	Sigma, Deisenhofen
Phosphoric acid	Merck, Darmstadt
Pluronic F-127	Molecular Probes, Göttingen
PMA (phorbol-12-myristate-13-acetate)	Sigma, Deisenhofen
PMSF (phenylmethylsulfonylfluoride)	Sigma, Deisenhofen
Potassium chloride	Merck, Darmstadt
Potassium hydrogen phosphate	Merck, Darmstadt
Protease inhibitor cocktail for mammalian tissues	Sigma, Deisenhofen, P8340
Ribonuclease A	Sigma, Deisenhofen, R5500
Sodium cyanoborohydride	Sigma, Deisenhofen, S8628
Sodium dodecylsulfate (SDS)	Bio-Rad, Munich
TIRON [4,5-dihydroxy-1,3-benzene-disulfonic acid]	Sigma, Deisenhofen, D7389,
Trifluoroacetic acid (TFA)	Merck, Darmstadt

TRIS (tris[hydroxymethyl]aminomethane)	Merck, Darmstadt
TRIS Ultrapure (for ECL solutions)	ICN, Irvine, USA, Cat.No. 819623
Vitamin D ₃ (1,25-(OH) ₂ vitamin D ₃)	Calbiochem, Läufelingen, CH
Xanthine oxidase	Sigma, Deisenhofen, X4500
Zymosan A from <i>saccharomyces cervisiae</i>	Sigma, Deisenhofen, Z4250
β-Mercaptoethanol	Sigma, Deisenhofen

3.2 Tests, kits and other materials

BioRad protein assay dye reagent	Bio-Rad, Munich, Art.#500-0006
BioRad protein assay kit	Bio-Rad, Munich, Art.# 500-0001
BioRad RC DC protein assay kit	Bio-Rad, Munich, Art.# 500-0001
Bio-Rad Precision Plus unstained protein standards	Bio-Rad, Munich
Bio-Rad Precision Plus stained protein standards (dual color)	Bio-Rad, Munich
BenchMark Prestained Protein Ladder	Invitrogen, Karlsruhe
Premixed Protein Molecular Weigth Marker low range	Boehringer/Roche, Mannheim
Biochrom buffer set P for amino acid analysis	Biochrom, Cambridge, GB
GB gel blotting paper	Schleicher + Schüll, Dassel
Protran nitrocellulose membrane 0.45µm	Schleicher + Schüll, Dassel

Immuno-Blot PVDF membrane	Bio-Rad, Munich
Glass hydrolysis tubes	Wheaton, Milville, NJ, USA
Hyperfilm ECL	Amersham Pharmacia Biotech, Freiburg
Spectrum Float-A-Lyzer (MW cut off: 5000 Da)	Roth, Karlsruhe

3.2.1 Isolation of leucocyte subclasses

Dynabeads M-450 CD3 (panT)	Dynal, Hamburg
Dynabeads M-450 CD14	Dynal, Hamburg
Dynabeads M-450 CD15	Dynal, Hamburg

3.2.2 Immunoprecipitation

Pierce Seize Primary Immunoprecipitation kit	Pierce, Bonn
Pierce Seize Classic (G) Immunoprecipitation kit	Pierce, Bonn
Pierce Seize X Protein G Immunoprecipitation kit	Pierce, Bonn
Pierce ImmunoPure Immobilized Protein G	Pierce, Bonn

3.2.3 2-D Elpho

Sypro Ruby gel stain	Bio-Rad, Munich, Art.# 170-3125
Sypro Ruby blot stain	Bio-Rad, Munich, Art.# 170-3148
Pierce GelCode E-zinc stain kit	Pierce, Bonn

3.3 Cell culture media and additives

RPMI 1640 with 20mM HEPES, w/o glutamine	Gibco, Karlsruhe, #42401-018
Dulbecco's modified Eagle's medium (DMEM)	BioWhittaker, Verviers, Belgium, #BE12-7078
Fetal calf serum (FCS), tested for MM6 cells	Gibco, Karlsruhe, charge 12476024
Glutamine 200mM	Gibco, Karlsruhe, #25030-024
Penicillin/streptomycin	Gibco, Karlsruhe, #15140-122
OPI (oxalacetate, pyruvate, insulin) media supplement	Sigma, Deisenhofen, O5003
NEAA (non essential amino acids) 1%	Gibco, Karlsruhe, #11140-035
Glucose 1M	
Phosphate buffered saline (PBS) w/o Ca and Mg	BioWhittaker, Verviers, Belgium #BE17-512F
Hanks' salt solution (HSS)	Biochrom, Berlin

3.4 Cell lines

Table 3-1. Cell lines used in the present investigation.

Cell line (type)	Obtained from:
MonoMac 6 (human monocytic leukemia)	H. Ziegler-Heitbrock, Munich [133]
PLB-985 (human acute myeloid leukemia)	DMSZ, Braunschweig
PLB-985gp91 Δ 488-497 (NADPH oxidase knock out mutant of PLB-985)	M. Dinauer, Indianapolis, USA [134]
N11 (murine microglia)	R. Schinzel, Würzburg
N11/6 (NADPH oxidase knock out mutant of N11/6)	R. Schinzel/A. Neumann, Würzburg

3.5 Cell culture conditions and experimental conditions in cell culture experiments

3.5.1 Mono Mac 6, PLB 985 and PLB 985gp91 Δ 488-497 monocytic cells

All cell culture media and additives were from Gibco, Karlsruhe, unless stated otherwise. The cell culture media were prepared according to the following recipes:

Monocytic cell growth medium (5.5 mM (1 g/l) glucose):

To 450 ml RPMI 1640 medium (5.5 mM glucose, 20mM HEPES, w/o glutamine, cat. #42401-018) was added:

50 ml inactivated FCS (low LPS, Gibco, Karlsruhe, cat. # 16000-044, tested lot #12476024) to a final concentration of 10 %, 5 ml glutamine to a final conc. of 2 mM, 2.5 ml penicillin to a final conc. of 100 u/l, 2.5 ml streptomycin to a final conc. of 100 μ g/l and 5 ml OPI medium supplement to a final conc. of oxalacetate 1 mM, pyruvate 1 mM and insulin 9 μ g/ml, respectively.

Monocytic cell experimental medium (30 mM (5.5 g/l) glucose):

Same as above. Additionally, 1M sterile glucose solution was added to a final concentration of 30 mM glucose.

Culture conditions:

Cells were kept in growth medium (see above) at 37⁰C in a humidified 5 %CO₂ atmosphere. Cells were split 1:10 twice weekly.

Predifferentiation of Mono Mac 6 and PLB 985 cells:

For subsequent experiments, cells were split 1:10 and Mono Mac 6 cells were pre-differentiated by incubation with TNF α (1nM/ml which equals 17ng/ml) for 3 d according to Ziegler-Heitbrock et al.

[135; 136] and PLB 985 cells were pre-differentiated by incubation with 50 nM 1,15-(OH)₂-vitamin D₃ for 5 d according to Perkins et al. [137] in growth medium. After this period of time, the cells were found to produce ROS in the lucigenin chemiluminescence test as a feature of monocytic differentiation.

Experimental conditions:

Pre-differentiated Mono Mac 6 or PLB 985 cells were stimulated by 20 nM PMA in normal glucose (5.5mM) or high glucose (30mM) growth medium as indicated. Pre-differentiated cells were seeded at approx. 0.25 – 0.50 x 10⁶ cells/ml in 6 wells or culture flasks in experimental medium. The stimulating agents or inhibitors listed in **Table 3-2** were added as indicated in each experiment (see Results). For controls, the solvents EtOH and DMSO were added to a final concentration of 0.05% and 2%, respectively.

3.5.2 N11 and N11/6 murine microglial cells

Microglial cell growth and experimental medium (final conc. 11 mM / 2 g/l glucose):

To 450 ml DMEM medium (1 g/l glucose, BioWhittaker, Verviers, Belgium, cat. #BE12-7078) was added: 50 ml inactivated FCS to a final concentration of 10 %, 5 ml glutamine to a final conc. of 2 mM, 2.5 ml penicillin to a final conc. of 100 u/l and 2.5 ml streptomycin to a final conc. of 100 µg/l.

Table 3-2. Stimulators and inhibitors used in cell culture experiments.

	Stock solution	Final concentration	Dilution	Solvent	Source (cat.-no.)
Arachidonic acid	10mM	100µM	1:100	Ethanol	Sigma (A3925)
DPI[Diphenylene-iodinium chloride]	10mM + 1mM	100µM	1:100	DMSO	Sigma (D2926)
fMLF	87.5µg/ml	437.6ng/ml (1 µM)	1:200	Ethanol	Sigma (F3506)
HMAP (apocynine/acetovanillone)	200mM (33.2mg/ml)	2mM	1:100	70%Ethanol	Sigma (A10809)
Lactosylceramide	5mM (4.8mg/ml)	5µM	1:1000	DMSO	Calbiochem (427572)
LeukotrieneB4	30nM/100µl	2nM/ml	20 µl/3 ml	Ethanol	Sigma (L0517)
LPS (from E.coli)	1mg/ml + 2µg/µl	20ng/ml	1:100	PBS 1:10	Sigma (L8274)
Menadion	2mM + 200µM	2µM	1:100	DMSO	Sigma (5625)
TNF alpha	588nM	1nM (17ng/ml)	1:588	PBS	Sigma (T 6674)
PMA	0.1mM + 2µM	20nM	1:100	Ethanol	Sigma (P 8139)
Zymosan, opsonised	6.25mg/125µl	1.5mg/ml		Hank's buffer	Sigma (Z 4250)

Table 3-2. (cont.).

	Stock solution	Final concentration	Dilution	Solvent	Source (cat.-no.)
Benfotiamine	10mM (4.66mg/ml)	50µM	1:200	RPMI	Sigma (B9636)
4-OHCA	12.5 ml (2.36mg/ml)	250µM	1:50	Ethanol	Sigma (C2020)
CCCP	12.5mM (2.55mg/ml)	2.5µM	1:5000	DMSO	Sigma (C2759)
Rotenone	10mM (3.94mg/ml)	5µM	1:2000	DMSO	Sigma (R8875)
TTFA	20mM (4.44 mg/ml)	10µM	1:2000	DMSO	Sigma (T9888)
Antimycin A	3mM (1.59 mg/ml)	0.3µM	1:10000	Ethanol	Sigma (A8674)
Allopurinol	15mM (2.04mg/ml)	300µM	1:50	0.1M NaOH	Sigma (A8003)
Indomethacin	25mM (8.94mg/ml)	500µM	1:50	Ethanol	Sigma (I7378)
NDG	0.25mM	5µM	1:50	Ethanol	Sigma (N5023)
L-NAME	5mM (1.35mg/ml)	100µM	1:50	H ₂ O	Sigma (N5751)
Lucigenin	10mM / 1mM	500µM / 50µM	1:20	PBS	Sigma (M8010)
NADPH	10mM	200µM	1:20	H ₂ O	Sigma (N6505)
Ionomycin		5µg/ml = 6.7 µM			Sigma (I0634)
Vitamine D3 [1,25-(OH) ₂ -Vit.D3]		50nM			Calbiochem(679101)

3.6 Equipment

Table 3-3. Equipment used in the present investigation.

Cell counter	Advia 120 hematology system	Bayer Diagnostics, Fernwald
1-D Electrophoresis chambers	Mini elpho chamber Protean II	Harnischmacher, Kassel Bio-Rad, Munich
2-D Electrophoresis chamber	Multiphor II	Amersham Pharmacia Biosciences, Freiburg
Amino acid analysis	Eppendorf/Biotronic LC3000 cation exchange AA analyser (Ninhydrin post column derivatisation)	Eppendorf, Hamburg
Blotting device	Semidry blotting chamber	Hölzl, Wörth
	Multiphor II semidry blot chamber	Amersham Pharmacia Biosciences, Freiburg
Centrifuges	Haereus Biofuge fresco, rotor 3324	Haereus, Hanau
	Hettich Micro 20	Hettich, Tuttlingen
	Haereus Megafuge 2.0R, rotor 8160	Haereus, Hanau
	Hettich Rotixa/P	Hettich, Tuttlingen
Chemi-luminescence	Tropix chemiluminescence plate reader	Applied Biosciences, Foster City, CA, USA
Homogenisator	Potter S tissue homogenisator	Braun Biotech, Melsungen
HPLC	Shimadzu series 10A, equipped with SIL-10A programmable autosampler and RF-10AXL fluorescence detector	Shimadzu, Kyoto, Japan
Microscope	Zeiss Axioplan	Zeiss, Göttingen
	Zeiss Aviovert 25	

Table 3-3. Continued

Cell counter	Advia 120 hematology system	Bayer Diagnostics, Fernwald
pH-meter	pH 545 Multi Cal	WTW, Weilheim
Photometer	Eppendorf BioPhotometer	Eppendorf, Hamburg
Power supplies	Pharmacia Multidrive XL Pharmacia EPS 3500XL Pharmacia 601	Amersham Pharmacia Biosciences, Freiburg
Shakers	Roto-shake Genie	Scientific Industries, Bohemia, NY, USA
Ultrasound bath	Transsonic 460/H	Elma, Singen
Vacuum concentrator	Speedvac centrifugal evaporator	Christ, Osterode
Vibration mill	Micro dismembrator U	Braun Biotech, Melsungen

3.7 *In vitro* chemical carboxymethylation of proteins

HSA, BSA, Ferritin and hemoglobin were chemically carboxymethylated using glyoxylic acid and NaBH₃CN as described by Reddy et al. [38]. In general, a protein containing x mol of lysine residues was incubated with an equimolar amount of glyoxylic acid and an 3 fold molar excess of NaBH₃CN in 0.2 M sodium phosphate buffer pH 7.8 at 37⁰C for 4h or 24h, respectively, as indicated in **Table 3-4**. The reaction was stopped by transferring the reaction mixture to 1 or 10 ml dialysis tubes (Spectrum Float-a-lyzer, Roth, Karlsruhe, MW cut off: 5000 Da) for subsequent dialysis against 4 l of 0.2 Na phosphate buffer pH 7.8 for 2 x 24 h. The buffer was changed once.

Table 3-4. Composition of the reaction mixtures and conditions for the *in vitro* carboxymethylation of human serum albumin (HAS), bovine serum albumin (BSA), hemoglobin A and cationised ferritin by glyoxylic acid.

Human serum albumin (HSA), low endotoxin (MW 66422 Da; 59 lysine residues / 585 amino acids)			
	Control (C)	low CML-modified (L-CML)	high CML-modified (H-CML)
Protein	1000 mg	1000 mg	1000 mg
Glyoxylic acid	–	97.9 mg	97.9 mg
NaBH ₃ CN	161.2 mg	161.2 mg	161.2 mg
Buffer (0.2M Na-phosphate pH 7.8)	8.5 ml	8.5 ml	8.5 ml
Time	24 h	4 h	24h

Bovine serum albumin (BSA), low endotoxin (MW 66432 Da; 59 lysine residues / 583 amino acids)			
	Control (C)	low CML-modified (L-CML)	high CML-modified (H-CML)
Protein	1000 mg	1000 mg	1000 mg
Glyoxylic acid	-	97.9 mg	97.9 mg
NaBH ₃ CN	161.2 mg	161.2 mg	161.2 mg
Buffer (0.2M Na-phosphate pH 7.8)	8.5 ml	8.5 ml	8.5 ml
Time	24 h	4 h	24h

Hemoglobin HbA (MW 61986 Da; 44 lysine residues / 574 amino acids ($\alpha_2\beta_2$))			
	Control (C)	low CML-modified (L-CML)	high CML-modified (H-CML)
Protein	10 mg	10 mg	10 mg
Glyoxylic acid	-	1.7 mg	1.7 mg
NaBH ₃ CN	2.8 mg	2.8 mg	2.8 mg
Buffer (0.2M Na-phosphate pH 7.8)	1.0 ml	1.0 ml	1.0 ml
Time	24 h	4 h	24h

Table 3-4. Continued

Ferritin, cationized (MW 440 kDa, 24 apoferritin subunits; 27 lysine residues / 175 amino acids (apoferritin))			
	Control (C)	high CML-modified (H-CML)	
Protein	10 mg	10 mg	
Glyoxylic acid	-	1.7 mg	
NaBH ₃ CN	2.8 mg	2.8 mg	
Buffer (0.2M Na-phosphate pH 7.8)	1.0 ml	1.0 ml	
Time	24 h	24h	
Abbreviations: MW: molecular weight; Da: Dalton.			

3.8 Determination of CML content by amino acid analysis

The CML content of the carboxymethylated proteins was determined from acid hydrolysates (7 M HCl) by amino acid analysis (ASA). An aliquot corresponding to approx. 1 mg of protein was transferred to a vacuum hydrolysis tube (Wheaton, Milville, NJ, USA), diluted by 12M HCl (>36.5% w/w) to a final concentration of 7 M HCl, cooled in liquid nitrogen and evacuated after the contents solidified. Samples were hydrolysed at 110 °C for 24 hours under vacuum. The hydrolysates were filtered and evaporated to dryness.

ASAs were performed by cation exchange HPLC, post column ninhydrin reaction and detection at 570 nm using an Eppendorf/Biotronic AA-analyser LC3000 and the Biotronic ready-to-use buffer and reagents set P for analysis of physiological samples (Amersham Biosciences, Freiburg). The lyophilised sample was taken up in 400 µl sample dilution buffer and cleared by centrifugation. 20µl of the diluted (1:5 with sample dilution buffer) supernatant was injected for analysis. A Benson

amino acid standard was run in parallel and amino acids were identified according to their retention time. Samples were spiked with additional CML standard at a concentration of 100 nmol/ml and the CML peak was identified by coelution.

3.9 *In vitro* lipid peroxidation of RNase

The lipid peroxidation of RNase by the polyunsaturated fatty acids (PUFAs) oleic acid, linoleic acid and arachidonic acid, respectively, was investigated under various oxidative conditions and under the influence of antioxidative agents. **Table 3-5** lists the composition of the reaction mixtures.

Table 3-5. Composition of the reaction mixtures for the lipid peroxidation of RNase (final conc. 1 mM) by oleic acid, linoleic acid and arachidonic acid (final conc. 100 mM), respectively.

Reaction mixture	
Oleic acid [18:1 (Δ 9)]	6.8 mg RNase and 14.1 mg oleic acid were dissolved in 500 μ l PBS.
Linoleic acid [18:2 (Δ 9,12)]	6.8 mg RNase and 14.0 mg linoleic acid were dissolved in 500 μ l PBS.
Arachidonic acid [20:4 (Δ 5,8,11,14)]	6.8 mg RNase and 15.2 mg arachidonic acid were dissolved in 500 μ l PBS.

The poly-unsaturated fatty acids (PUFAs) were dispersed by sonification for 60 min in a ultrasound bath at 37⁰C (Elma Transonic, Singen, Germany) according to [138], then RNase was added. Suspensions were initially fine disperse and became gradually biphasic (oleate) or monophasic (linoleate, arachidonate) at day 2-5.

Table 3-6 summarises the reaction conditions used for each PUFA.

Table 3-6. Reaction conditions for the lipid peroxidation of RNase by polyunsaturated fatty acids.

Condition	
Aerobic (O ₂)	Reaction mixture was left under aerobic condition
Xanthine oxidase (XOD)	2.5µl of a 100 mM hypoxanthine solution and 5mU xanthine oxidase per 500µl were added freshly every hour during daytime (12 hours/day) as a superoxide anion-generating system
Xanthine oxidase /aminoguanidine	additionally 10µl of a 500 mM aminoguanidine 500mM solution was added per 500 µl to a final conc. of 10mM aminoguanidine
Xanthine oxidase/Tiron	5 µl of a 1 M Tiron solution was added per 500 µl to a final conc. of 10mM Tiron
H ₂ O ₂	6µl H ₂ O ₂ (30%, 8.8M) was added freshly every hour during daytime (12 hours/day) per 500 µl to a final conc. of approx. 100mM
H ₂ O ₂ /aminoguanidine	10µl of a 500 mM aminoguanidine solution was added per 500 µl to a final conc. of 10mM aminoguanidine

3.10 Synthesis of CML standard

In cooperation with Dr. B. Christian, Institute of Organic Chemistry, University of Tuebingen (group of Prof. E. Bayer), CML was synthesised according to the method of M. Lederer, University of Hohenheim (personal communication) as described below. The protocol used is a modification of the method of Liardon et al. [139]. In the original method, the reduction step was performed by Pd catalysed hydration in a H₂ atmosphere. The reaction scheme is depicted in **Figure 3-1**. Additional amounts of

CML for the planned synthesis of modified peptides were synthesised by Dr. Echner, Tuebingen.

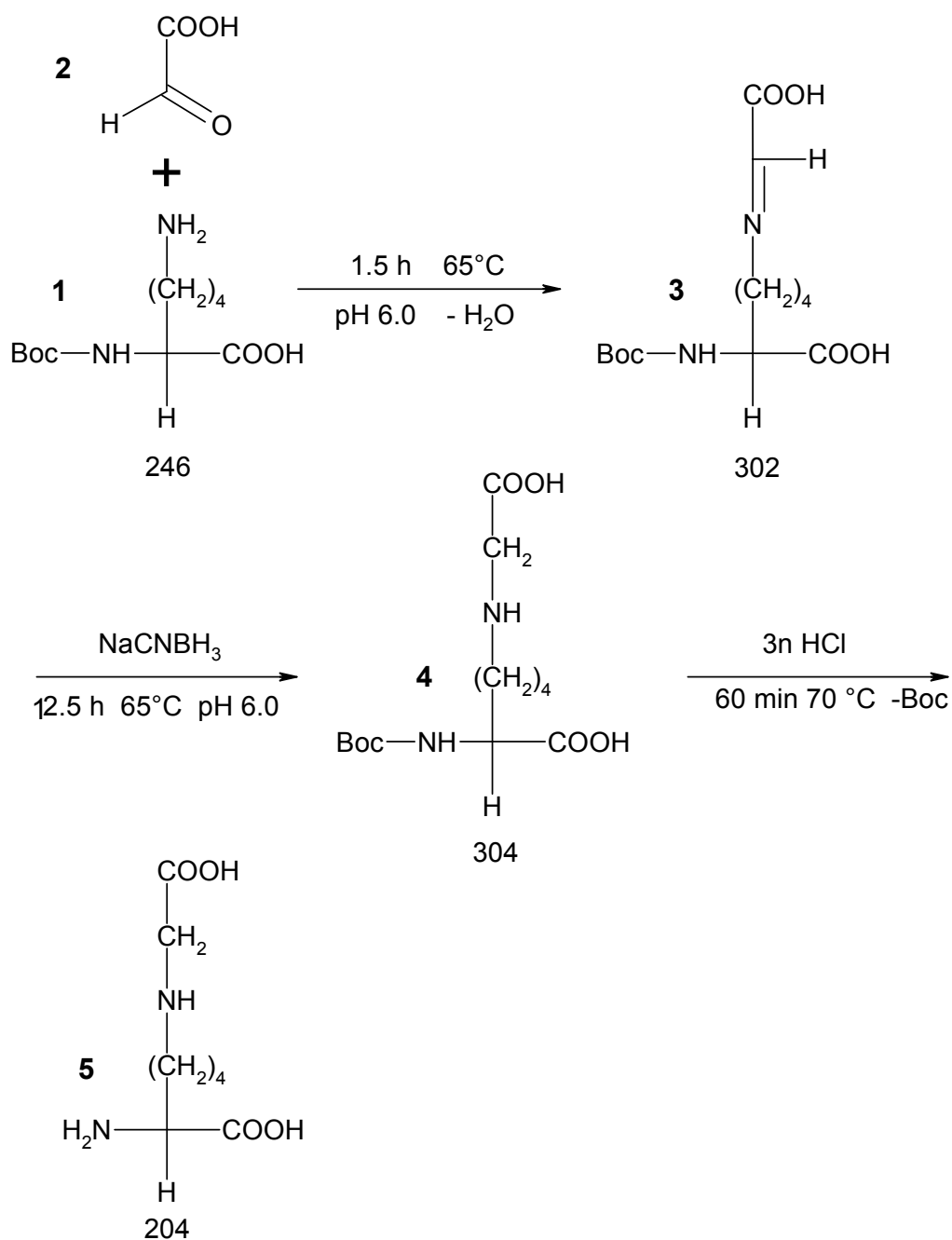


Figure 3-1. Synthesis of N^ϵ -(carboxymethyl)-lysine starting from N^α -Boc-lysine (1) and glyoxylic acid (2) which form a Schiff's base (3) in situ. The Schiff's base is reduced in the presence of sodium cyanoborohydride to N^α -Boc- N^ϵ -(carboxymethyl)-lysine (4). Subsequently, the Boc group is split off under acidic conditions to yield N^ϵ -(carboxymethyl)-lysine (5).

Synthesis protocol

N^α-tert.-Boc-L-lysine (**1**) was purchased from Calbiochem, Läufelingen, CH, glyoxylic acid (**2**) and NaCNBH₃ was purchased from Sigma, Deisenhofen. Citrate buffer was prepared according to Sörensen by dissolving 2.1 g citric acid monohydrate in 20 ml H₂O and was adjusted to pH 6 by adding 1M NaOH. Microanalysis was performed at the Microanalytical Laboratory at the Institute for Inorganic Chemistry at the University of Tuebingen.

Synthesis of N^α-Boc-N^ε-(carboxymethyl)-lysine (4**)**

N^α-Boc lysine (**1**) (985.24 mg, 4 mmol) and sodium glyoxylate (**2**) (684.18 mg, 6 mmol) was dissolved in 8 ml of citrate buffer. The solution was adjusted to a pH of 6 (pH-electrode) using 1 M NaOH and stirred for 1.5 h at 65 °C. Subsequently, NaCNBH₃ (384.8 mg, 6.12 mmol) was added and the solution stirred continuously for 12.5 h at 65 °C. Samples were taken regularly and analysed using thin-layer chromatography (TLC). After 14 h of reaction time, TLC analysis could not detect any remaining N^α-Boc lysine in the solution. After completion of the reaction, the solution was concentrated in a rotatory evaporator. The residue of the solution was dissolved in methanol and desalted using a short column packed with cellulose. After washing with additional methanol, the collected filtered solution was dried. In a second desalting step, the residue was dissolved in methanol and separated through a long column packed with cellulose. *Yield of 4*: 1080.6 mg (3.56 mmol; 88.9 % of expected value)

Synthesis of N^ε-(carboxymethyl)-lysine (5**)**

N^{α} -Boc- N^{ϵ} -(carboxymethyl)-lysine (**4**) (1080.6 mg, 3.56 mmol) was dissolved in 10 ml of 3M HCl and heated for 1 h to 70 °C. After removing the HCl in a vacuum concentrator, the residue was recrystallized in water-ethanol. *Yield of 5*: 728.4 mg (2.62 mmol; 73.9 % of expected value). *Elemental analysis*: $C_8H_{16}N_2O_4$: calculated (in %) C 47.1, H 7.8, N 13.7; found (in %) C 44.91, H 7.10, N 12.61, Cl 1.20

Characterisation of N^{ϵ} -(carboxymethyl)-lysine (CML) for use as a standard compound

The synthetic product was further characterised by LC-MS, cation-exchange HPLC and reversed-phase HPLC. Identification of the synthesis product by MS (**Figure 3-2, C**) showed that the product contained CML (MW 204.3 $[M+H]^+$ with m/z of 205.4) besides traces of lysine ($[M+H]^+$ with m/z of 147.4). Cation exchange HPLC (**Figure 3-2, A**) and sensitive RP-HPLC using OPA-derivatisation and fluorescence detection (**Figure 3-2, B**) revealed a single peak for CML and no other amino compound.

The CML content of the synthesis product was estimated by comparison with a CML standard synthesised and characterised by Dr. M. Lederer, Stuttgart. In amino acid analysis (**Figure 3-2, A**), 95% of the expected concentration (210.6 $\mu\text{mol/l}$ as compared to 220 $\mu\text{mol/l}$ expected) was found and in RP-HPLC, (**Figure 3-2, B**) 90% of the expected concentration (1.0 $\mu\text{mol/l}$ as compared to 1.1 $\mu\text{mol/l}$ expected) was found. These data together with the results from elemental analysis indicate that the raw product had a CML content of 90-95% and contained no other amino group bearing compound. Therefore, it was suited for identification of CML during chromatography and for the synthesis

of CML-containing peptides. For use as a quantitative standard, further purification will be required.

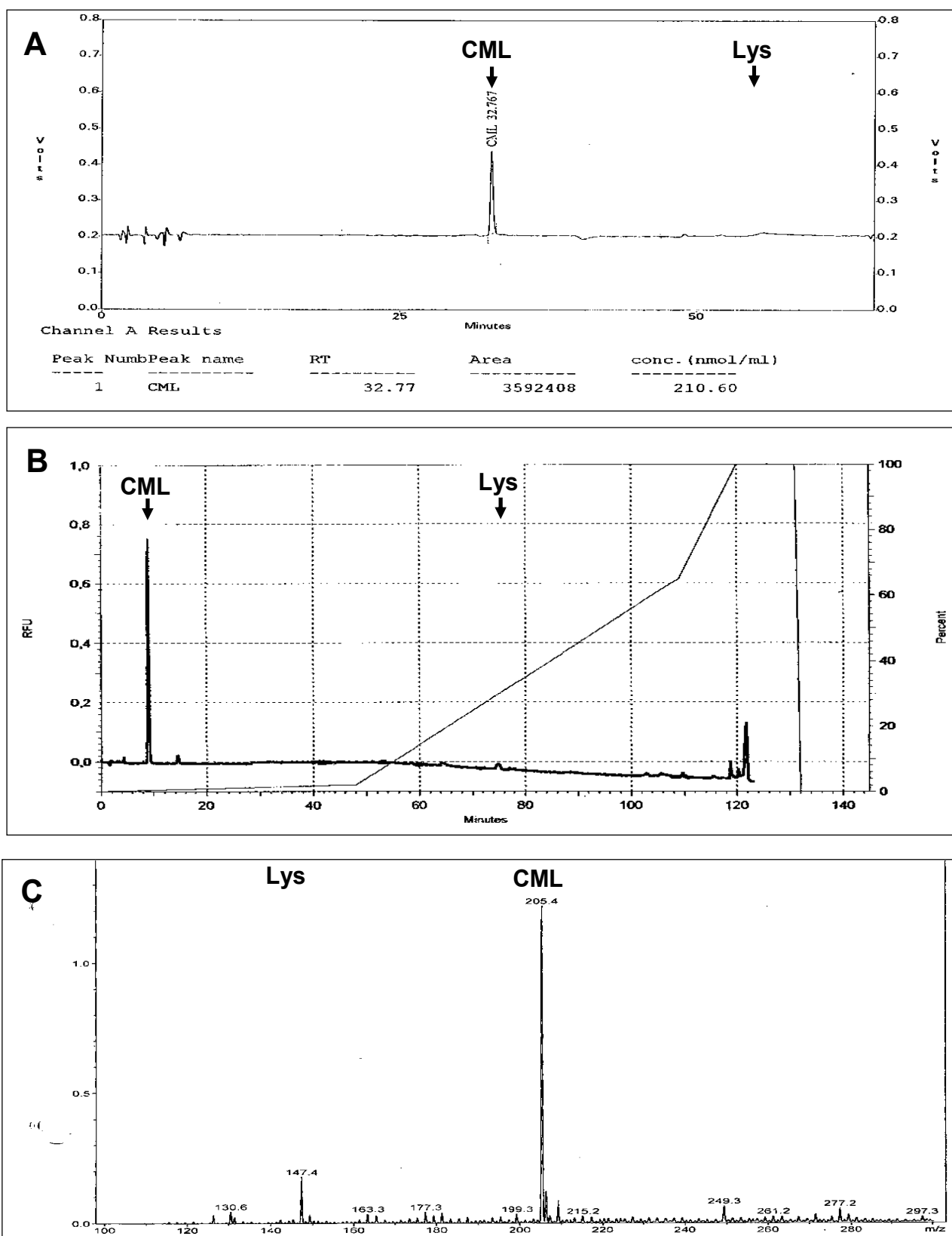


Figure 3-2. Legend see following page.

Figure 3-2. Characterisation of synthetic CML by cation exchange HPLC (A), by RP-HPLC (B) and by ESI-MS (C). The product was dissolved at 4.5 mg/ml. In (A) a 1:100 dilution (which would equal 220 $\mu\text{mol/l}$ CML) and in (B) a 1:20000 dilution (which would equal 1.1 $\mu\text{mol/l}$) was analysed. Chromatographic separations (A, B) gave a single peak of CML as identified by coelution with CML standard. In (C) the sample was diluted to 10 pmol/ μl in 50% methanol/1% formic acid and injected at a rate of 5 $\mu\text{l}/\text{min}$. ESI-MS (C) of the synthesis product revealed the characteristic mass of CML ($M+H^+$ m/z 205) besides traces of lysine ($M+H^+$ m/z 147). Conditions: **A:** Eppendorf/Biotronic LC 3000 amino acid analyser (Eppendorf, Hamburg, Germany), Eppendorf cation exchange resin, column 125 x 4 mm, 20 μl injection volume, isocratic elution, Eppendorf ready-to-use buffer, ninhydrin post column derivatisation, 125 $^{\circ}\text{C}$, detection 570nm. For external calibration, the Benson amino acid standard P with additional CML at a concentration of 100 nmol/ml was used (not shown). The peak for carboxymethyllysine (CML) and lysine (Lys) was identified by coelution with standards at 32.7 and 60.3 min, respectively; **B:** GROM-SIL 100 ODS-0 AB C18 reversed phase column, 5 μm , 200x4 mm, flow 0.4 ml/min, 21 $^{\circ}\text{C}$, injection 10 μl , eluent A: 1% ACN / 1% TFA, eluent B: 45% ACN / 5% TFA in 15 mM NaH_2PO_4 , pH 7.2, gradient: 0-2.5% B (0-44min), 2.5-60% B (44-110min); 60-100% B (110-120min), OPA pre-column derivatisation, fluorescence detection, excitation 340nm, emission 455nm; **C:** Bruker Daltronics esquire3000 plus ESI-MS; pos. ionisation mode, capillary exit 103.0 V, scan from 100 to 300 m/z . Abbreviations: CML: carboxymethyllysine; Lys: lysine; RFU: rel. fluorescence units

3.11 Preparation of cell lysates and protein extracts

For Western-blotting, 1% Triton lysates were prepared from cell culture cells. The composition of the cell lysis buffer was: 50 mM Tris-HCl (pH 8), 150 mM NaCl, 0.02% sodium azide, 1% Triton X-100, 0,5 mM PMSF and 14 $\mu\text{g}/\mu\text{l}$. aprotinin. PMSF and aprotinin were freshly added from stock solutions of 100mM PMSF in EtOH and 70mg/50ml aprotinin (Trasylol®) in H_2O , respectively.

Suspension cells (or trypsinated and scraped off adherent cells) were counted using an Advia120 automatised cell counter (Bayer Diagnostics, Fernwald, Germany). Viability was shown to be

>85% by trypan blue exclusion testing. Typically, approx. 4×10^6 suspension cells (or approx. 5×10^5 adherent cells) were harvested by centrifugation (900 rpm equal to $125 \times g$, 3 min, 4° , Haereus Megafuge 2.0R) and washed 3 times in PBS (900 rpm, 3 min, 4°). The cell pellet was resuspended in 200 μ l lysis buffer (or 50 μ l per 10^6 cells if cell counts were low) with freshly added aprotinin and PMSF, vortexed for 10 sec and centrifuged (13000 rpm equal to $16000g$, 5 min., $4^\circ C$) using a microcentrifuge (Haereus Biofuge). The protein concentrations of the supernatants were determined with a modified Bradford reaction (Bio-Rad protein assay, Bio-Rad, Munich, Germany) against a calibration curve made from BSA standard (Bio-Rad). Protein concentrations were typically in the range of 2 - 4 μ g protein / μ l. Supernatants were stored at $-70^\circ C$.

Protein extracts from tissues were prepared using the homogenisation buffer given below. 10 – 100 mg of tissue were frozen in liquid nitrogen and powdered in a liquid nitrogen-cooled vibration mill (Micro-Dismembrator U, Braun Biotech, Melsungen, Germany) using a 3 ml teflon shaking flask at 2000 rpm for 1 min. Powdered tissue was placed in 1.5 ml ice-cold tissue homogenisation buffer (10 mM $NaHCO_3$ pH 7.0, 0.25 M sucrose, 5 mM NaN_3 , freshly added protease inhibitor cocktail (10 μ l/100 μ g tissue, Sigma, P8340) and 100 μ M PMSF) and further homogenised in a motor-driven Potter-Elvehjem tissue homogenisator (Potter S, Braun Biotech, Melsungen, Germany) at 1500 rpm for 2 min and 20 ups and downs. The crude homogenates were centrifuged (13000 rpm, 10 min, 4°) and protein concentrations of the supernatants were determined with a modified Bradford reaction (Bio-Rad protein assay, Bio-Rad,

Munich, Germany), typically resulting in 0.1 to 0.3 μg protein / μl . Protein extracts were stored frozen at -70°C .

3.12 Western blots / dot blots

Aliquots of cell lysates or tissue homogenates, equivalent to 10 to 30 μg protein, were denatured with 0.2 volumes of Laemmli buffer (25 % glycerol, 2 % sodium dodecylsulfate (SDS), 5 % β -mercaptoethanol in 60 mM Tris/HCl pH 6.8) at 95°C for 5 min, loaded in pockets and separated by sodium dodecylsulfate polyacrylamide gel electrophoresis (SDS-PAGE) on 1.5 mm thick 7.5% polyacrylamide gels. For separation of low molecular weight proteins, e.g. hemoglobin, 15% separation gels were used. Recipes for stacking and separation gels are given in **Table 3-7**. Proteins were transferred to nitrocellulose membranes by semi-dry-electroblotting (transfer buffer: 48 mM Tris, 39 mM glycine, 0.040 % SDS, 20 % (v/v) methanol). Transfer conditions were 1 h 45 min at a current of 0.8 mA / cm^2 . Blotting efficiency was controlled by reversible Ponceau Red protein staining of the membranes. After blotting, the nitrocellulose membranes were blocked with NET-G buffer (150 mM NaCl, 50 mM Tris/HCl pH 7.4, 5 mM EDTA, 0.05 % Triton X-100, 0.25 % gelatine) and incubated with the appropriate specific first antibody overnight at 4°C . The primary antibodies used in this study and the appropriate dilutions are listed in **Table 3-8**. After washing with NET-G buffer, the membranes were incubated with the appropriate species-specific horseradish peroxidase-conjugated anti-IgG as listed in **Table 3-9** for 1 h at room temperature. Immunoreactive proteins were detected by enhanced chemiluminescence using the ECL system (Amersham

Pharmacia Biotech, Freiburg, Germany) and subsequent autoradiography. The protocol for immunostaining is given below. Exposure times were in the range from 1 min to 60 min depending on the experiment and on the antibodies used. Details for each experiment are given in the Results section.

For reblots, membranes were stripped using the protocol given below and the immunostaining was repeated using a new primary antibody.

Table 3-7. Recipes for the preparation of polyacrylamide gels (SDS-PAGE).

Mini gel (1.5 mm thickness)	Separation gel 7.5 %	Separation gel 15 %	Stacking gel
Acrylamide 30%	2.5 ml	5.0 ml	0.45 ml
H ₂ O	5.0 ml	2.5 ml	2.35 ml
1.5M TRIS pH 8.8/ 2% SDS	2.5 ml	2.5 ml	0.85 ml
TEMED	16.5 µl	16.5 µl	5 µl
APS 10% (200mg in 2ml H ₂ O)	67.5 µl	67.5 µl	37.5 µl

Preparation of a 10-fold concentrated electrophoresis running buffer:

30 g of TRIS base, 144 g of glycine and 10 g of SDS are dissolved in 1 l of H₂O.

Preparation of 10-fold concentrated NET-G buffer:

25 g of gelatine is dissolved in approximately 500 ml of H₂O at 37⁰C in a water bath. Subsequently, 87.66 g of NaCl, 60.55 g of TRIS base and 19.10 g of EDTA are added and the solution is filled up with H₂O to a final volume of 1 l.

Immunostaining protocol for Western blot / dot blot membranes:

1. Membranes are blocked for 3 x 15min in NET-G buffer
2. Primary antibody is added and membranes are incubated overnight at 4⁰C on a laboratory rocker
3. Membranes are washed for 3 x 15min in NET-G buffer
4. Secondary antibody/HRP-conjugat is added and membranes are incubated for 60 min at room temperature on a laboratory rocker
5. Membranes are washed for 4 x 15min in NET-G buffer

Protocol for the immunodetection by enhanced luminol chemiluminescence (ECL):

All steps are performed in the dark.

1. Equal volumes of ECL solution A and B (see below) are added to immunostained membranes for 3 min in the dark
2. Membranes are put in a film developer cassette and covered with transparent cover sheets. Film (Hyperfilm ECL, Amersham Pharmacia Biotech) is placed on top and cassette is closed.
3. Film is exposed for the indicated time (1 – 60 min) and developed.

Preparation of ECL-solution A:

880 μ l of a 0.5 M luminol solution (final conc. 4.41 mM) and 864 μ l of a 0.5 M p-iodophenol solution (final conc. 4.32 mM) are dissolved in 100 ml of 0.1 M TRIS/HCl pH 9.35.

Preparation of ECL-solution B:

25 μ l of a 30% hydrogen peroxide solution is added to 100ml 0,1M TRIS/HCl pH 9.35. Both solutions are stored at 4°C under light protection.

Preparation of a 0.5 M luminol solution:

0.885 g of luminol is dissolved in 10 ml H₂O.

Preparation of a 0.5 M p-iodophenol solution:

1.10 g of p-iodophenol is dissolved in 10ml DMSO.

Stripping protocol for reblots.

1. Membranes are washed in NET-G buffer for 30-60 sec.
2. Membranes are incubated in stripping buffer for 30 min at 55°C in a closed water bath.
3. Membranes are washed in NET-G buffer for 3 x 15 min and immunostained as given above.

Preparation of stripping-buffer (500 ml).

4 g of TRIS (final conc. 66 mM) is dissolved in 450 ml H₂O. The pH is adjusted to 6.8 by the addition of HCl. 2.5 ml of β -mercaptoethanol (final conc. 0.5 % v/v) and 10 g SDS (final conc. 2 % w/v) are added and the volume is adjusted to 500 ml by the addition of H₂O.

3.13 Antibodies

The primary and secondary antibodies used in the present study are listed in **Table 3-8** and **Table 3-9**, respectively.

Table 3-8. Primary antibodies used in the present study.

Antibody	Dilution (Western Blot)	Second. antibody	Source	Isotype
CML antiserum (polyclonal, rabbit)	(1 :1000) to 1 :8000	Anti-rabbit (1: 3000)	Prof. Schleicher, Tuebingen	
Anti-CML 2F8 (monoclonal, mouse)	1 :5000	Anti-mouse (1: 3000)	Novo Nordisk, Bagsvaerd, Denmark	
Anti-CML CMS10 (monoclonal, mouse)	1 :5000	Anti-mouse (1: 3000)	TransGenic, Kumamoto, Japan	IgG 1
Anti-CML NF1G (monoclonal, mouse)	1 :5000	Anti-mouse (1: 3000)	TransGenic, Kumamoto, Japan	IgG 2a
Anti-AGE-2 (polyclonal, rabbit)	1 :1000	Anti-rabbit (1: 3000)	Prof. Makita, Sapporo, Japan	
Anti-AGE-3 (polyclonal, rabbit)	1 :1000	Anti-rabbit (1: 3000)	Prof. Makita, Sapporo, Japan	
Anti-CML 4G9 (monoclonal, mouse)	1:5000	Anti-mouse (1:3000)	Roche, Penzberg	IgG 1
Anti-CEL/(CML) IF2A1 (monoclonal, mouse)	1:1000	Anti-mouse (1:3000)	NovoNordisk, Bagsvaerd, Denmark	
Anti-CEL KNH-30 (monoclonal, mouse)	1:1000	Anti-mouse (1:3000)	Tansgenics, Kumamoto, Japan	IgG1

Table 3-9. Secondary antibodies used in this study.

Antibody-HRP conjugate	Source (cat.-#)
Goat anti-rabbit IgG-HRP	Santa Cruz, Heidelberg, (sc-2004)
Goat anti-mouse IgG-HRP	Santa Cruz, Heidelberg, (sc-2005)
Anti-goat IgG-HRP	Santa Cruz, Heidelberg, (sc-2020)

Abbreviations: HRP: horse radish peroxidase

The specificity of the polyclonal rabbit anti-CML antiserum has been characterised previously [140] as shown in **Figure 3-3**.

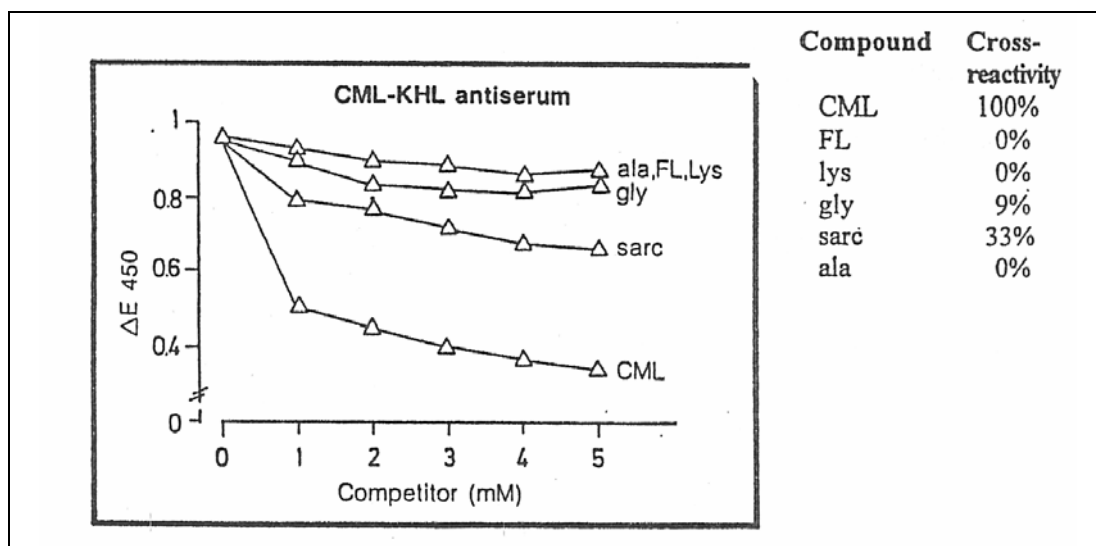


Figure 3-3. Specificity of the rabbit anti-CML antiserum used. Reaction mixtures contained 0-5 mM of the free hapten (CML) or other competitors. Crossreactivities were deduced from the competition curves (lys = lysine; FL = fructose-lysine, ala = alanine, gly = glycine, sarc = sarcosine) (taken from [140]).

3.14 HPLC determination of urinary CML excretion

3.14.1 Study group and sample collection

First morning urine samples were obtained from 51 diabetic patients (DM; age 57 +/- 14 years, HbA1c 8,0 +/- 1,8 %) and from 42 controls (C: age 45 +/- 17 years). Characteristics of patient and control groups are summarised in **Table 3-10**. As assessed from the clinical record, 72% of the patients (29 out of 42 patients with data available) showed signs of diabetic neuropathy (reduced vibration sensation) and 37 % (16 out of 43 patients who received examination) showed non-proliferative or proliferative retinopathy. Inclusion criteria for all participants were: absence of gross proteinuria (< 300 mg/l), absence of renal impairment (serum creatinine \leq 1.0 mg/dl) and absence of inflammatory signs and symptoms by clinical record and by laboratory parameters (normal white blood count, no elevation of C-reactive protein). HbA1c was measured by cation exchange HPLC (Tosoh 2.2 HLC-723, Tosoh Corp., Tokyo, Japan), urinary protein by a modified Biuret reaction on a BM/Hitachi 747 clinical chemistry analyser and urinary albumin by nephelometry (Dade Behring BN II, Marburg, Germany). Urine was stored frozen at –20°C for up to 2 years. Urinary creatinine, protein and albumin were measured directly prior to sample work up.

Table 3-10. Characteristics of diabetic patients and control subjects.

(+/- SD)	DM (n=51)	Controls (n=42)
Sex (m/f)	27/24	19/23
Age (years)	57 +/- 14	45 +/- 17
Type of DM (I / II)	9/42	none
BMI (kg/m ²)	29.5 +/- 5.5	25.6 +/- 2.7
Duration of DM (years)	10.0 +/- 6.5	0
Diabetic neuropathy (prevalence)	72 % *	none
Diabetic retinopathy (prevalence)	37 % **	none
HbA1c (%)	8.0 +/- 1.8	w.n.l.
Fasting glucose (mg/dl)	172 +/- 73	n.d.
Proteinuria (mg/l)	77 +/- 66	59 +/- 45
Albuminuria (mg/l)	30 +/- 24	n.d.
Serum-creatinine (µmol/l)	79.6 +/- 8.8	70.7 +/- 8.8
<p>*: data on neuropathy were available from 42 patients, **: examination for retinopathy was performed in 43 patients. Data are mean +/- SD. BMI: body mass index; w.n.l.: within normal limits; n.d.: not determined</p>		

3.14.2 Preparation of the urine samples

A volume of urine equivalent to 1 mg creatinine was evaporated to dryness with a Speedvac centrifugal evaporator (Christ, Osterode, Germany). 420 μ l of 12M HCl (>36.5% w/w) and 300 μ l H₂O was added to a final concentration of 7 M HCl. The solution was transferred to vacuum hydrolysis tubes (Wheaton, Milville, NJ, USA), cooled in liquid nitrogen and evacuated after the contents solidified. Samples were hydrolysed at 110 °C for 24 hours under vacuum. The hydrolysate was filtered, evaporated to dryness, resuspended in 1000 μ l redryness solution (H₂O/EtOH/Triethylamine 2:2:1 (v/v/v)) to remove traces of HCl, evaporated to dryness and resuspended in 200 μ l 15 mM NaH₂PO₄, pH 7.2. For analysis of free CML one volume of urine, equivalent to 0.5 mg creatinine, and two volumes of acetonitrile were allowed to stand overnight at 4 °C for precipitation and centrifuged at 4000 rpm for 5 min. The supernatant was evaporated to dryness and resuspended in 100 μ l H₂O.

3.14.3 Sample derivatisation and HPLC analysis

All steps of pre-column derivatisation with OPA were performed with the programmable autosampler Shimadzu SIL-10A (Shimadzu Corp., Kyoto, Japan) using the following protocol: 200 μ l of appropriately diluted sample (1:250 for urine hydrolysates and 1:100 for deproteinised urine) was incubated with 200 μ l buffer 1 (0.2 M Na₃BO₃, 5 mM EDTA, pH 10) and 100 μ l OPA-reagent (50 mg OPA/50 μ l 3-mercaptopropionic acid in 5 ml methanol) for 3 min, stopped with 200 μ l buffer 2 (1 M KH₂PO₄, pH 4.0) and immediately injected for HPLC-analysis (injection volume 10 μ l). HPLC analysis was performed in an air-

conditioned laboratory environment with a room temperature set at 21 °C using a Shimadzu series 10A HPLC device, equipped with a Shimadzu RF-10AXL fluorescence detector (excitation 340 nm, emission 455 nm) and a GROM-SIL 100 ODS-0 AB RP-column (5 µm, 200*4 mm) from Grom (Herrenberg, Germany). Eluents were A: 1 % ACN / 1 % THF and B: 45 % ACN / 5 % THF in 15 mM NaH₂PO₄, pH 7.2. As gradient was used: 0-1.25 % B (0-17 min at 0.4 ml/min), 1.25-100 % B (17-18min at 0.4 ml/min), 100 % B (18-28 min at 0.8 ml/min) and 100 % A (29-39 min at 0.8ml/min).

3.15 Immunohistochemistry and Western-blotting in muscle and nerve tissue

Immunohistochemistry of nerve tissue was performed in cooperation with Dr. M. Haslbeck, Erlangen and Dr. A. Bierhaus, Tuebingen/Heidelberg, as described in [141]. Specimens were obtained from patients with polyneuropathies of various etiologies and of healthy controls. Tissue samples were frozen immediately after biopsy in isopentane and cooled in liquid nitrogen. Segments of the biopsy sample were fixed in cold 4% glutaraldehyde in 0.1 cacodylate buffer at pH 7.4, embedded in epoxy resin, cut for semithin sections and stained with methylene blue. For immunohistochemical staining a specific rabbit anti-CML antiserum was used, characterised by us previously [41; 140]. As shown in **Figure 3-3**, the antiserum showed only little or no crossreactivity with the related compounds lysine, alanine, glycine or fructoselysine. The antiserum was used because of its higher stability compared to the immunopurified antibodies. The bound antibodies were visualised using the alkaline phosphatase anti-alkaline phosphatase (APAAP) immunostaining method as

described earlier [141]. Faint haematoxylin counterstaining was used to reveal cellular structures. Negative controls for the staining specificity of the antiserum were performed with unspecific rabbit immunoglobulin instead of the specific antibody and also after preincubation of the CML antiserum with CML-modified human serum albumin (CML-HSA). For Western blot detection of CML-modified proteins, aliquots of 50 – 100 mg muscle or 10 - 30 mg nerve tissue were frozen in liquid nitrogen and powdered in a liquid nitrogen-cooled vibration mill (Micro-Dismembrator U, Braun Biotech, Melsungen, Germany) using a 3 ml teflon shaking flask at 2000 rpm for 1 min. Powdered tissue was placed in 1.5 ml ice cold buffer (10 mM NaHCO₃ pH 7.0, 0.25 M sucrose, 5 mM NaN₃, freshly added protease inhibitor cocktail (Sigma, P8340) and 100 µM PMSF) and further homogenised in a motor-driven Potter-Elvehjem tissue homogenisator (Potter S, Braun Biotech, Melsungen, Germany) at 1500 rpm for 2 min and 20 ups and downs. The crude homogenates were centrifuged (13000 rpm, 10 min, 4°) and supernatants (10 to 30 µg protein/lane) were taken for Western blot analysis as described above. The protein concentrations of the supernatants were determined with a modified Bradford reaction (Bio-Rad protein assay, Bio-Rad, Munich, Germany) typically resulting in 0.1 mg protein / ml.

3.16 Immunohistochemistry and Western-blotting of CML-modified proteins in cartilage

Immunohistochemistry of cartilage tissue was performed in cooperation with Dr. W. Schwab, Dresden, as described in [142]. Osteochondral specimens were obtained during knee surgery from a patient with osteoarthritis and from a patient with healthy

cartilage. Specimens were fixed in 4% buffered formalin, decalcified for 2 weeks in EDTA solution and embedded in paraffin. Sections were cut (5 μ m) and mounted on silane-coated slides. The sections were dewaxed, washed in phosphate-buffered saline (pH 7.4) and treated with 0.3% hydrogen peroxide for 30 min followed by the incubation with rabbit anti-CML antiserum (dilution 1:2000, Prof. Schleicher, Tuebingen) for 1 h at 37°C. The primary antibody was incubated with a biotinylated anti-rabbit IgG antibody and then detected with a streptavidin/biotin-peroxidase complex (Vectastain Elite; Vector, Burlingame, Calif.; USA). The peroxidase activity was visualised with 3,3'-diaminobenzidine and counterstained with hemalaun. For specific negative controls the primary antibody was replaced with a non-specific rabbit IgG. The specificity of the polyclonal CML antiserum was proofed in preabsorption experiments with CML-human serum albumin. All control sections were completely negative. For Western-blotting, protein extracts were prepared as described above except for prolonging the intervals of the vibration mill to 3 x 1min. The crude homogenates were centrifuged (13000 rpm, 10 min, 4°) and supernatants (10 μ g protein/lane) were taken for Western blot analysis.

3.17 Density gradient preparation of granulocytes

Granulocytes were isolated from buffy coats which were prepared by the blood bank on the same day. Aliquots of 20 ml of buffy coat were carefully layered on a biphasic Histopaque (Sigma, Deisenhofen) density gradient as depicted in **Figure 3-4** and centrifuged for 25 min at 633 g and 18°C without brakes. The granulocytic layer at the 1.077 / 1.119 interface was transferred

into a new 50 ml tube and washed twice by centrifugation (462 x g, 15 min, 15°C). The pellet was resuspended in 5 ml PBS and 45 ml erythrocyte lysis buffer and kept on ice on a shaker for 15 min to lyse contaminating erythrocytes. The erythrocyte lysis buffer was prepared by dissolving 8.29 g of NH_4Cl , 1.00 g of KHCO_3 and 0.037 g of $\text{Na}_2\text{-EDTA}$ in 1000 ml of H_2O . The granulocytic cell suspension was sedimented (340 g, 10 min, 4°C) and washed once by centrifugation in PBS containing 15% FCS. Cell count and identification of granulocytes was performed in a Advia 120 hematology cell counter (Bayer Diagnostics, Fernwald). Automatic classification of leukocyte subclasses by the hematology system using flow cytometry and myeloperoxidase activity revealed that the cell preparation contained >95% granulocytes (not shown).

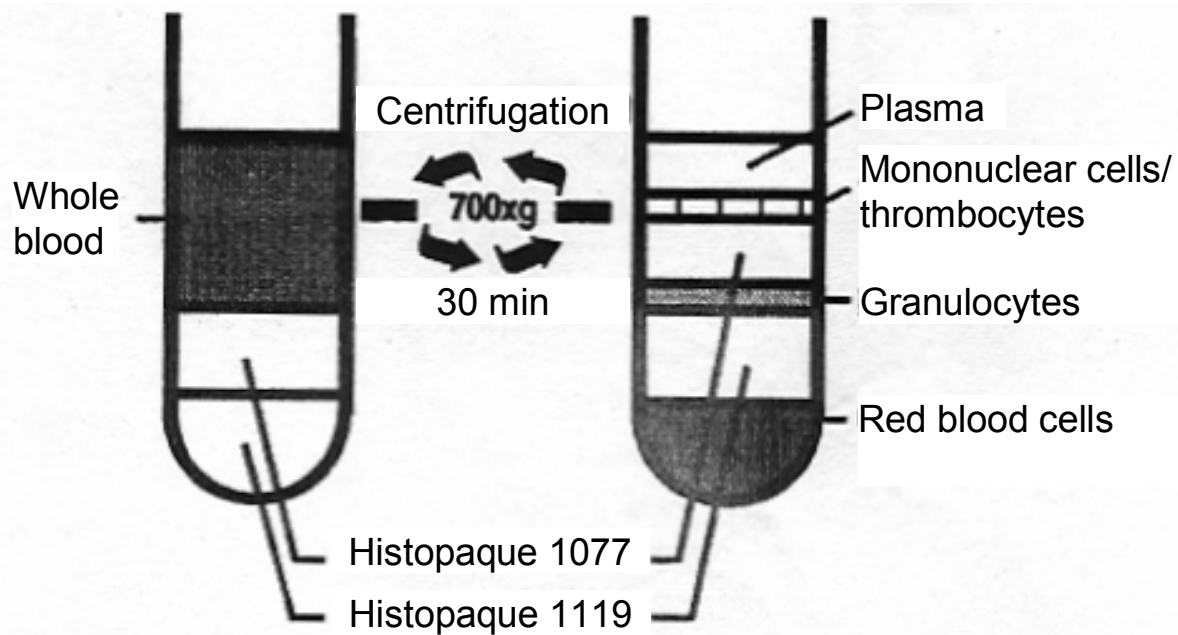


Figure 3-4. Ex vivo isolation of granulocytes: buffy coats were separated by density centrifugation using a biphasic Hyperpaque gradient.

3.18 Preparation of leukocyte subclasses

Sedimented blood cells from a freshly drawn 3 ml EDTA blood sample were washed twice with 10 ml of PBS containing 0.6 % sodium citrate and 2 % FCS by centrifugation (4000 rpm, 3 min, 4⁰C). The washed blood cells were resuspended in 5 ml of PBS containing 0.6 % sodium citrate and 2 % FCS and the sequential isolation of leukocyte subclasses was performed according to the instructions of the manufacturer. The work-flow is depicted in

Figure 3-5.

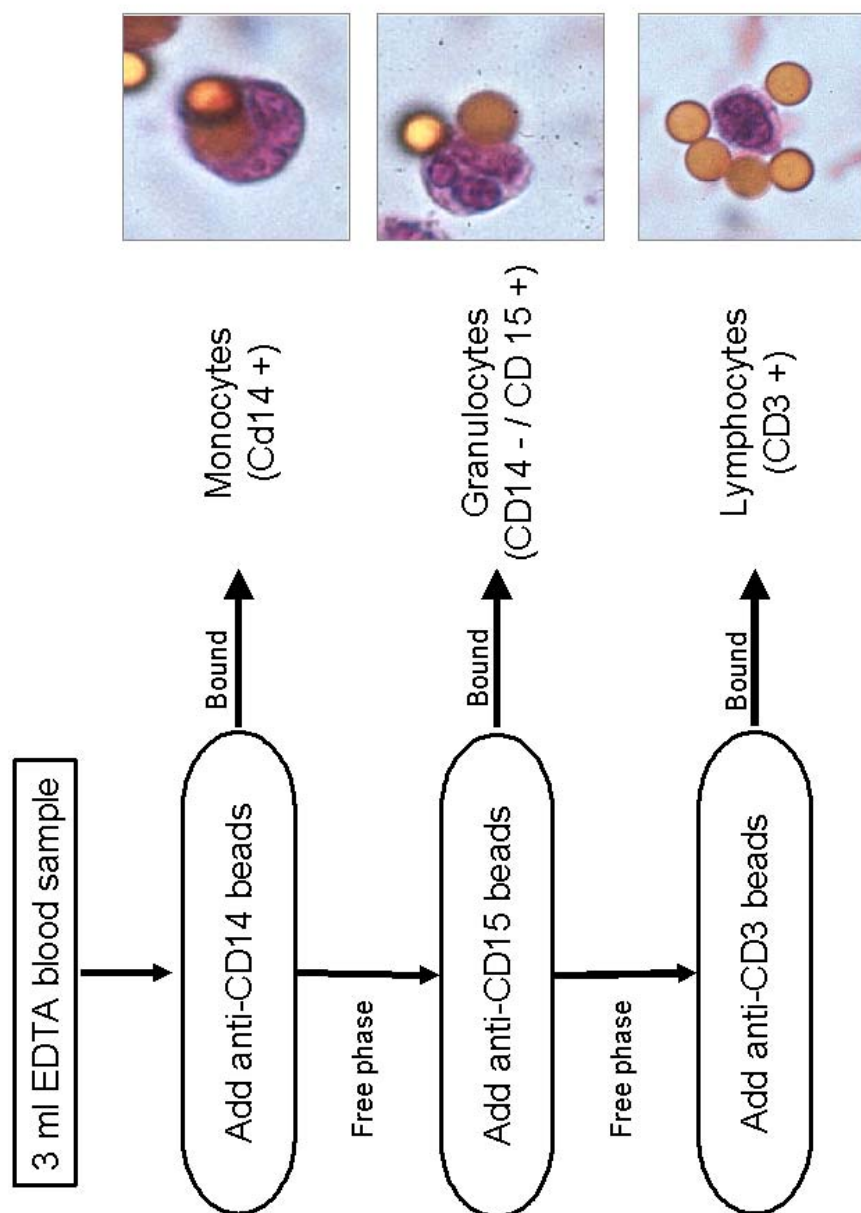


Figure 3-5. Preparation of leukocyte subclasses: leukocytes from 3 ml blood samples were sequentially extracted by the appropriate CD specific antibody-coated magnetic beads. The bound cell fraction was washed and lysed for subsequent Western-blotting.

All steps were performed at 4°C or on ice. Resuspended cells were incubated for 15 min on a rotary wheel with 40 µl of magnetic beads coated with an antibody specific for the appropriate CD-class and then separated by a magnet. The bound fraction of cells was washed twice in PBS/0.6% citrate/2% FCS and four times in PBS/0.6% citrate and a smear was prepared from an aliquot for microscopic examination. Cell lysates were prepared with 100 µl of lysis buffer and an equivalent

of 10µg protein was denatured in Lämmli's buffer for subsequent Western blot analysis. Purity of the leukocyte fractions, as evaluated by microscopic examination, was found to be > 90 % for monocytes, > 80 % for granulocytes and > 95 % for lymphocytes.

3.19 Luminol and lucigenin chemiluminescence assay for granulocytes

The generation of myeloperoxidase-derived hypochlorite anions was measured as luminol chemiluminescence and the generation of NADPH oxidase-derived superoxide anions was measured as lucigenin chemiluminescence on a Tropix chemiluminescence plate reader with a programmable 2 channel reagent dispenser (Applied Biosystems, Foster City, USA) according to the method of Dr. Bruchelt, Tuebingen [143]. Granulocytes were freshly prepared from buffy coats by density gradient centrifugation. 250000 cells/well were suspended in 200 µl Hank's buffer on a 96-well plate and stimulated by 25 µl of a 15 mg/ml solution of opsonised zymosan (final conc. 1.5 mg/ml). The plate was inserted immediately and the chemiluminescence reaction was started by pipetting 25 µl of a 500 µM luminol or lucigenin solution, respectively, through the programmable reagent channel P of the plate reader. The chemiluminescence signal was recorded and integrated over 15 min.

3.20 Lucigenin chemiluminescence assay for cell culture cells

The measurement of lucigenin chemiluminescence is used as a measure of cellular superoxide anion production and NADPH oxidase activity [144-147]. The mechanism of superoxide anion-

induced chemiluminescence is shown in **Figure 3-6**. In the present study, the measurement of cellular superoxide anion production was performed as described by Griendling et al. [144] with modifications. A lower concentration of lucigenin (50 μ M) has been used. This has been recommended by Munzel et al. [146] to prevent the problem of unspecific redox cycling [148; 149]. For chemiluminescence measurement a Tropic chemiluminescence plate reader set at 37⁰C with a programmable 2 channel reagent dispenser was used.

For measurement of cell suspensions, cells were counted using an Advia 120 automated cell counter, and cell suspensions were diluted to a concentration of 5 x 10⁶/ml and kept on ice. 50 μ l equivalent to 250000 cells were used for each test. The reaction mixture was pipetted in the order given in **Table 3-11**.

Table 3-11. Pipetting scheme for the lucigenin chemiluminescence assay.

		Final amounts
415 μ l	Reaction buffer	
25 μ l	Lucigenin 1mM	50 μ M
10 μ l	NADPH 10mM	200 μ M
50 μ l	Cell suspension /homogenate	250000 cells
Total: 500 μ l		

Measurements were performed in triplicates: 3 x 100 μ l of the reaction mixture were pipetted in 96-plate wells, the plate was inserted in the reader, and the reaction was started by dispensing 25 μ l of a 100 nM solution (final conc. 20 nM) and chemiluminescence was integrated over 15 min.

For measurements of cell homogenates, cells were counted and cell pellets equal to approx. 2×10^6 cells were washed and lysed using the lysis buffer given below. The volume of lysis buffer was calculated and added at a ratio of 100 μ l per 0.5×10^6 cells.

In experiments, where the effects of inhibitors or stimuli on superoxide anion production was tested, cell suspensions or homogenates were preincubated with the indicated substances for 20 min before the samples were pipetted to the reaction mixture.

Composition of the lucigenin chemiluminescence reaction buffer (modified from [144]):

50 mM	sodium phosphate, pH 7.0
1 mM	EGTA
150 mM	sucrose

Composition of the cell lysis buffer for the lucigenin chemiluminescence assay (modified from [144]):

20 mM	potassium phosphate, Ph 7.0
1 mM	EGTA
0.5 mM	PMSF
14 μ g/ml	Aprotinin
20 μ l/ 2×10^6 cells	Mammalian protease inhibitor cocktail (Sigma P8340)

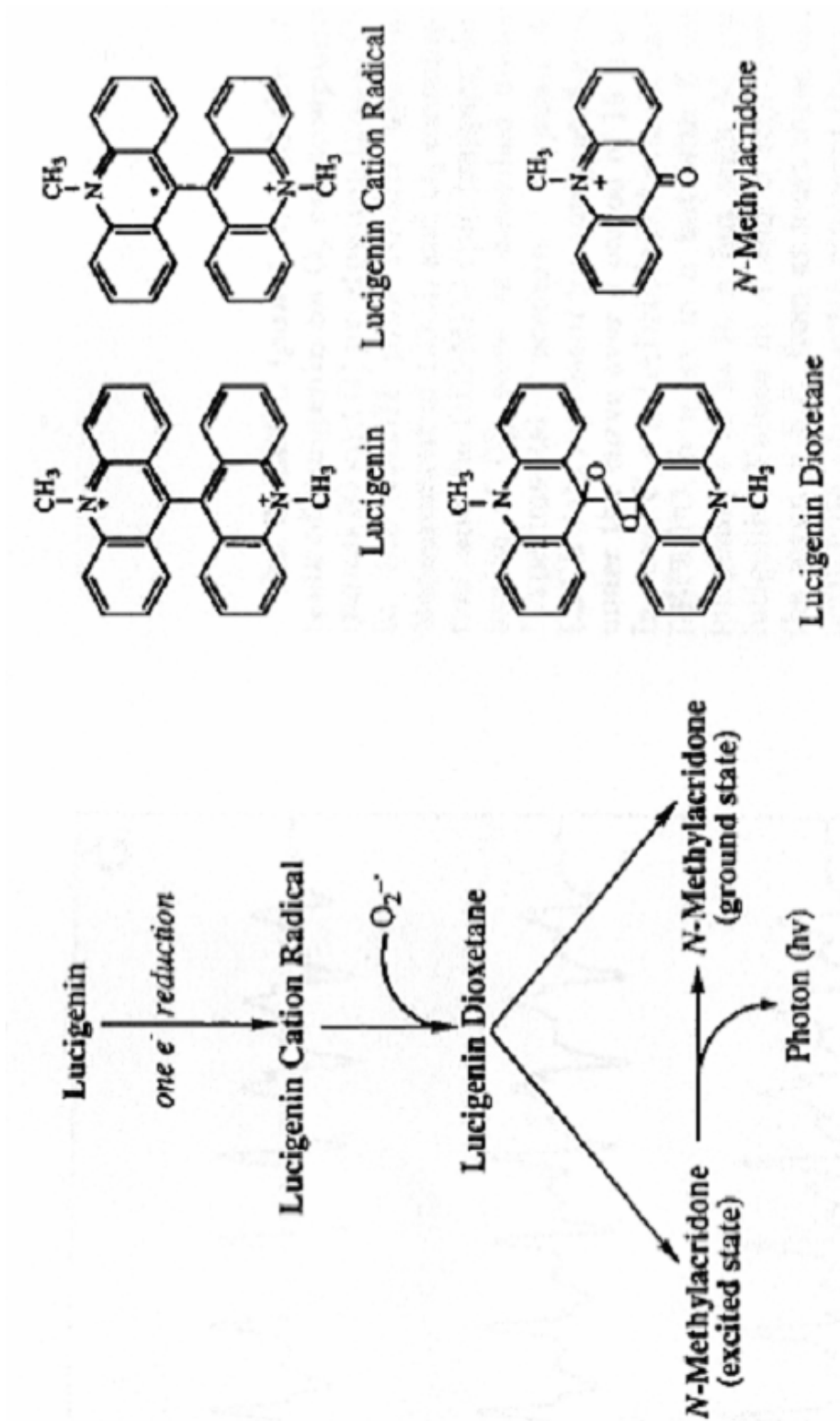


Figure 3-6. Lucigenin chemiluminescence. Schematic illustration of the reaction leading to lucigenin-derived chemiluminescence by superoxide anions (taken from [147]).

3.21 Statistical analysis

The unpaired Student's-t-test (two-sided) was used to compare mean values among the different groups and linear regression analysis was used to assess correlations. All data are shown as the mean +/- SD, unless otherwise specified.

4 RESULTS

4.1 Chemical carboxymethylation of model proteins and characterisation of the used anti-CML antibodies

Figure 4-1 and **Figure 4-2** show the anti-CML Western blots of HSA, BSA, ferritin and hemoglobin which were chemically carboxymethylated *in vitro* using glyoxylic acid as the C2 precursor. The CML content of the products was determined by ASA using a cation exchange amino acid analyser with ninhydrin post-column derivatisation (**Figure 4-3** and **Figure 4-4**). For peak identification and quantification synthetic CML was used as a standard. As shown for HSA, carboxymethylation proceeded rapidly and after 4 h approx. 33 % of all lysine residues and after 24 h more than 50 % of all lysine residues were modified (**Figure 4-3** and **Figure 4-4**).

These CML-modified proteins were used to estimate and compare the sensitivity of the CML-antibodies used in this study (**Figure 4-5**). The commercially-obtained monoclonal anti-CML antibody CMS10, (Trangenics, Kumamoto, Japan) did not show any reaction (data not shown), be it in Western-blotting or IHC. The other antibodies (polyclon. anti-CML antiserum (rabbit); mab 4G9 (Roche); mab 2F8 (NovoNordisk, Bagsvaerd, Denmark); mab NF1G (Transgenics, Kumamoto, Japan)) were shown to be highly sensitive with a detection limit down to an amount of 1 ng of CML-protein which equals 0.5 to 1.0 pmoles of CML residues, depending on the protein used. The calculation e.g. for highly modified CML-HSA (H-CML-HSA) reads as follows: the detection limit is 1 ng of H-CML-HSA. (**Figure 4-5**). 1 ng of HSA (MW 66.5 kDa) equals 15 fmol of HSA. HSA contains 59 mol lysine residues

/ mol HSA. In H-CML-HSA, 51% of its lysine residues are carboxymethylated (**Figure 4-3**). Therefore, 1 ng of H-CML-HSA contains: $15 \text{ fmol} \times 59 \times 0.51 = 442.5 \text{ fmol}$ CM-lysine which equals approx. 0.5 pmol CM lysine.

The antibodies were specific for AGE-modified proteins and did not crossreact with non-carboxymethylated control proteins up to amounts as high as 0.015 μ g of control protein. Monomeric CML was recognised only by the monoclonal antibody 4G9 at very high amounts (250 ng or 1.25 nmol on dot blot), but did not react with the other CML antibodies at these quantities on dot blots (data not shown). Epitope recognition of the CML modification was independent from the protein environment since it was equal in different proteins. Therefore the antibodies truly represent modification-specific antibodies and are not directed against the protein compound.

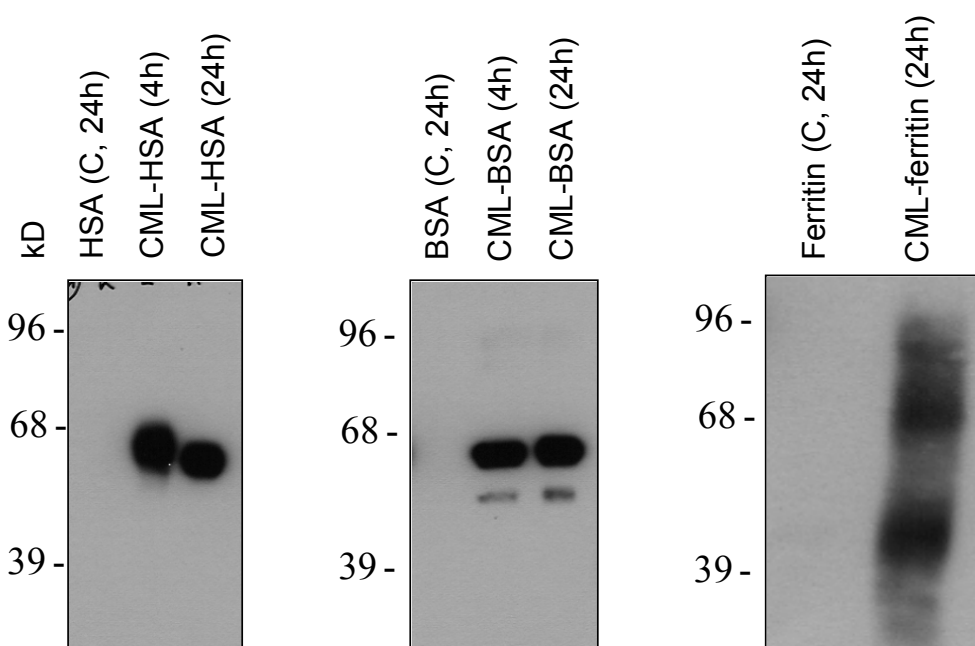


Figure 4-1. Western blot analysis of *in vitro* carboxymethylated human serum albumin (CML-HSA), bovine serum albumin (CML-BSA) and cationised ferritin (CML-ferritin). The proteins were incubated with an equimolar amount of glyoxylic acid and a 3-fold molar excess of NaBH_3CN in 0.2 M sodium phosphate buffer at pH 7.8 and 37°C for 4 and 24 h, respectively. As controls, the proteins were incubated for 24 h without glyoxylic acid. 0.1 μg protein per lane was loaded on a 7.5 % polyacrylamide gel, separated by SDS-PAGE, transferred onto a nitrocellulose membrane and immunoblotted against a specific rabbit anti-CML antiserum (Prof. Schleicher, Tuebingen, dilution 1:8000). The CML-modified proteins were visualised by enhanced chemiluminescence (ECL). Conditions: secondary antibody: anti-rabbit-IgG-HRP conjugate; dilution 1:3000; exposure 3 min). Abbreviations: kD: kilo Dalton; CML: carboxymethyllysine

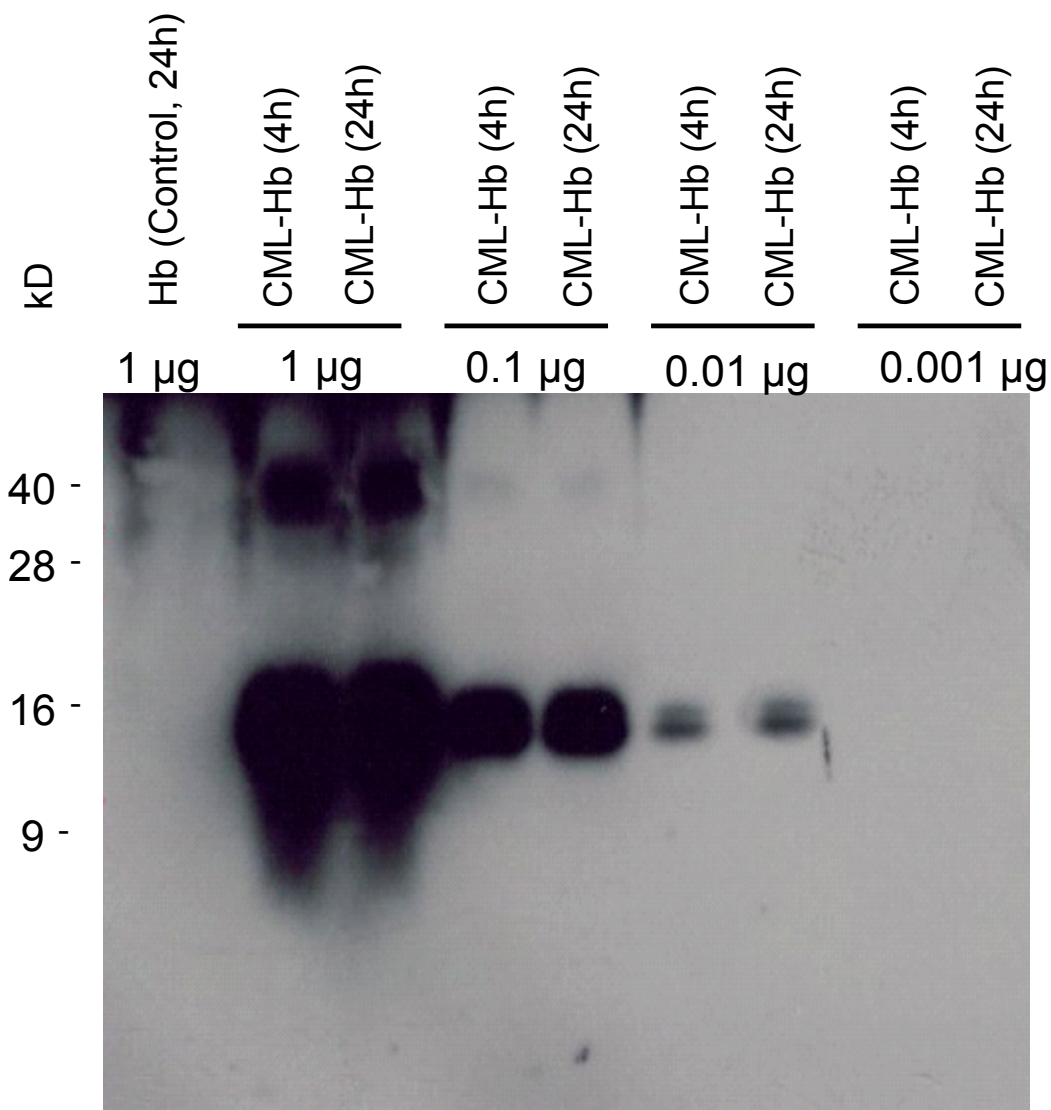


Figure 4-2. Semiquantitative Western blot analysis of in vitro carboxymethylated hemoglobin (CML-Hb). Purified HbA was incubated with an equimolar amount of glyoxylic acid and a 3-fold molar excess of NaBH_3CN in 0.2 M sodium phosphate buffer at pH 7.8 and 37°C for 4 and 24 h, respectively. As control, the protein was incubated for 24 h without glyoxylic acid. The carboxymethylation was verified by SDS-PAGE of 0.001 to 1 μg protein/lane on a 15 % polyacrylamide gel using a specific rabbit anti-CML antiserum (Prof. Schleicher, Tuebingen, dilution 1:8000). The carboxymethylated proteins were visualised by enhanced chemiluminescence (ECL). Conditions: secondary antibody: anti-rabbit-IgG-HRP conjugate, dilution 1:3000; exposure 3 min. Abbreviations: kD: kilo Dalton; CML: carboxymethyllysine.

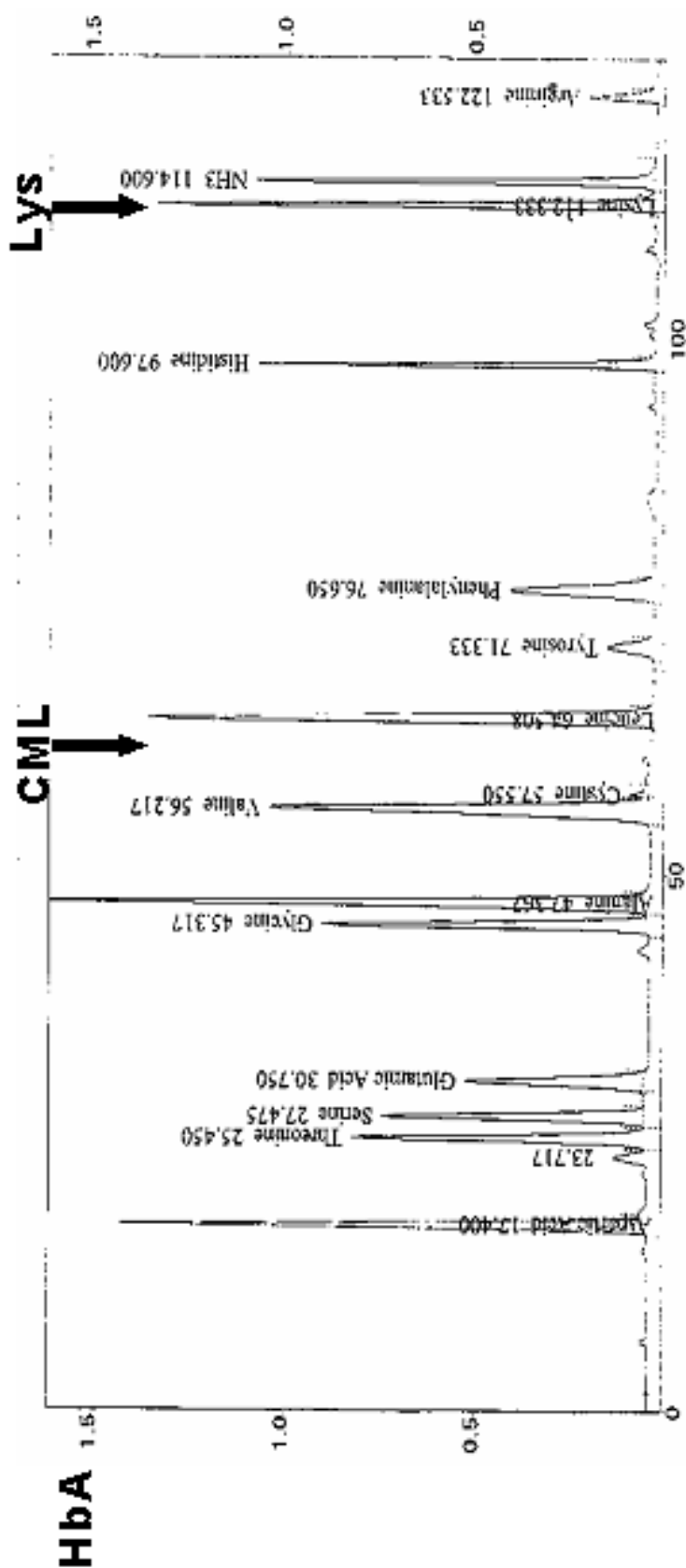


Figure 4-3. Determination of the CML-content of unmodified and CML-modified hemoglobin by amino acid analysis. 1 mg of hemoglobin A was incubated without (unmodified HbA, upper chromatogram) or with (CML-HbA, lower chromatogram) an equimolar amount of glyoxylic acid and a 3-fold molar excess of NaBH_3CN at 37°C for 24h. The samples were hydrolysed (7 M HCl, 110°C , 24 h). The lyophilised hydrolysates were diluted to 0.5 mg/ml and analysed on an Eppendorf/Biotronic LC 3000 amino acid analyser (Eppendorf, Hamburg, Germany). For external calibration, the Benson amino acid standard P with additional CML at a concentration of 100 nmol/ml was used. (cont.)

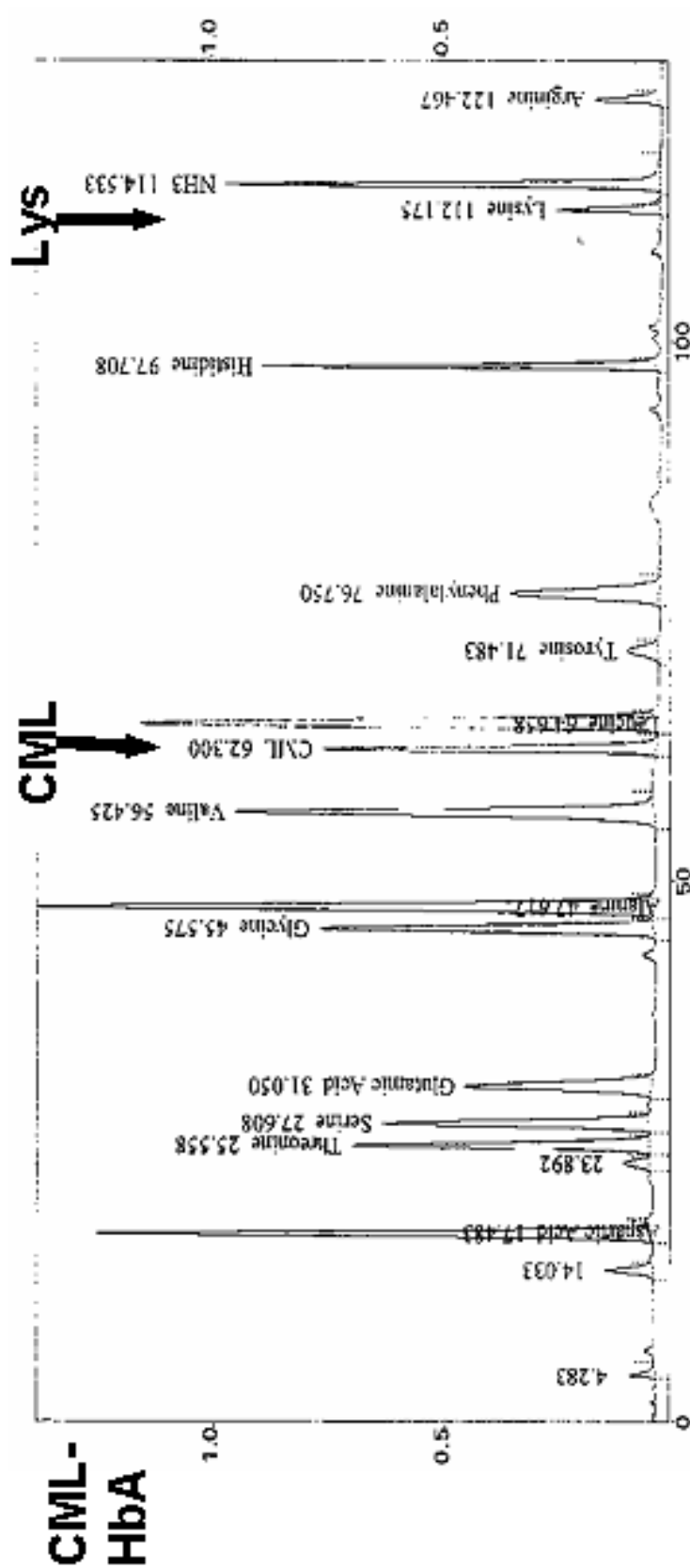


Figure 4-3 (cont.). Conditions: Eppendorf cation exchange resin, column 125 x 4 mm, 20 μ l injection volume, gradient and Eppendorf ready-to-use buffer set P for physiological samples, ninhydrin post column derivatisation, 125 $^{\circ}$ C, detection 570nm. The peak for lysine (Lys) and carboxymethyllysine (CML) was identified by coelution with standards at 112.1 and 62.3 min, respectively. In unmodified HbA, CML was below the detection limit. In CML-HbA, 76% of the total lysine residues were carboxymethylated after 24 h which is equivalent to 33.6 mol CML / mol HbA (α 2 β 2 tetramer).

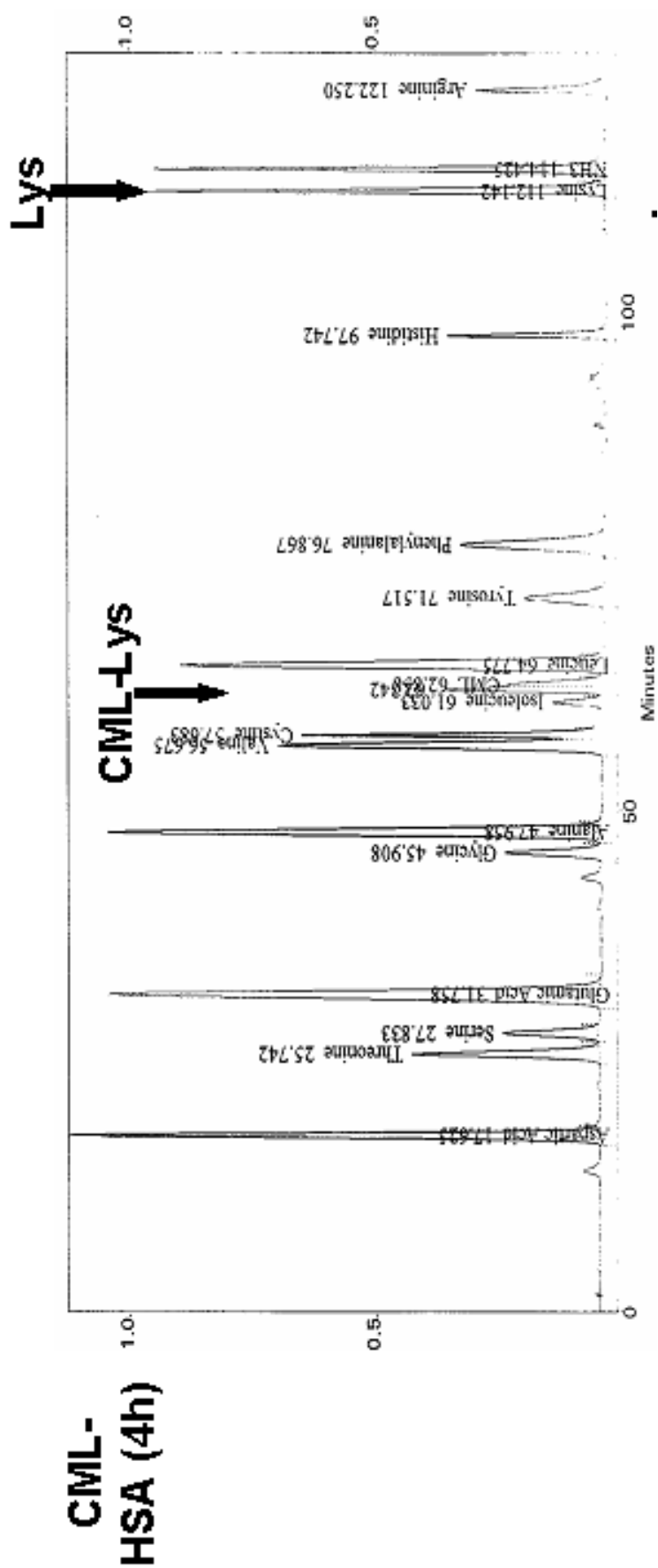


Figure 4-4. Amino acid analysis of CML-modified human serum albumin (CML-HSA). For each analysis, 1 mg of HSA was carboxymethylated *in vitro* for 4 h (low-modified CML-HSA, upper trace) or for 24 h (high-modified CML-HSA, lower trace) and subjected to an amino acid analysis as described in **Figure 4-3**. (cont.).

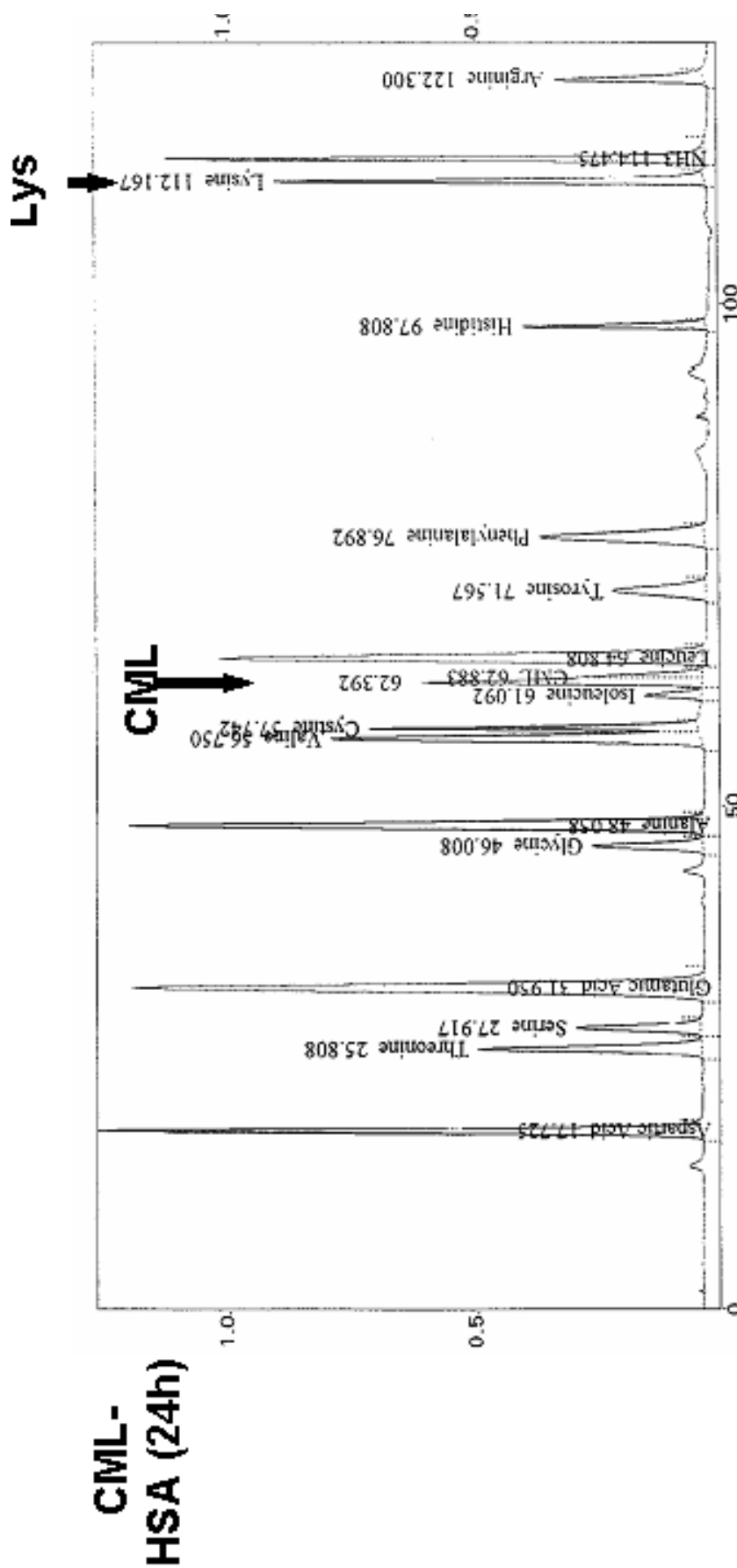


Figure 4-4 (cont.). In low-modified CML-HSA (4 h) approx. 33 % of the total lysine residues (equivalent to 19.5 mol CML / mol HSA) and in high-modified CML-HSA (24 h) approx. 51 % of the total lysine residues (equivalent to 30.1 mol CML / mol HSA) were carboxymethylated. Abbreviations: Lys: lysine; CML: carboxymethyllysine.

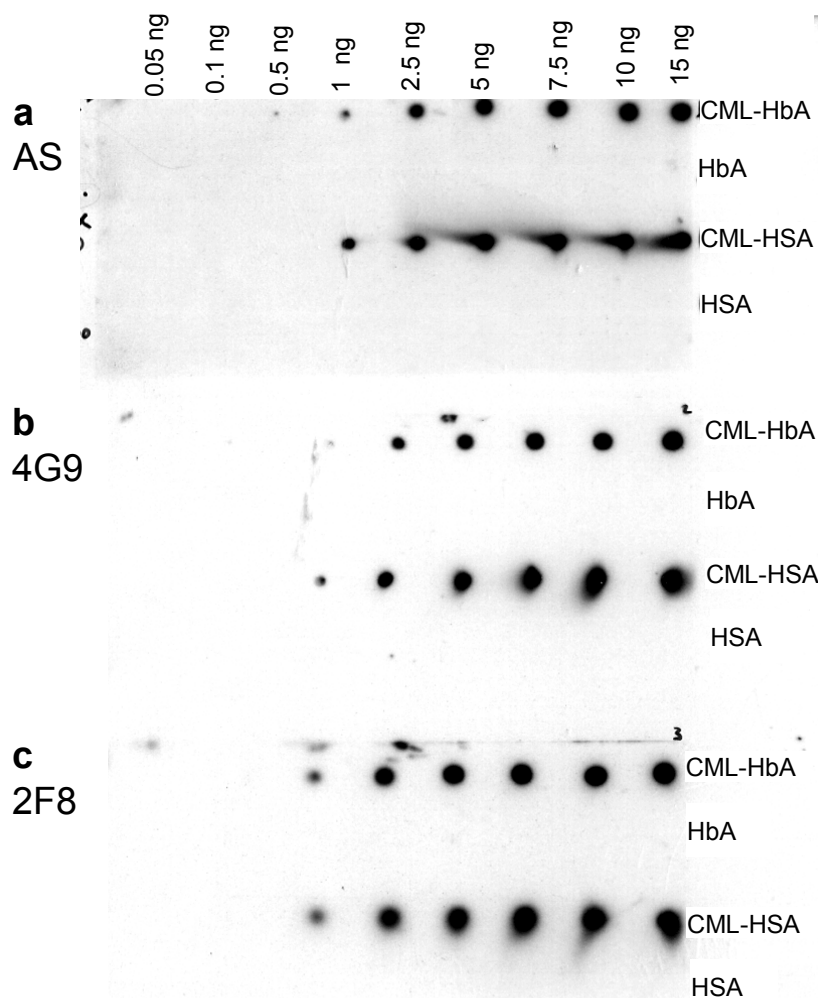


Figure 4-5. Sensitivity and specificity of the anti-CML antibodies used in the present study. Serial dilutions of unmodified (no CML detectable) and CML-modified Hb (33.6 mol CML / mol Hb) and unmodified (no CML detectable) and CML-modified HSA (30.1 mol CML / mol HSA) were probed against a specific CML-antiserum (AS) and two monoclonal anti-CML antibodies (4G9, 2F8) as indicated. The antiserum and the monoclonal antibodies 4G9 and 2F8 were highly sensitive with a detection limit of approx. 1 ng CML-modified protein per dot (equaling 0.5 to 1.0 pmol of carboxymethylated lysine residues) and were used for subsequent studies. Conditions (prim. antibody/sec. antibody): **a:** rabbit anti-CML antiserum 1:8000 (Prof. Schleicher, Tuebingen, Germany) / anti-rabbit-IgG-HRP conjugate 1:2000; **b:** mouse monoclonal anti-CML 4G9 1:500 (Roche, Penzberg, Germany) / anti-mouse-IgG-HRP conjugate 1:3000; **c:** mouse monoclonal anti-CML 2F8 (NovoNordisk, Bagsvaerd, Denmark) 1:5000 / anti-mouse-IgG-HRP conjugate 1:3000; ECL detection; exposure 1 sec.

4.2 CML excretion is increased in urine in diabetic subjects and CML formation can be demonstrated *in vivo* in tissues and in circulating leukocytes

4.2.1 Increased *in vivo* formation and excretion of protein-bound CML in diabetic subjects

4.2.1.1 Validation of the HPLC method

Upon variation of the gradient using various columns, filled with modified C18 reverse phase materials, conditions for base line separation of CML in hydrolysed and in deproteinised urine were elaborated as described in methods. **Figure 4-6** shows chromatograms of an urine sample after acid hydrolysis (**A/B**) and of an urine sample after acetonitrile precipitation (**C/D**) of a representative diabetic patient. CML eluted at RT 8.7 – 9.1 min (**Figure 4-6, A/C**) and peak identity was confirmed by the coelution of an added CML standard (**Figure 4-6, B/D**). Throughout all samples, the CML peak was found to be narrow and fully baseline-separated from the chemically-related homolog carboxyethyllysine CEL (RT 10.5 min; **Figure 4-6 B**). Using other columns (GromSIL ODS-3 CP, GromSIL ODS-4 HE, GromSIL ODS 5-ST, GromSIL OPA3, all from Grom, Herrenberg, Germany), CML could not be fully separated neither from the preceding peak (caused by the abundant physiological amino acid serine) nor from CEL. For six-point calibration, standard solutions from 0.05 to 1.5 $\mu\text{mol/l}$ (corresponding to 0.14 - 4.26 pmol) were prepared from a CML standard in H_2O . 200 μl of each standard concentration was derivatised and analysed in triplicates. Linearity of the standard calibration curve was verified in a range from 0.14 pmol to 4.26 pmol CML. The calibration line was: $\text{CML (pmol)} = 0.009 + 0.318 \times \text{area} (10^6 \text{ au}); (R=0.994)$. For

validation of the analytical procedure, a processed patient sample was diluted (1:250 for hydrolysed urine and 1:100 for deproteinized urine), spiked with 0.1 or 0.5 $\mu\text{mol/l}$ CML standard (corresponding to 0.28 and 1.4 pmol CML), aliquotted, and measured in eighthfold replicates. The peak areas were calculated from measurements of unspiked and spiked sample pairs. The coefficient of variation (CV) for the peak area was 5.1 % (in series) and 7.5 % (from day to day) for the calibration level of 0.28 pmol CML on column and 2.17 % (in series) and 6.7 % (from day to day) for the calibration level of 1.4 pmol CML on column. Recovery of CML during acid hydrolysis was 90-95 %. The detection limit of the method was 0.07 pmol CML on column (signal/noise = 4).

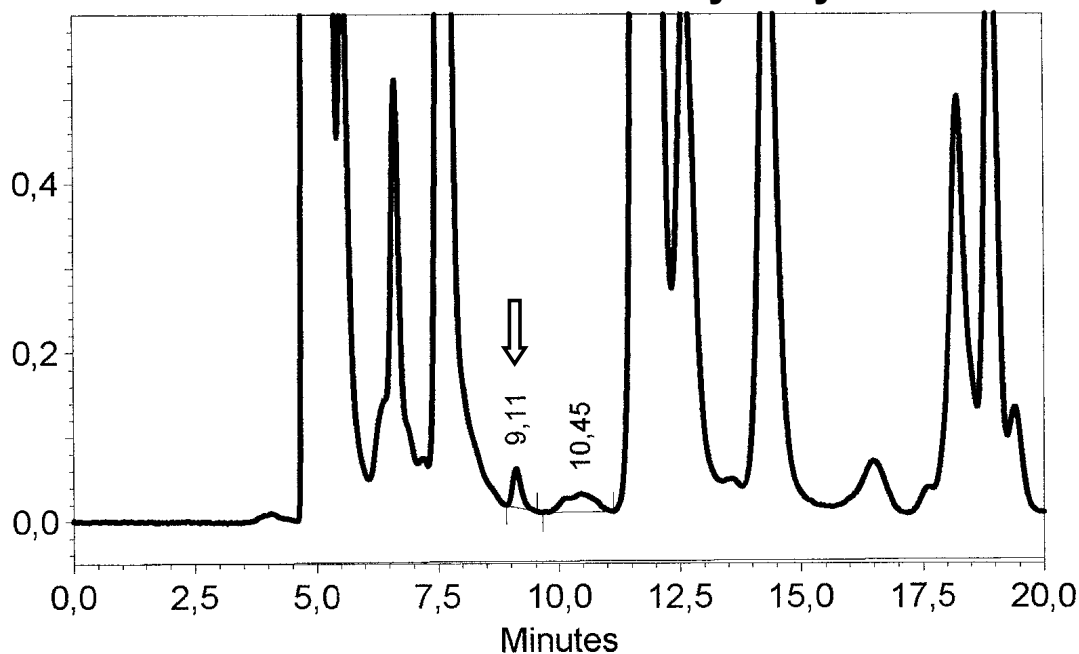
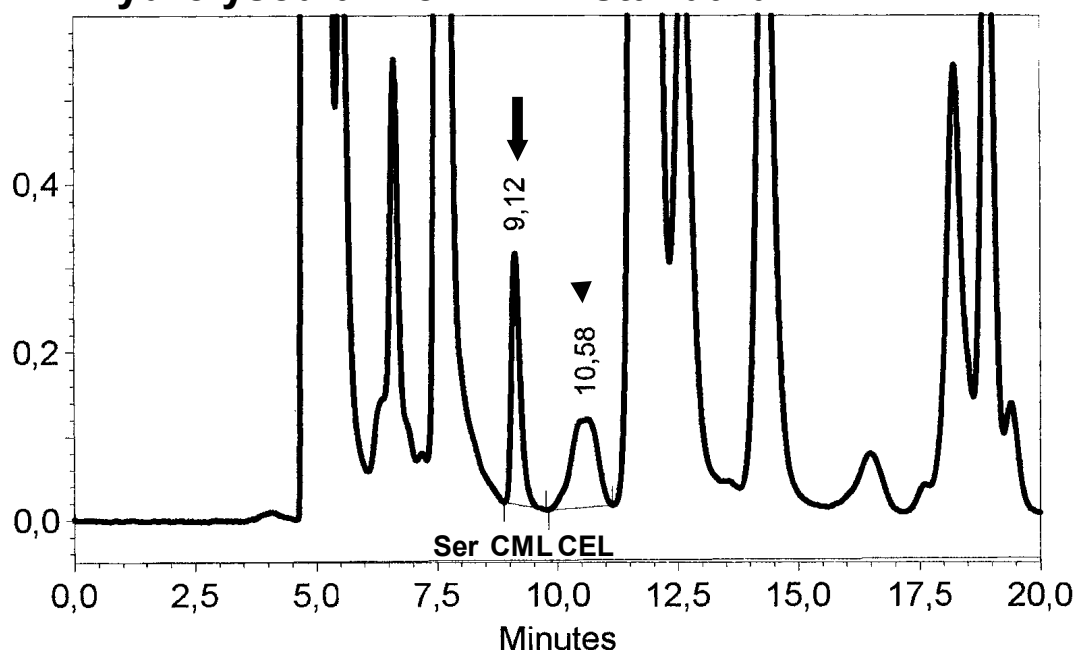
A: Determination of total CML in hydrolysed urine**B: Hydrolysed urine + CML standard**

Figure 4-6. Determination of urinary total and free carboxymethyllysine (CML) in a representative diabetic patient. Urine samples were either hydrolysed (7M HCl, 110^oC, 24 h) and diluted 1:250 (A/B) or deproteinised by precipitation with acetonitrile and diluted 1:100 (C/D) for subsequent derivatisation with o-phthaldialdehyde (OPA). OPA-derivates were analysed by RP-HPLC and fluorescence detection (340nm/455nm). In B and D, diluted samples were spiked with 0.5 $\mu\text{mol/l}$ CML standard (filled arrows) corresponding to 1.4 pmol CML on column (cont.).

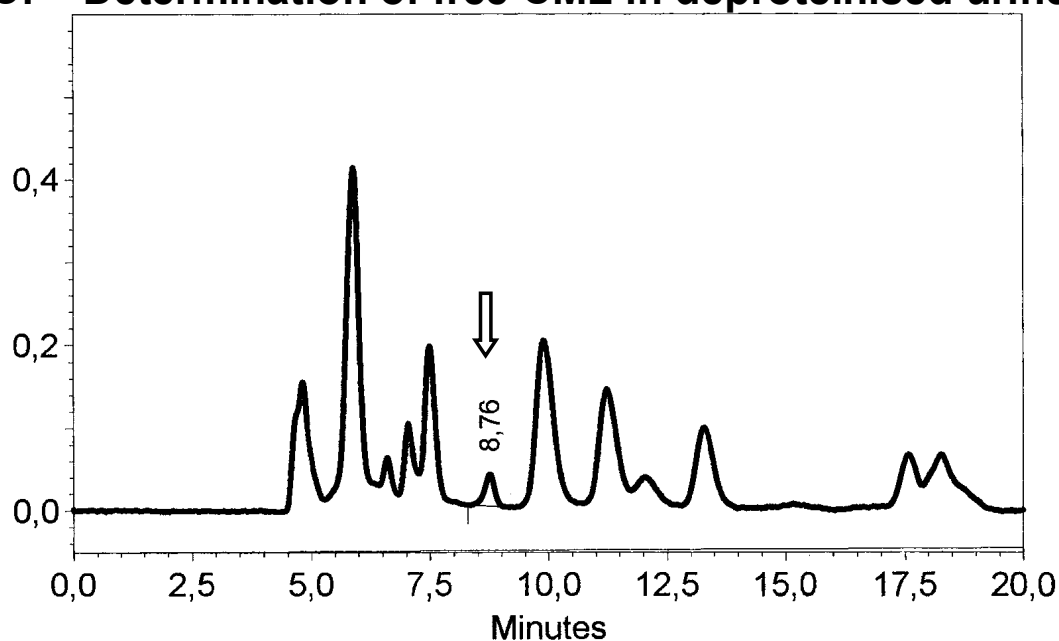
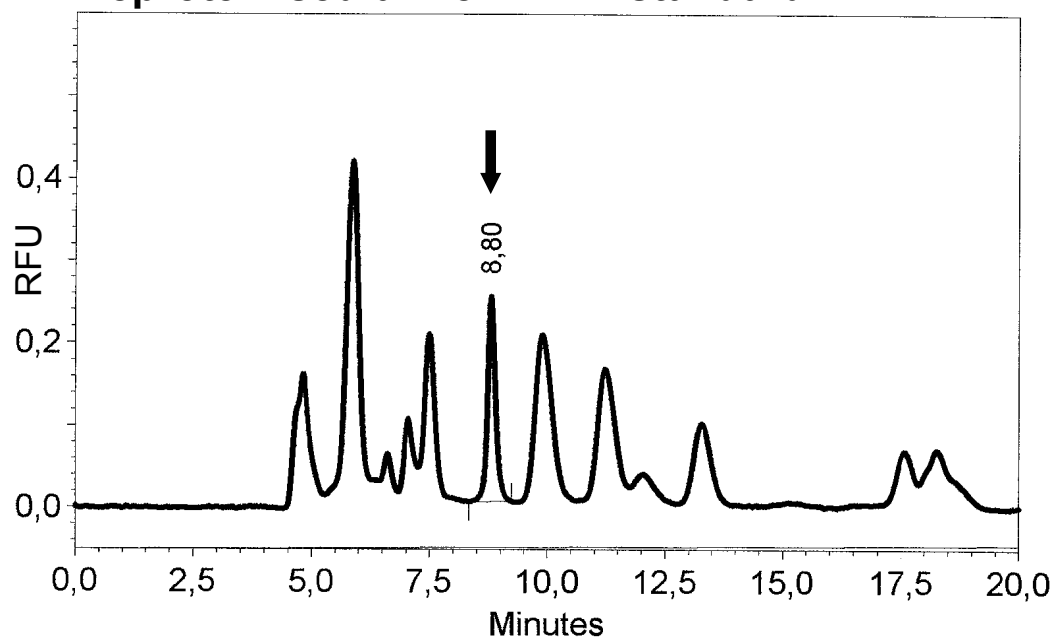
C: Determination of free CML in deproteinised urine**D: Deproteinised urine + CML standard**

Figure 4-6 (cont.). Endogenous CML was identified at RT 8.7 – 9.1 min (A/B; open arrows) by coelution. CML was fully baseline separated from its homolog carboxyethyllysine (CEL) and from serine (Ser) as demonstrated in B, where also CEL was added (arrowhead; 1.4 pmol on column) for peak identification. Conditions RP-HPLC: injection 10µl, column GROM-SIL ODS-0 AB C18, 5 µm, 200x4 mm, eluent A: 1% ACN / 1% TFA, eluent B: 45% ACN / 5% TFA in 15 mM NaH₂PO₄, pH 7.2; gradient: 0-1.25% B (0-17 min), 1.25-100% B (17-18 min), 100% B (18-20), flow 0.4 ml/min).

4.2.1.2 Urinary CML excretion in diabetic and non-diabetic subjects

In **Figure 4-7**, the urinary excretion of total and free CML of 51 diabetic patients (DM) is compared to 42 non-diabetic controls (C). In diabetic patients, the excretion of total CML is increased by about 30 % (DM: 0.58 +/- 0.21; C: 0.45 +/- 0.14 $\mu\text{mol}/\text{mmol}$ creatinine ; $p < 0.001$). Urinary excretion of free CML was not statistically different between both groups, although it tended to be higher in diabetic patients (DM: 0.22 +/- 0.15 versus C: 0.18 +/- 0.13 $\mu\text{mol}/\text{mmol}$ creatinine; ns). To assess the peptide- and protein-bound fraction of CML, the difference between total and free CML was calculated. 'Bound CML' contained about 60 % of total CML and consisted of protein- and peptide-bound CML which has not been precipitated. Patients with diabetes had a significantly higher excretion of bound CML compared to controls (DM: 0.36 +/- 0.17; C: 0.27 +/- 0.14; $P < 0.05$). As shown in **Figure 4-8** the calculated fraction of bound CML correlates significantly with urinary protein excretion ($R = 0.46$, $p < 0.001$) and with albumin excretion ($R = 0.73$, $p < 0.001$), whereas the correlation of total CML excretion with protein excretion ($R = 0.28$, $p = 0.047$) and albumin excretion ($R = 0.29$, $p = 0.037$) was at the border of significance (data not shown). Excretion of free CML did not correlate with protein or albumin excretion. Neither total nor free nor bound CML did correlate with age, duration of DM or HbA1c. The urinary CML excretion in subgroups with diabetic neuropathy or retinopathy did not differ from the total group of diabetic patients (data not shown). Since previous reports have shown that CML formation in certain tissues such as skin, vertebral discs or eye lens collagen is increased with age [42; 43;

150], the urinary free and total CML excretion in 19 young healthy subjects (30 +/- 6 years) was compared to 23 older subjects (59 +/-11 years) who were age matched to the study group of diabetic patients. Urinary excretion of total CML did not differ in both groups (0.45 +/- 0.09 vs. 0.44 +/- 0.17 $\mu\text{mol}/\text{mmol}$ crea; ns). Urinary excretion of free CML was found to be lower in young controls (0.12 +/- 0.10 vs. 0.23 +/- 0.15 $\mu\text{mol}/\text{mmol}$ crea; $p < 0.01$) compared to old controls.

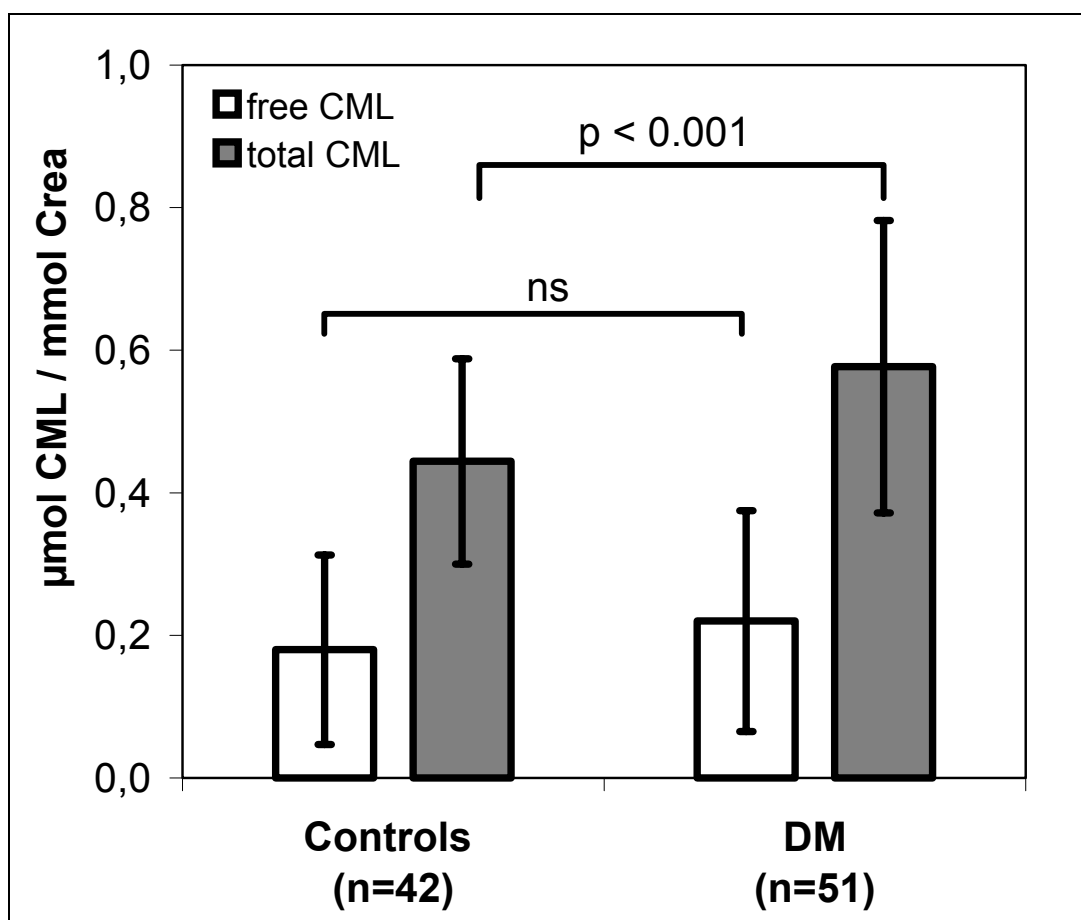


Figure 4-7. Comparison of urinary free (open bars) and total (filled bars) CML excretion in non-diabetic and diabetic subjects. Average values for free CML in controls versus diabetic subjects were 0.18 +/- 0.13 and 0.22 +/- 0.15 $\mu\text{mol}/\text{mmol}$ creatinine, respectively (ns). Average values for total CML in controls versus diabetic subjects were 0.45 +/- 0.14 and 0.58 +/- 0.21 $\mu\text{mol}/\text{mmol}$ creatinine, respectively ($p < 0.001$). (all values +/- SD; ns = non significant, DM = diabetes mellitus).

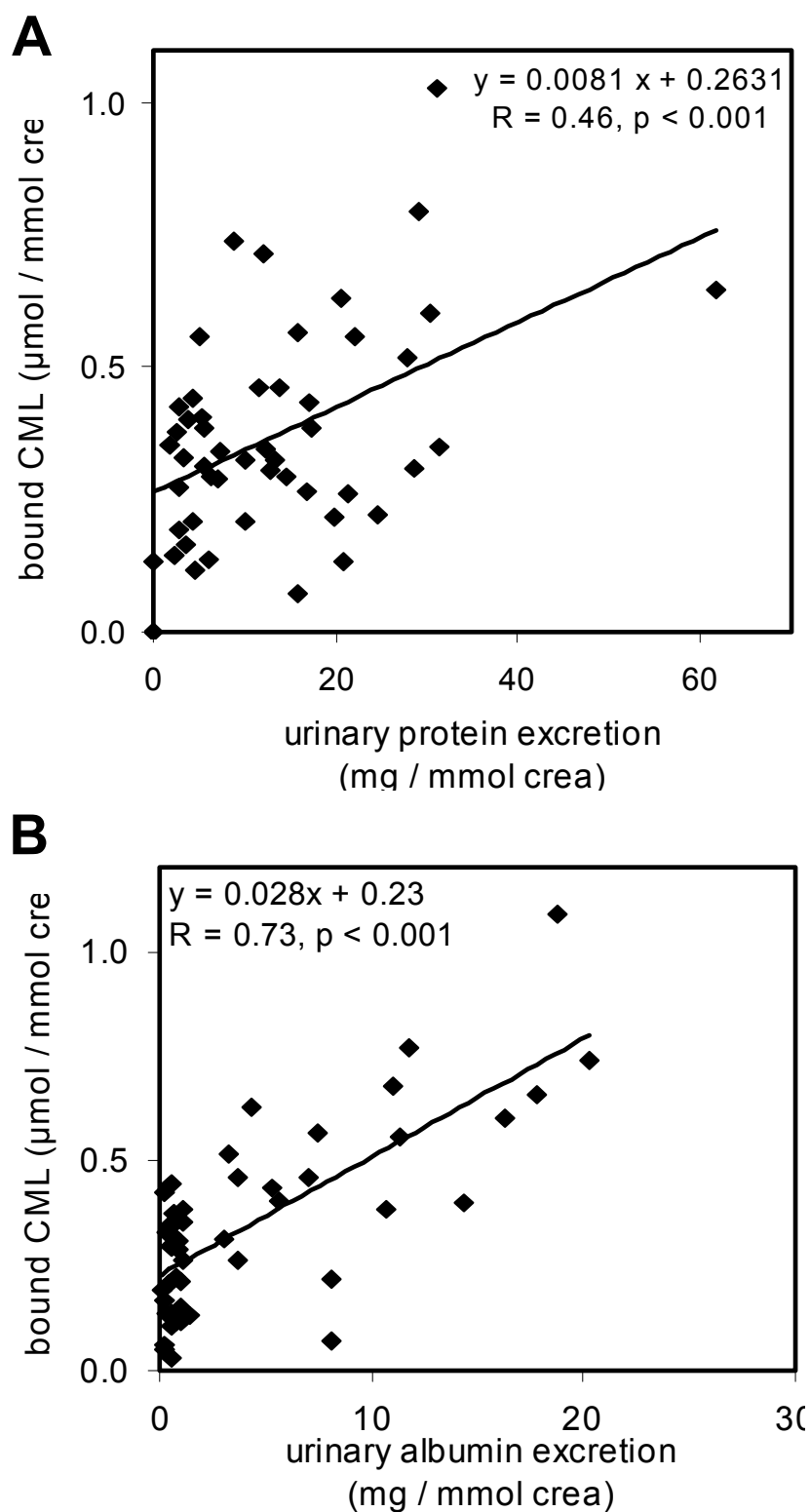


Figure 4-8. Correlation between the excretion of peptide- and protein-bound CML and the excretion of protein (A) and albumin (B) in the urine of 51 diabetic patients. The fraction of bound CML was calculated from the difference of total CML (measured in acid hydrolysates of urine) and free CML (measured in deproteinised urine samples).

4.2.2 Demonstration of increased *in vivo* accumulation of CML in nerve, muscle and vascular tissues in diabetes mellitus and in chronic inflammatory and chronic degenerative diseases

4.2.2.1 CML in noninflammatory and inflammatory peripheral polyneuropathies

In cooperation with M. Haslbeck, Erlangen and A. Bierhaus, Heidelberg/Tuebingen, the histological localisation of CML in sural nerve biopsies of 4 controls and 31 peripheral polyneuropathies (PN) of various etiologies [131; 141] were compared. In normal controls and in demyelating (chronic inflammatory demyelating polyneuropathy (CIDP)) or degenerative PNs (Charcot-Marie-Tooth disease type I (CMT I)) no or only very faint CML staining was observed. CML was detected in the perineurium and in epineural, perineural and endoneural vessels of diabetic PN (**Figure 4-9**), vasculitic PN (**Figure 4-11**) or in PN due to vitamin B12 deficiency and in the perineurium of alcohol-induced PN (not shown). In vasculitic PN all biopsies showed epineural or perivascular infiltrates of CD4, CD8 or CD68 positive mononuclear cells and cytoplasmatic CML staining was found within the mononuclear inflammatory cells (**Figure 4-11**). In diabetic PN the colocalisation of CML, RAGE and the activated form of NF κ B was found on epineural vessels and in the perineural space (IHC: Dr. A. Bierhaus, Heidelberg, data not shown).

The increased CML formation observed by IHC was verified by immunoblotting. On Western blots (**Figure 4-10**), a single distinct protein with an apparent MW of approx. 50 kDa was found to be immunoreactive to the polyclonal CML antibody. This CML-

modified protein band was much more prominent in diabetic PN compared to an age-matched healthy control. It is of note that in nerve tissue no CML reative band was visible at 67 kDa, the mass of serum albumin (**Figure 4-10**), indicating that a tissue protein rather than a serum protein is CML-modified.

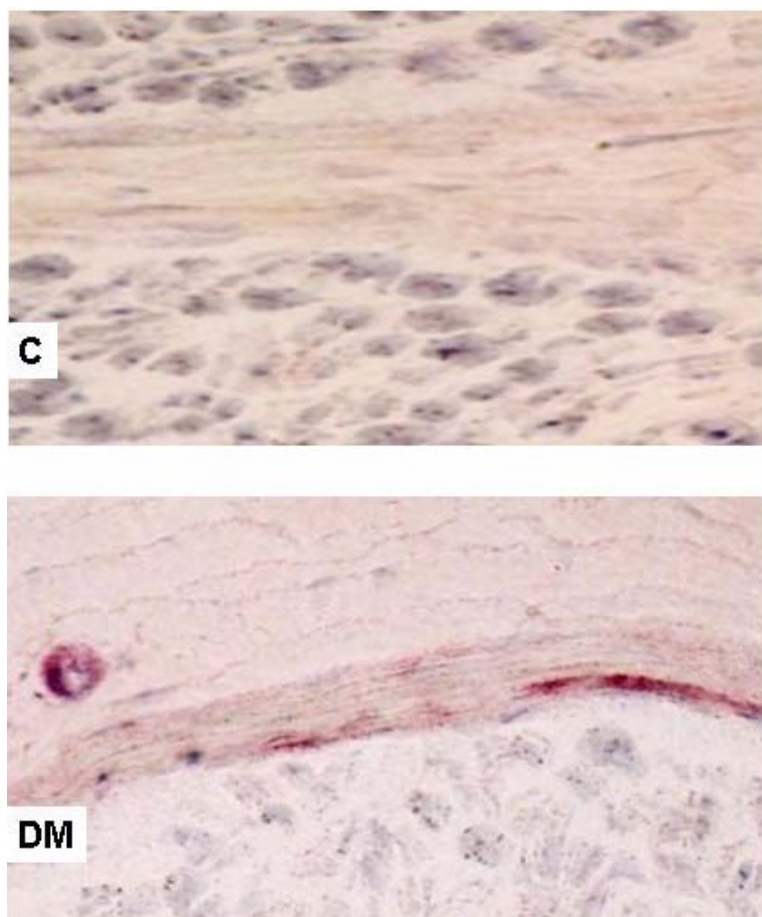


Figure 4-9. Anti-CML immunohistochemical stains of sural nerve tissue from a 64-year-old patient with diabetic polyneuropathy (DM) and a healthy age-matched 66-year-old subject (control, C). Semithin sections of nerve biopsy samples were immunostained with a specific anti-CML antiserum and counterstained with faint haematoxylin. CML-immunoreactive structures were visualised by the alkaline phosphatase anti-alkaline phosphatase (APAAP) method. In DM, perineural and vascular CML depositions were visible as bright red color complexes as compared to only faint scattered staining in the healthy subject (C). Control experiments for the staining specificity, performed with unspecific rabbit immunoglobulin and with anti-CML antiserum which was preabsorbed with CML-HSA, were negative (not shown). The immunohistochemistry was performed in cooperation with Dr. M. Haslbeck, Erlangen, Germany.

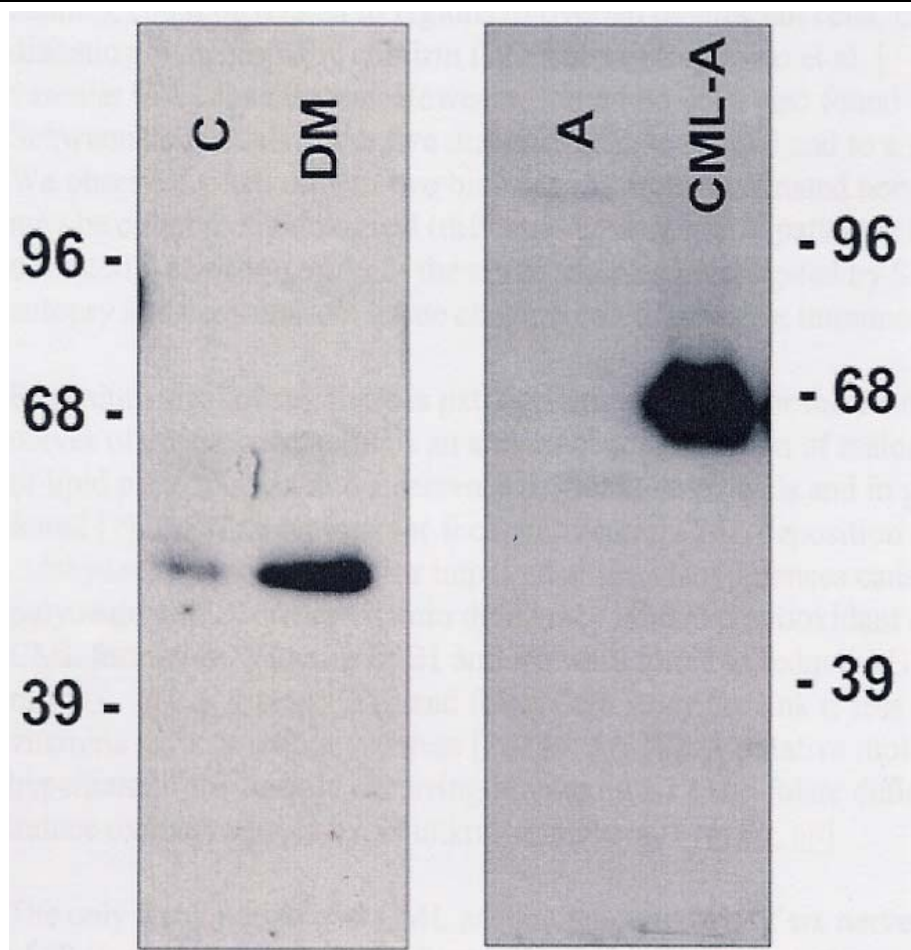


Figure 4-10. Western blot analysis of CML-modified proteins in nerve biopsy samples from a 64-year old man with diabetic polyneuropathy (DM) and a 56-year-old normal control (C). Tissue protein extracts (10 μg protein/lane) were separated by SDS-PAGE on 7.5% polyacrylamide gels, transferred to nitrocellulose membranes and probed against a specific rabbit anti-CML antiserum (Prof. Schleicher, Tuebingen, dilution 1:8000). For comparison, CML-modified albumin (CML-A, 0.1 μg) and unmodified albumin (A, 0.1 μg) was loaded. CML-immunoreactive proteins were visualised by enhanced

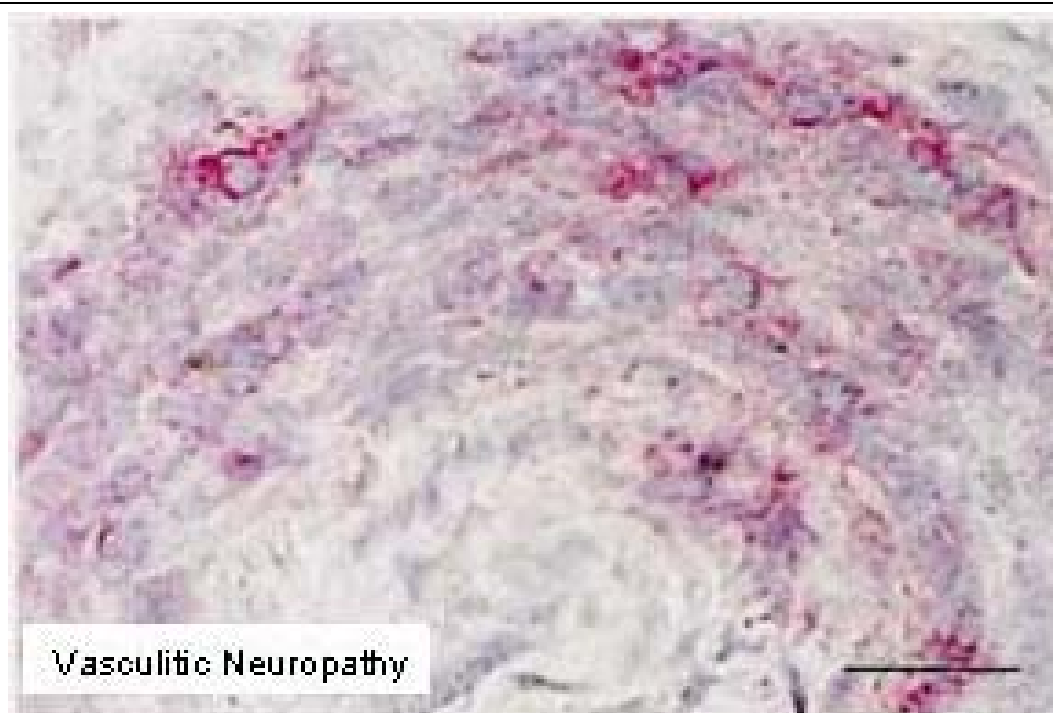


Figure 4-11. *CML-positive epineural-perivascular mononuclear cells in a 75-year-old woman with vasculitic neuropathy (polyclonal anti-CML (rabbit) / APAAP method). Bar 100 μ m. Conditions as in Figure 4-9. The immunohistochemistry was performed in cooperation with M. Haslbeck, Erlangen.*

4.2.2.2 CML in noninflammatory and inflammatory myopathies

In Western blots (**Figure 4-12**) the pattern of CML-modified proteins in skeletal muscle from patients with diabetes or atherosclerosis was compared to muscle diseases of inflammatory (polymyositis, dermatomyositis) or neuropathic etiology (HMSN I) and to a group of diseases with mitochondrial defects (CPEO syndrome, limb-girdle dystrophy, MELAS syndrome). For comparison, the left lane shows a sample from a healthy patient in which only faint CML immunoreactivity was observed. In inflammatory myopathies (polymyositis, dermatomyositis) the highest degree of CML modification was found on several distinct protein bands. Noninflammatory conditions (diabetes, atherosclerosis) showed a staining pattern

of CML-modified proteins different from inflammatory muscle diseases. Remarkably, the Western blot pattern of CML-modified proteins in diabetes is very similar to the pattern of a patient with atherosclerosis (micro- and macroangiopathy from heavy smoking). This correlates well to immunohistochemistry: in the diabetic patient, CML accumulation was confined to the wall of small vessels (**Figure 4-13 a**). In contrast to this finding, atrophic muscle from neuropathic myopathy (NP) showed only little CML modification on Western blot and was quantitatively comparable to control.

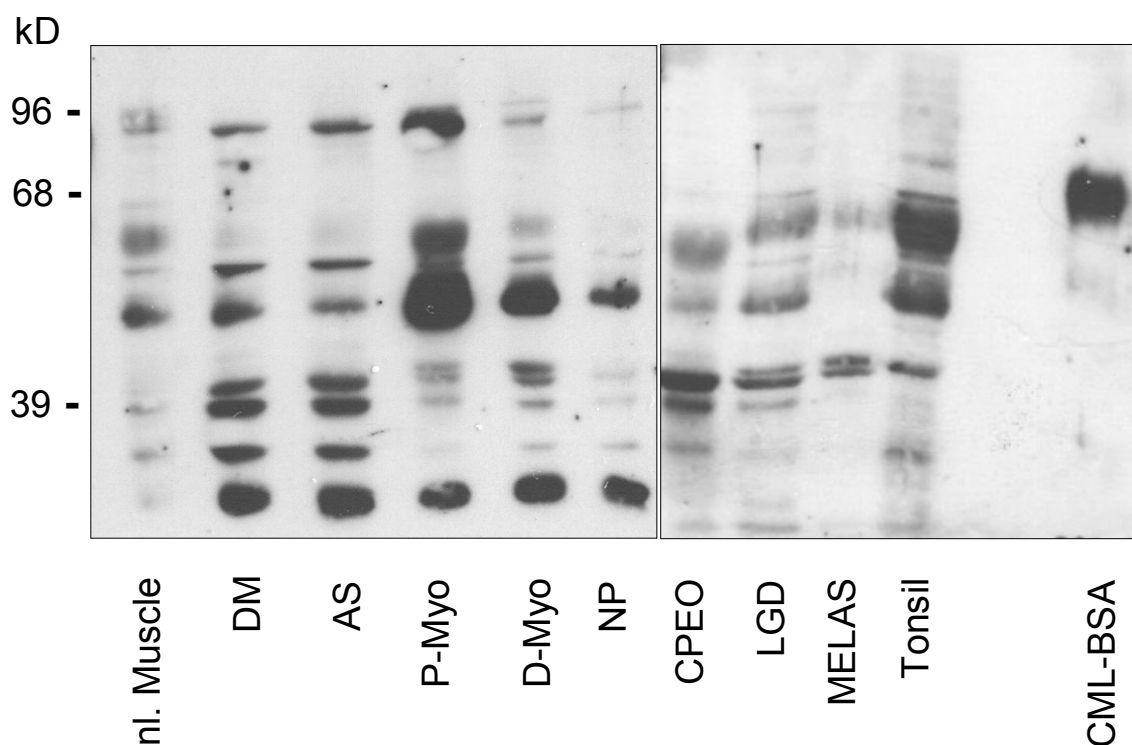


Figure 4-12. Anti-CML Western blots of skeletal muscle from patients suffering from diabetes mellitus and from other inflammatory and non-inflammatory diseases. For comparison, skeletal muscle from a healthy person (left lane) and lymphocyte-rich tissue (tonsil, right lane) was also examined. (30 μ g protein/lane; polyclonal anti-CML (rabbit)). (DM: diabetes mellitus type II; AS: atherosclerosis; P-Myo: polymyositis; D-Myo: dermatomyositis; NP: neuropathic myopathy HMSN type I; CPEO: CPEO-syndrome; LGD: limb-girdle dystrophy; MELAS: MELAS syndrome).

In cooperation with Dr. M. Haslbeck, Erlangen, the histological localisation of CML in skeletal muscle of patients suffering from inflammatory myopathies (polymyositis, dermatomyositis) or diabetes mellitus were compared to healthy controls. The histological findings correlated well with immunoblots of tissue extracts. Both forms of inflammatory muscle disease (dermatomyositis and polymyositis) were histologically characterised by infiltrating CML positive mononuclear cells. In polymyositis (**Figure 4-13 b**) most infiltrating mononuclear cells stained positive for CML, RAGE and NF κ B. In dermatomyositis (**Figure 4-13 c**) about 50 % of mononuclear cells stained positive for CML, RAGE and NF κ B (Dr. A. Bierhaus, personal communication).

In summary, the corresponding findings of marked protein-carboxymethylation in Western blot analysis and of immunohistochemically detectable CML-accumulation in the vessels indicate that (i) diabetic organ damage is in part due to vascular damage and that (ii) angiopathy in both diseases has common properties, e.g. the deposition of CML in the vessel wall.

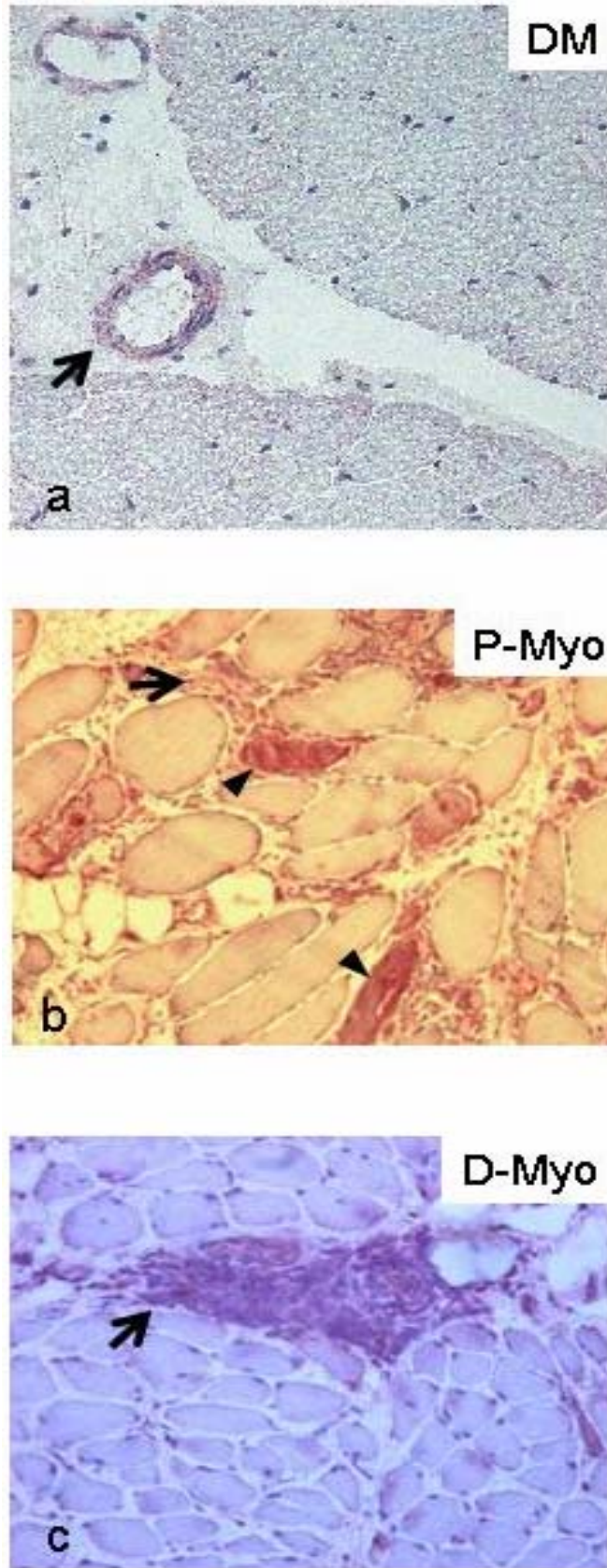


Figure 4-13. Legend see following page

Figure 4-13. Immunohistochemical detection of CML in skeletal muscle of patients with diabetes mellitus (a, DM), polymyositis (b, P-Myo) and dermatomyositis (c, D-Myo). Healthy muscle tissue stained negative for CML. In DM (a), CML accumulation was confined to the arteriolar wall. In polymyositis (b), CML deposits were found in infiltrating cells (arrow) and in degenerating muscle fibers (arrowheads). In dermatomyositis (c), CML was accumulating in infiltrating mononuclear cells. (Immunohistochemical staining of the tissue sections was performed in cooperation with M. Haslbeck, Erlangen; polyclonal anti-CML (rabbit), APAAP method).

4.2.2.3 CML accumulation in osteoarthritis

By Western blot analysis and IHC, the distribution of CML was studied in patients with severe osteoarthritis (OA) and in age-matched healthy controls [142]. **Figure 4-14** and **Figure 4-15** show IHC and Western blots of representative samples. In healthy cartilage, only faint CML immunoreactivity was found in the extracellular matrix (ECM) of the superficial layer, but not in deep layers of the cartilage tissue. In chondrocytes of healthy cartilage no CML was found (**Figure 4-14**, section a). In contrast, in the majority of OA cartilage samples, CML immunoreactivity was noted in the extracellular matrix of eroded cartilage and of chondrocytes (**Figure 4-14**, sections b-d). Considerable CML was found in the cytoplasm of most OA-affected chondrocytes (**Figure 4-14**, section d) and in chondrocytes of the calcified cartilage. Some chondrocytes showed CML in the nucleus. In Western blot analysis of CML in OA cartilage samples, bands in the molecular range between 39 and 68 kDa were found as shown in **Figure 4-15** (OA, left lane), whereas blots of healthy cartilage showed only trace amounts of CML (control C, right lane). For characterisation of the CML-modified proteins, the membranes were stripped and reprobated by Dr. Schwab,

Dresden. Reblotting of the membranes with antibodies against osteopontin, collagen II, aggrecan and COMP did not result in colocalisation with the CML immunoreactivity [142].

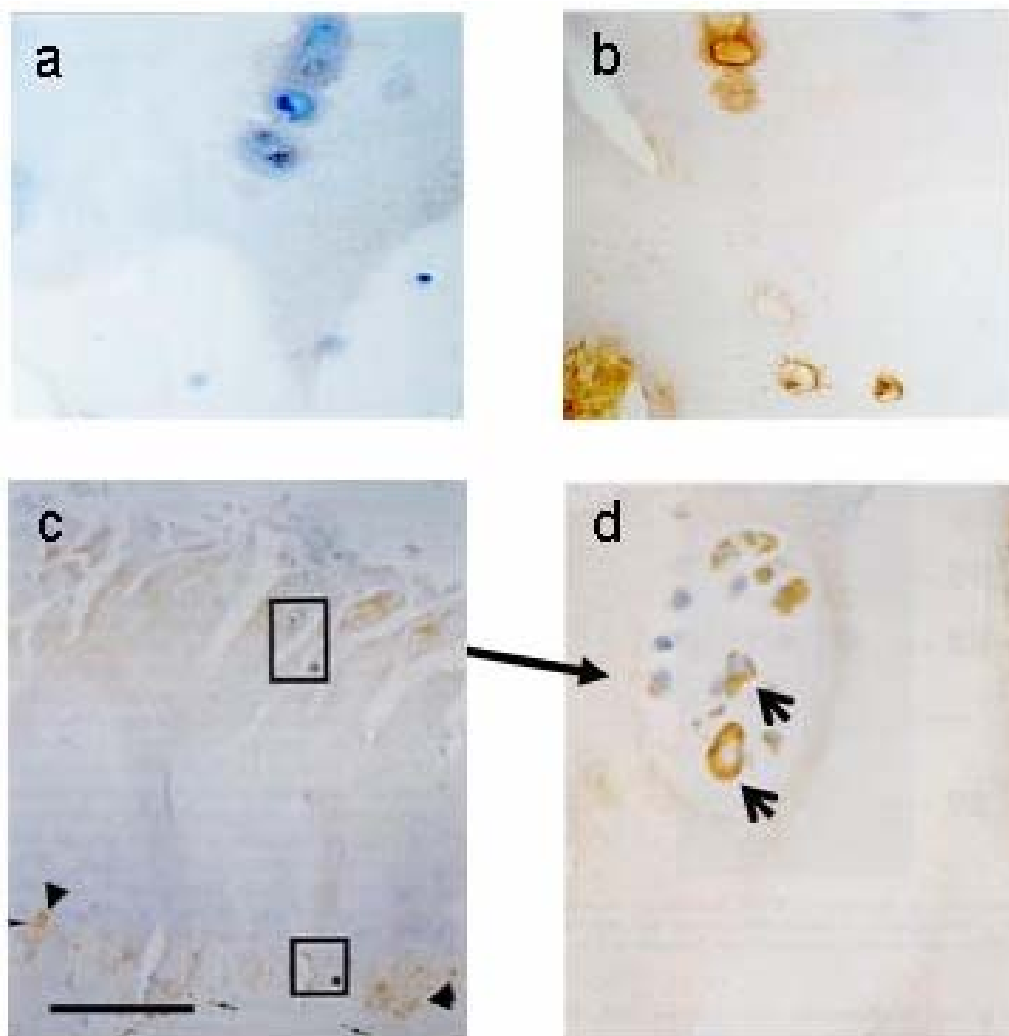


Figure 4-14. Immunohistochemical detection of CML in osteoarthritic knee joint cartilage (b-d) as compared to healthy cartilage tissue (a). CML is found in chondrocytes (b), in the superficial OA affected cartilage (upper frame in c), intracellular in chondrocytes (c, arrows), in the calcified cartilage (lower frame in c) and in osteocytes of the subchondral bone (c, arrowheads). In d, a higher magnification of a chondrocyte cluster (upper frame in c) is given and shows the intracellular localisation of CML deposits in chondrocytes. Bar 50 μ m. (Immunohistochemistry was performed in cooperation with W. Schwab, Dresden).

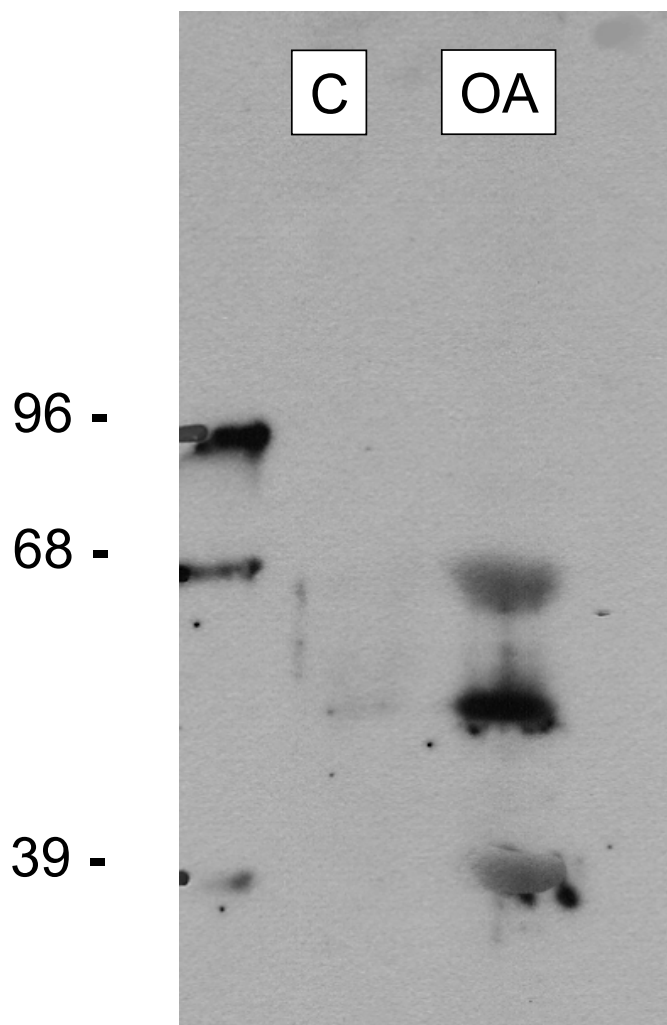


Figure 4-15. Anti-CML Western blot analysis of protein extracts of cartilage tissue from osteoarthritic (OA) and healthy (C) knee joint cartilage. Frozen cartilage biopsy samples were powdered in a liquid-nitrogen cooled vibration mill and further homogenised in a Potter-Elvehjem tissue homogenisator in 10 mM NaHCO₃, 0.25 M sucrose, pH7.0 with freshly added protease inhibitor cocktail and 100 µM PMSF. Protein extracts (10µg protein/lane) were separated by SDS-PAGE on 7.5% polyacrylamide gels, transferred to nitrocellulose membranes and probed against a specific rabbit anti-CML antiserum (Prof. Schleicher, Tuebingen, dilution 1:8000). CML-immunoreactive proteins were visualised by enhanced chemiluminescence. kD: kilo Dalton.

4.2.3 CML accumulation in circulating granulocytes

It was studied, whether CML modification of cellular proteins can be observed in circulating leukocytes of hyperglycemic diabetic patients as compared to normoglycemic non-diabetic controls. By immunoabsorption using antibody-coated magnetic beads, CD14-positive monocytes, CD14-negative/CD15-positive granulocytes and CD3-positive lymphocytes were prepared from EDTA blood samples of 8 diabetic patients (HbA1c in the range of 9.8 – 13.2%) and of 6 non-diabetic controls. Cell lysates were prepared and analysed by Western blotting (polyclonal rabbit anti-CML antiserum). In granulocytes, in 2 out of 8 diabetic patients a single CML-modified protein band was found with an apparent MW of approx. 25kDa (**Figure 4-16**) but not in granulocytes of normoglycemic controls. In monocytes and lymphocytes no CML modification was observed, neither in diabetics nor in controls.

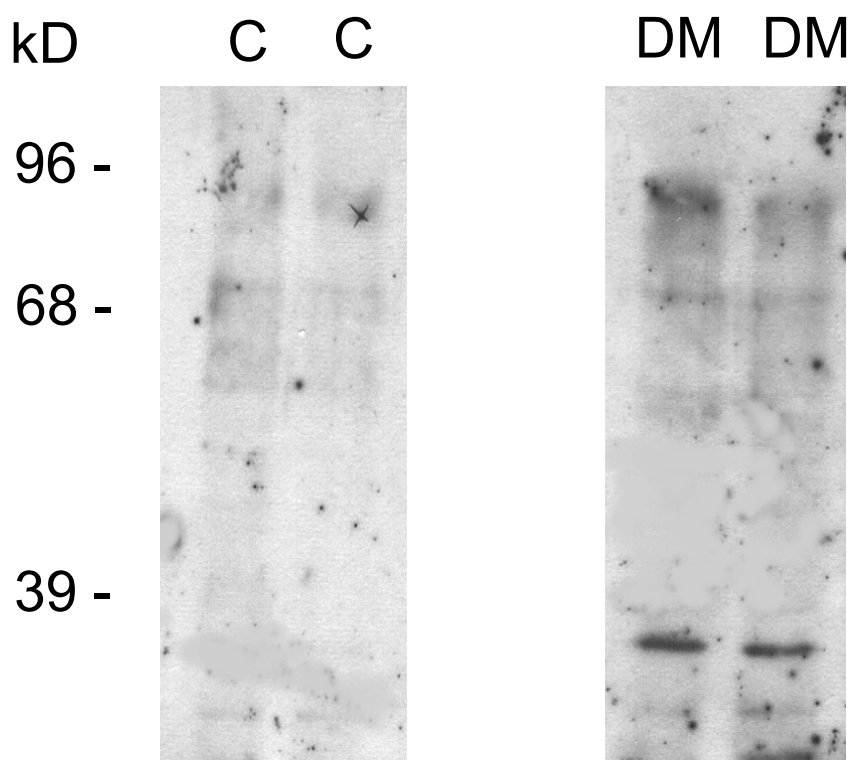


Figure 4-16. Western blot analysis of CML-modified proteins in ex vivo-isolated granulocytes. CD14-negative/CD15-positive granulocytes of two normoglycemic, healthy subjects (C) and two chronically hyperglycemic (HbA1c > 9%) patients with diabetes mellitus (DM) were isolated from anticoagulated whole blood by sequential immunoabsorption using anti-CD14- and anti-CD15-antibody coated magnetic beads. Cell lysates were separated by SDS-PAGE, transferred to nitrocellulose membranes and probed against a specific rabbit anti-CML antiserum. CML-immunoreactive proteins were visualised by enhanced chemiluminescence (ECL). Conditions: lysis buffer: 50 mM TRIS, 150 mM NaCl, 1% Triton with freshly added 0.5 mM PMSF / 14 µg/µl aprotinin; 7.5% polyacrylamide gels; 10 µg protein/lane; primary antibody: rabbit anti-CML antiserum (Prof. Schleicher, Tuebingen, Germany), dil. 1:8000, secondary antibody: anti-rabbit-IgG-HRP conjugate 1:3000; exposure 15 min. kD: kilo Dalton. Abbreviations: C. control; DM: diabetes mellitus; CD: cluster of differentiation.

4.3 Mechanism of CML formation in inflammation-associated cells

4.3.1 Lipid peroxidation leads to carboxymethylation of proteins *in vitro*

It has been described by Fu et al. [40] that the oxidative decomposition (lipid peroxidation) of PUFAs results in the formation of glyoxal and other carbonyl intermediates. Therefore, the involvement of the oxidative decomposition of polyunsaturated fatty acids (PUFAs) on the CML modification of RNase, a 13.7 kDa protein devoid of carbohydrate, was studied. Experiments were performed under atmospheric oxygen pressure. It was observed that the reaction mixture with the mono-unsaturated oleic acid became biphasic within 4 days, and the reaction mixtures, containing poly-unsaturated linoleic acid and arachidonic acid, were progressively solubilised as they autooxidised.

As shown in **Figure 4-17** lipid peroxidation of PUFAs led to a gradual carboxymethylation of RNase within 2 to 4 days. The degree of CML modification correlated with the number of C=C double bonds. The decomposition of arachidonate (20:4 (5,8,11,14)) resulted in the highest degree of carboxymethylation, followed by linoleate (9,12-octadecadienoic acid; (18:2)) and oleate (9-octadecenoic acid (18:1)). As revealed by SDS-PAGE (**Figure 4-17**), lipid peroxidation does not only lead to carboxymethylation of monomeric RNase (13.7 kDa), but also to multimerisation by crosslinking. Therefore, dot blots were used to estimate the influence of the superoxide-generating hypoxanthine/xanthine oxidase system and of H₂O₂ on CML formation. It was observed that H₂O₂ or the generation of

superoxide did not enhance the degree of CML modification above that by oxygen alone (data not shown).

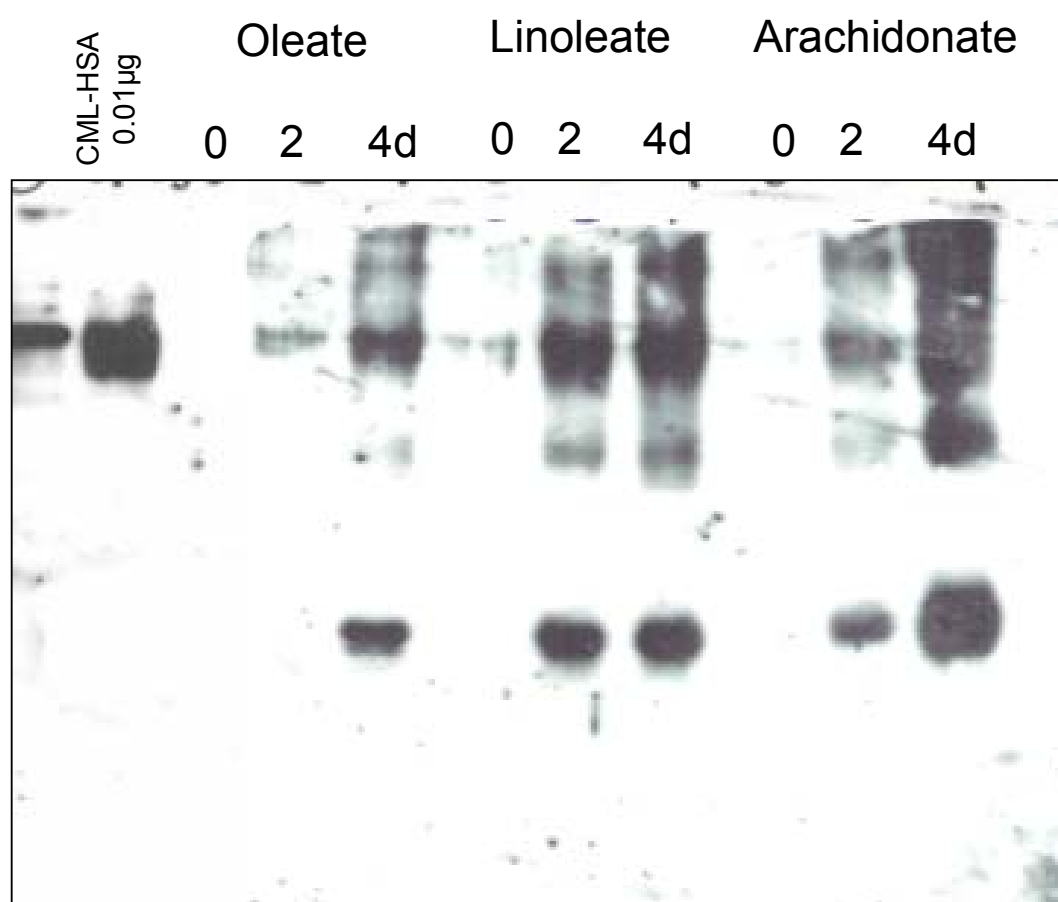


Figure 4-17. Anti-CML Western blot of ribonuclease (RNase) incubated with unsaturated fatty acids under aerobic conditions. 1 mM RNase was incubated with 100 mM of oleate, linoleate and arachidonate, respectively, for 0 – 4 days at 37°C. Subsequently, 10 µg of protein was separated by SDS-PAGE and immunoblotted against a specific anti-CML antiserum. CML-immunoreactive proteins were visualised by enhanced chemiluminescence (ECL). For comparison, 0.01 µg of highly-modified CML-HSA (33.6 mol CML/mol HSA) was loaded on the left lane. Conditions: 15% polyacrylamide gel; primary antibody: rabbit anti-CML antiserum (Prof. Schleicher, Tuebingen, Germany), dil. 1:8000, secondary antibody: anti-rabbit-IgG-HRP conjugate 1:3000; exposure 3 min.

4.3.2 The ,oxidative burst' of granulocytes leads to the carboxymethylation of serum proteins

Granulocytes were isolated from freshly-prepared buffy coats and suspended in RPMI, containing 5% FCS, and stimulated by opsonised zymosan (1.5 mg/ml) to study the effect of the granulocytic ROS production on serum proteins. As shown in

Figure 4-18 A/B, stimulation with opsonised zymosan resulted in an ,oxidative burst' with marked stimulation of myeloperoxidase (MPO, measured as luminol chemiluminescence) and of NADPH oxidase (measured as lucigemin chemiluminescence) for 120 min. The degree of protein-carboxymethylation of the serum proteins (as well as of intracellular proteins set free from lysed granulocytes) was analysed by Western-blotting (

Figure 4-18 C). A time-dependent CML modification predominantly on albumin (65 kDa), but also on other distinct proteins was observed. This experiment demonstrated the overall effect of the ROS set free during the granulocytic ,oxidative burst' on CML formation, but was not found suitable to study intracellular CML formation since granulocytic cells were completely lysed within 2 hours.

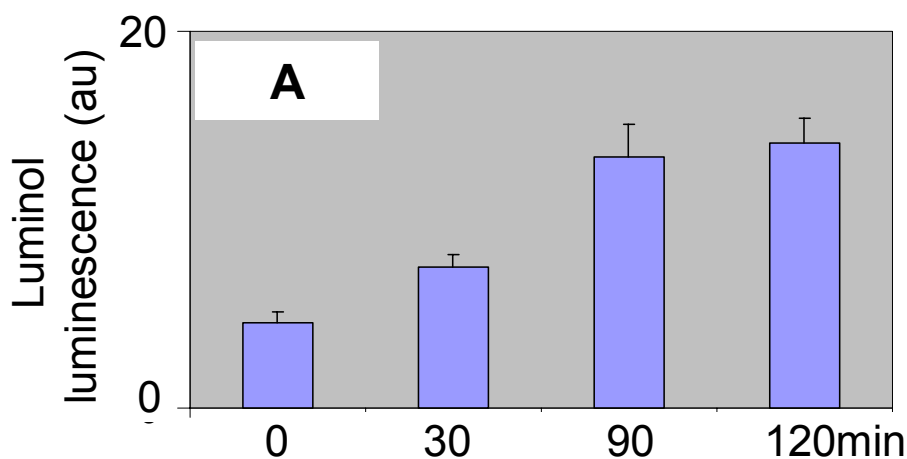


Figure 4-18. Legend see following page.

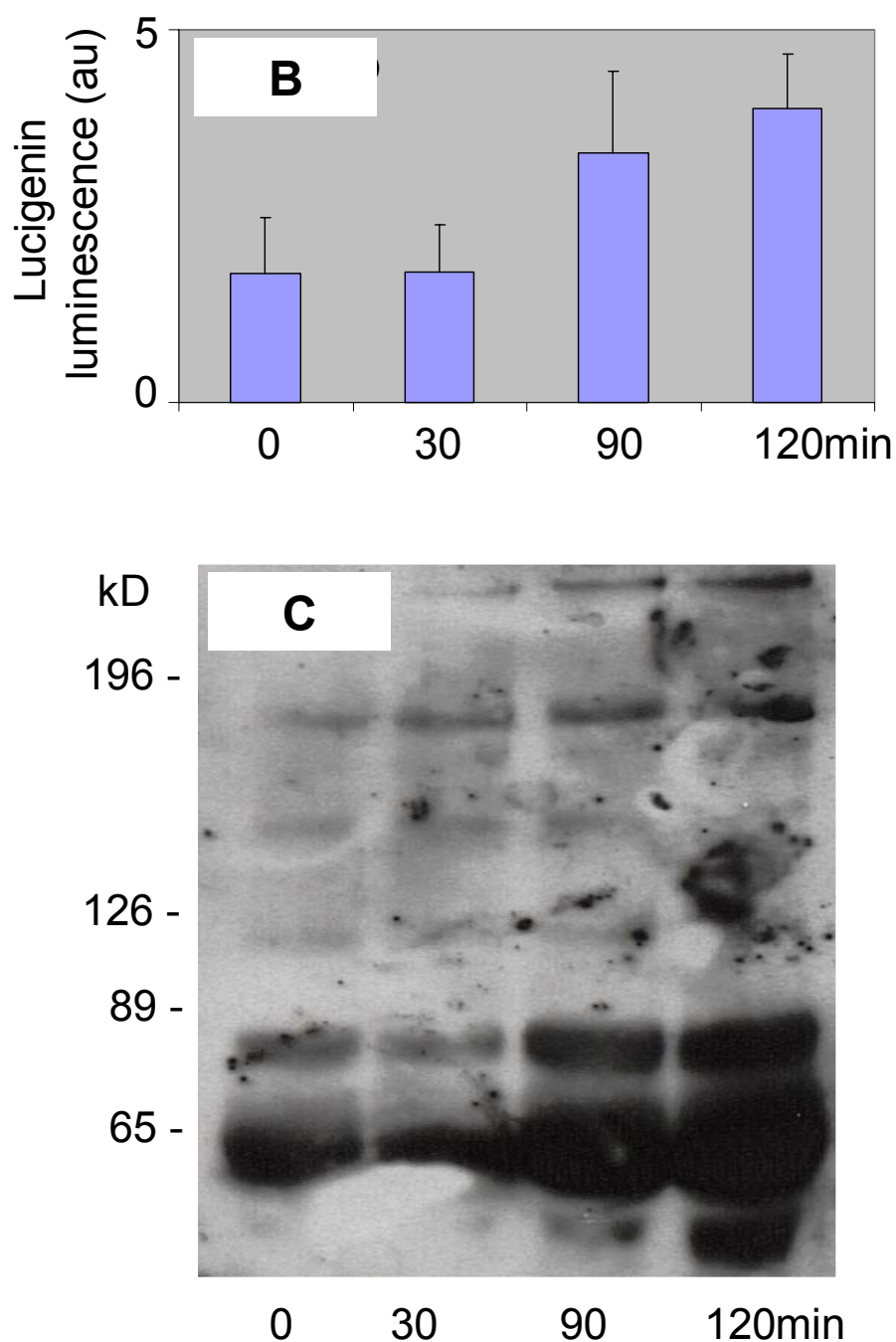


Figure 4-18. *The stimulation of ex vivo-isolated granulocytes by opsonised zymosan leads to an 'oxidative burst' and to the time-dependent carboxymethylation of serum proteins and cellular proteins.* Granulocytes were isolated from freshly-prepared buffy coats by density centrifugation. For the chemiluminescence assays (A,B), 250 000 cells each were suspended in 500 μ l of assay buffer and stimulated by 0.75 mg opsonised zymosan for 0 to 120 min. The generation of MPO-derived hypochlorite anions was measured by recording the luminol chemiluminescence (A) and the generation of NADPH oxidase derived superoxide anions was measured for 15 min

each by recording the lucigenin chemiluminescence (B) on a Tropic chemiluminescence reader (Applied Biosciences, Foster City, USA). Shown are the integrated chemiluminescence readings from 15 min of measurement in arbitrary units (au, 3 independent experiments, mean \pm SD). For the Western blot analysis of CML-modified proteins (C), 250000 cells each were suspended in 500 μ l of RPMI medium containing 5% fetal calf serum (FCS) and stimulated by 0.75 mg opsonised zymosan for 0 to 120 min resulting in complete cell lysis within 120 min. The reaction mixtures were cleared from cellular debris and zymosan by centrifugation (5000 rpm, 1 min). The supernatant was loaded (10 μ g of total protein/lane) on 7.5% polyacrylamide gels, separated by SDS-PAGE and immunoblotted against a specific rabbit anti-CML antiserum (Prof. Schleicher, Tuebingen, Germany, dil. 1:8000). CML-immunoreactive proteins were visualised by ECL detection (secondary antibody: anti-rabbit-IgG-HRP conjugate 1:3000; exposure 1 min).

4.3.3 In pre-differentiated monocytic cell lines, stimulation of ROS-generating mechanisms leads to CML modification of distinct cellular proteins

4.3.3.1 Experiments with pre-differentiated Mono Mac 6 cells

PMA stimulation leads to increased ROS formation, most likely from NADPH oxidase activity:

Mono Mac 6 cells were pre-differentiated as described by Ziegler-Heitbrock et al. [135; 136] in a monocytic direction until a PMA-induced oxidative burst could be observed (measured as lucigenin chemiluminescence, **Figure 4-19**). This chemiluminescence could be inhibited completely by the potent, yet unspecific, NADPH oxidase inhibitor DPI (100 μ M) and inhibited partly by the NADPH oxidase inhibitor HMAP (2mM) which has poor membrane penetration properties (**Figure 4-20**). Inhibitors for the respiratory chain (KCN, 5mM), for xanthine oxidase (allopurinol, 300 μ M), for NO-synthase (L-NAME, 5 μ M) and for cyclooxygenases (indomethacin 500 μ M) had no or only a

small effect in blocking the oxidative burst. Therefore, the observed oxidative burst most likely can be attributed to the activity of an inducible NADPH oxidase.

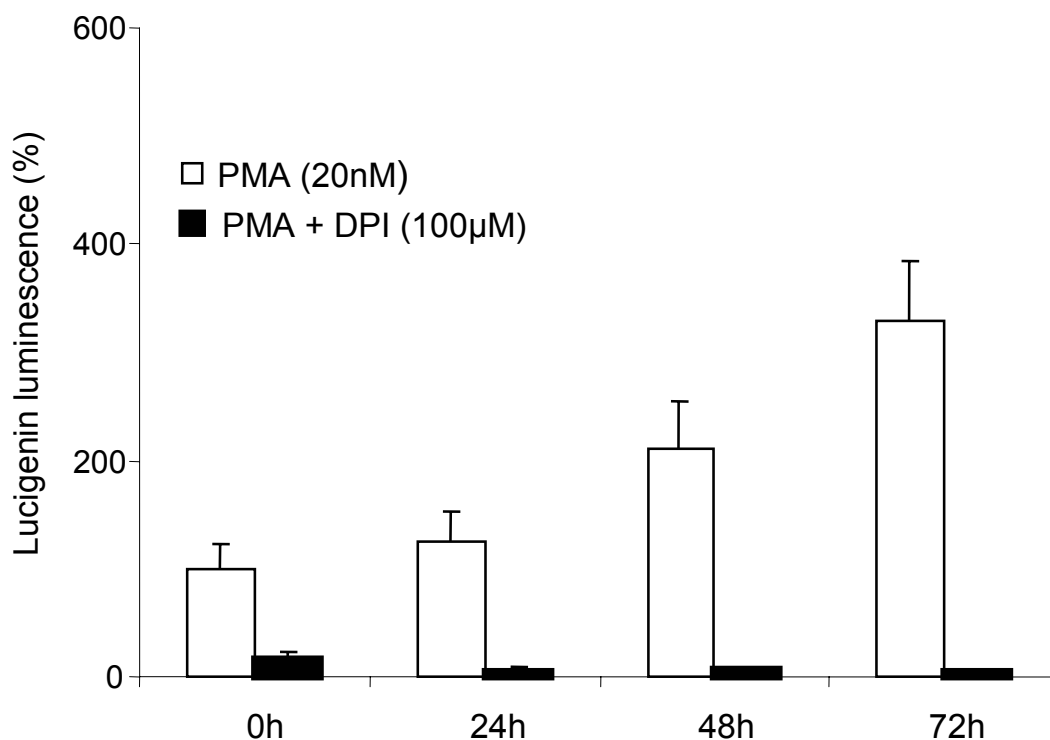
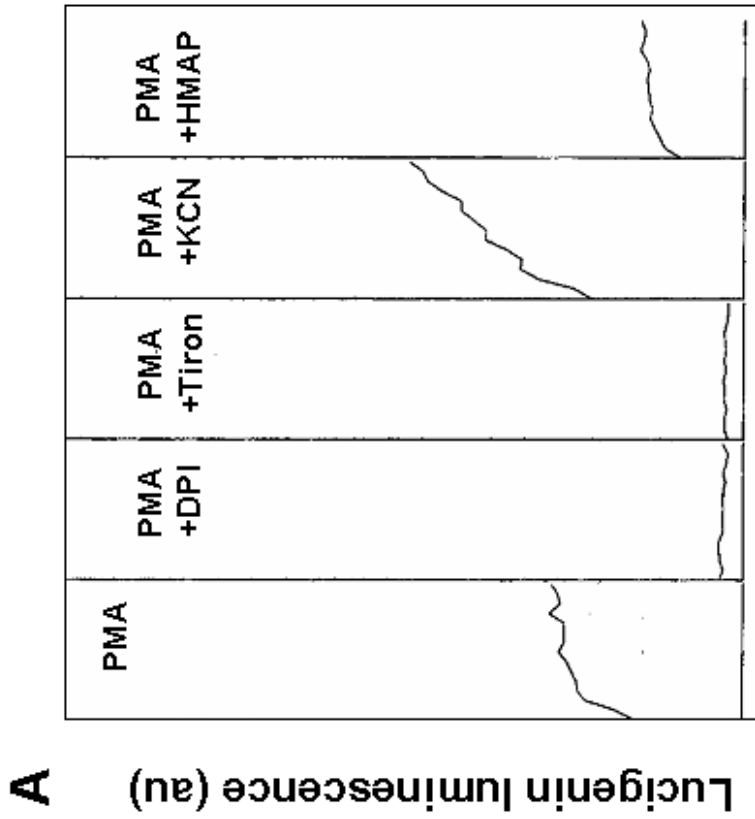
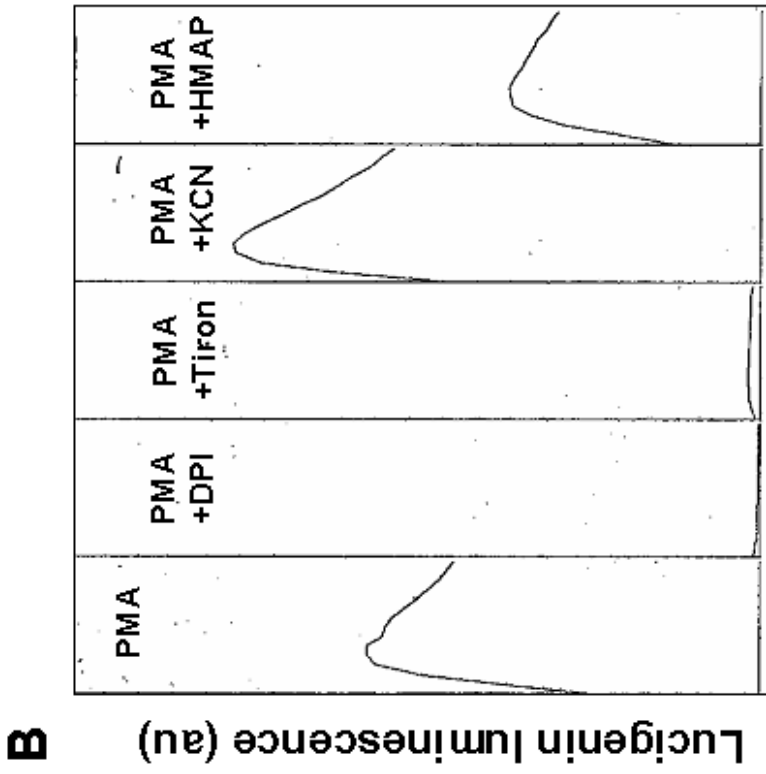


Figure 4-19. Pre-differentiated MonoMac6 cells exhibit monocytic features: stimulation by PMA results in an oxidative burst as determined by lucigenin chemiluminescence. Mono Mac 6 cells, which have been pre-differentiated with 1 nM $TNF\alpha$ for 3 days, were incubated with 20 nM PMA and without or with 100 μ M DPI in growth medium for 0 min to 72h. Aliquots of 250000 cells were washed, resuspended in 500 μ l of assay buffer containing 50 μ M lucigenin and 200 μ M NADH and stimulated with 20 nM freshly added PMA. The chemiluminescence was recorded over 15 min and integrated. Shown is the percentage of lucigenin chemiluminescence as compared to the initial signal of un-inhibited cells set to 100 % ($n = 3$, mean \pm SD).



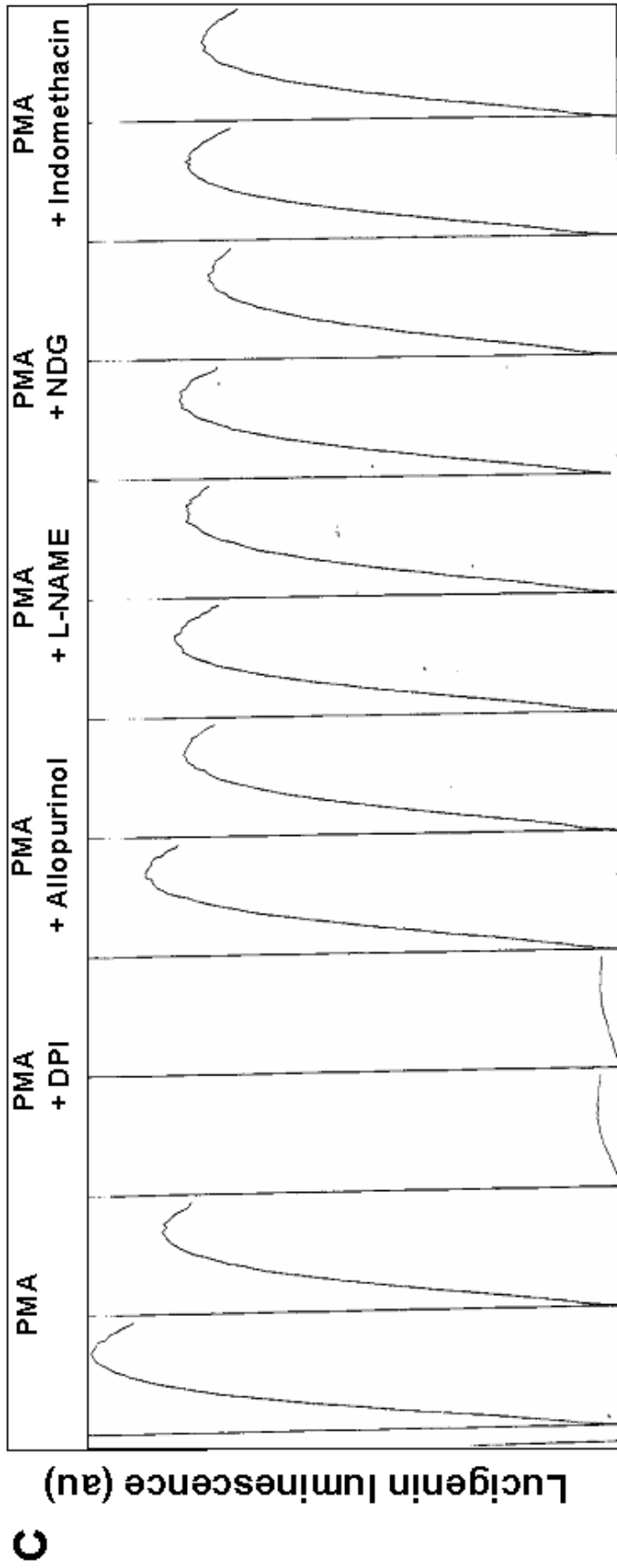


Figure 4-20. Characterisation of PMA-stimulated lucigenin chemiluminescence in Mono Mac 6 monocytic cells. Homogenates (A) or suspensions (B, C) from 250000 pre-differentiated cells, each, were preincubated without (first trace) or with (subsequent traces) various inhibitors of reactive oxygen species formation at the indicated concentrations. Then, 50 μM lucigenin and 200 μM NADH were added to a final volume of 500 μl . The cells were stimulated with freshly added 20 nM PMA and the chemiluminescence signal was recorded for 15 min. Lucigenin chemiluminescence was completely inhibited by 100 μM DPI, a potent, yet unspecific inhibitor for NADPH oxidase. Inhibitors for other cellular sources of ROS, such as inhibitors of the respiratory chain (5 mM KCN), of xanthine oxidase (300 μM allopurinol), of NO-synthase (100 μM L-NAME), of lipooxygenase (5 μM NDG) and of cyclooxygenase (500 μM indomethacin) had little effect. (au: arbitrary units).

Stimulation of differentiated Mono Mac 6 monocytic cells by PMA or opsonised zymosan leads to time-dependent intracellular CML formation under physiological ambient glucose concentrations and to an increased CML formation under high glucose conditions.

Under stimulation by PMA or opsonised zymosan, the carboxymethylation of cellular proteins could be observed within 8 to 24 h with a time-dependent increase for up to 72 h (**Figure 4-21**). At longer time points, cell lysis started to occur. As shown in **Figure 4-21**, several distinct cellular protein bands, predominantly in the molecular weight range between 96 and 20 kDa were found to be CML-modified. This was observed at physiological (5.5mM) glucose concentrations and was found to be increased at high glucose conditions (30mM).

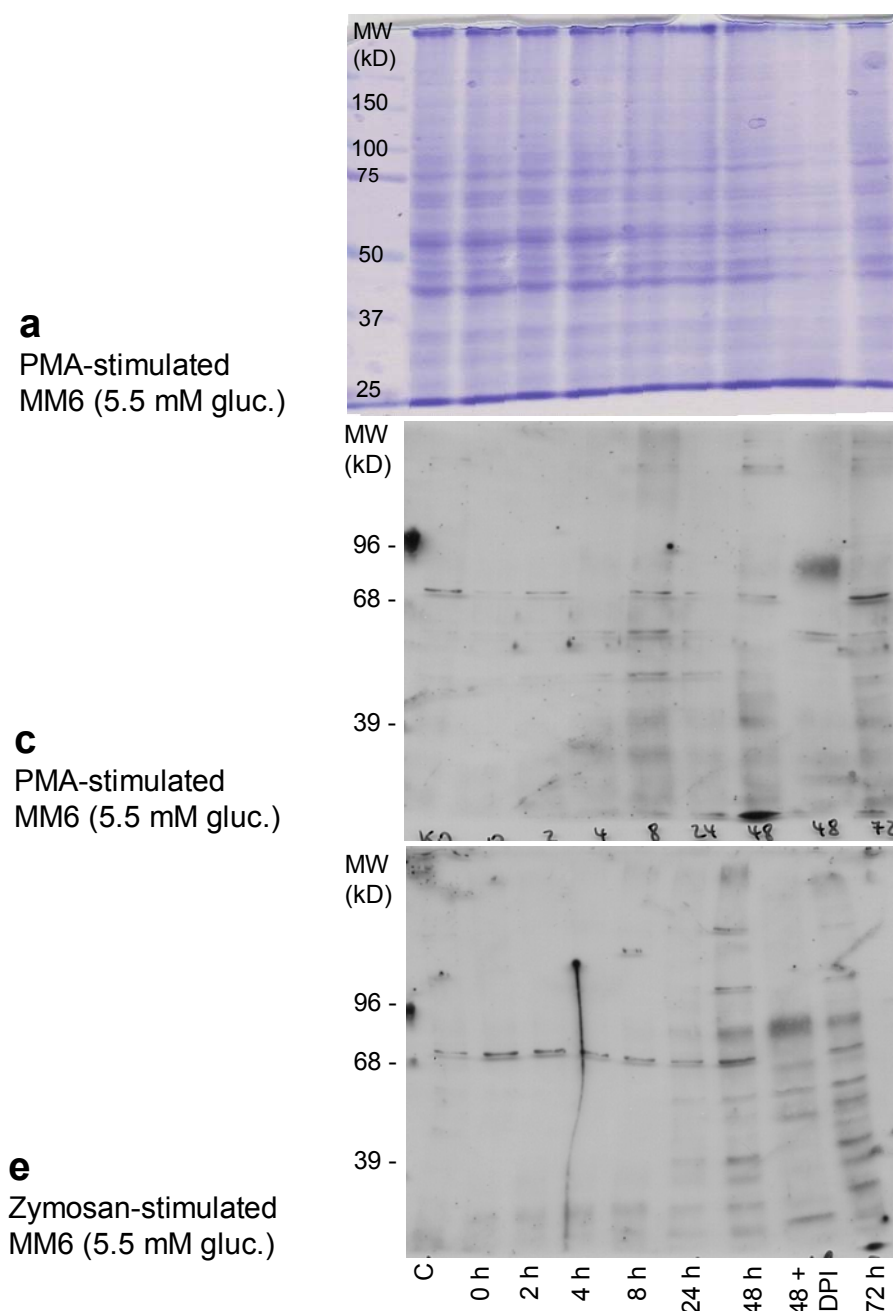


Figure 4-21. Western blot analysis of intracellular CML formation in stimulated Mono Mac 6 monocytic cells. Pre-differentiated cells were stimulated by 20 nM PMA (c, d) or by 1.5 mg/ml opsonised zymosan (e, f) under normoglycemic (5.5 mM glucose, left panel) or hyperglycemic (30 mM glucose, right panel) conditions for 0 to 72 h. Cells were harvested and equal amounts of cell lysates were separated by SDS-PAGE on 7.5% polyacrylamide gels. The gels were stained with Coomassie brilliant blue (a,b) or transferred to nitrocellulose membranes and immunoblotted against a specific rabbit anti-CML antiserum (c-f). CML-immunoreactive proteins were visualised by enhanced chemiluminescence detection (cont.).

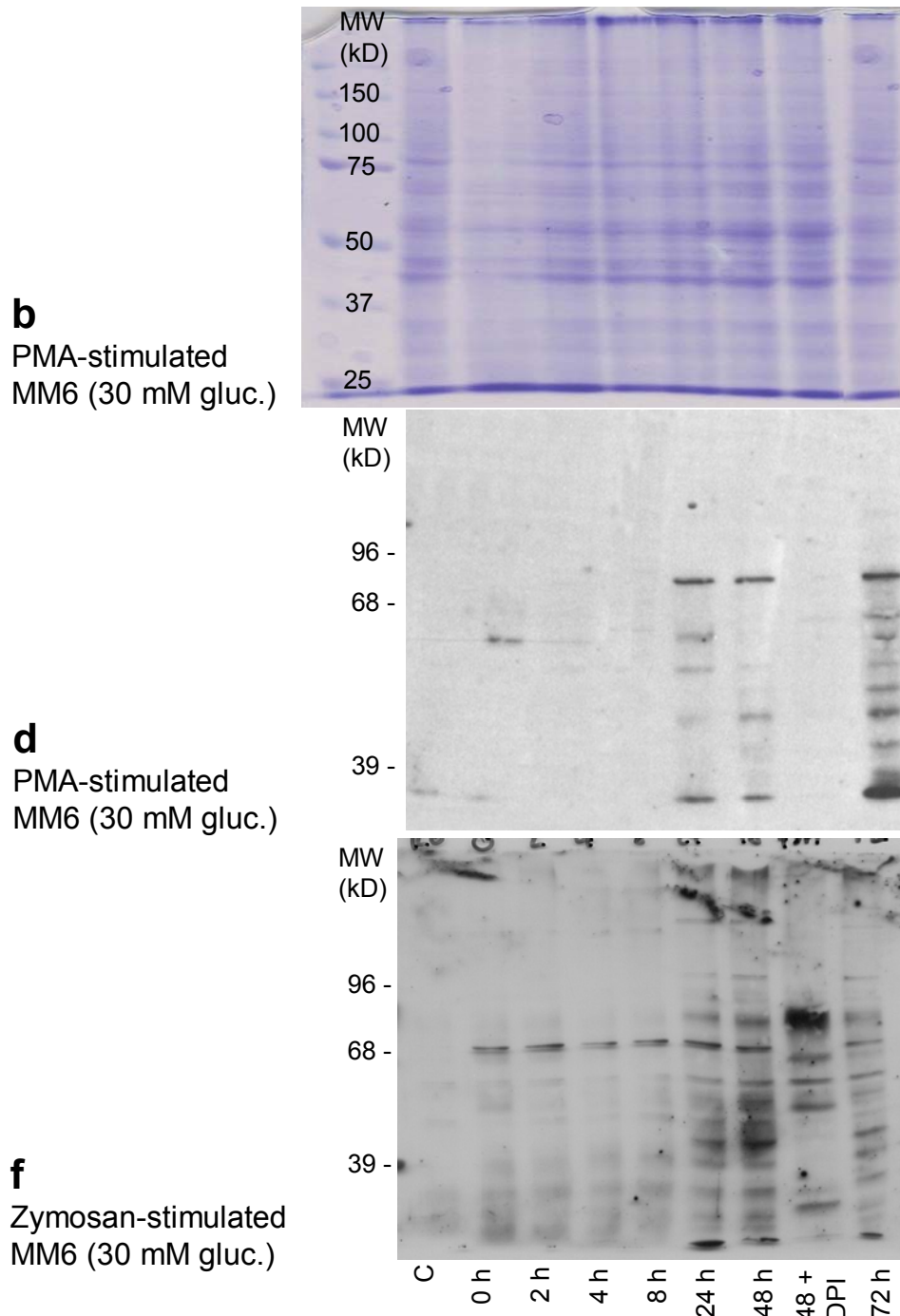


Figure 4-21(cont.). Upon stimulation by PMA or opsonised zymosan, CML was formed in a time-dependent manner within 8 to 72 h. CML formation was increased under high glucose (d, f) as compared to normal ambient glucose concentrations (c, e). Conditions: 30 µg protein/lane; primary antibody: rabbit anti-CML antiserum (Prof. Schleicher, Tuebingen, Germany), dil. 1:8000, secondary antibody: anti-rabbit-IgG-HRP conjugate 1:3000; exposure 4 min. Abbreviations: C: controls (unstimulated, pre-differentiated cells); DPI: diphenylene iodonium chloride; PMA: phorbol-12-myristate-13-acetate; MW: molecular weight; kD: kilo Dalton.

A 25 kDa CML-modified protein can be immunoabsorbed by surface-enhanced laser desorption/ionisation mass spectrometry (SELDI-MS):

In cooperation with Dr. R. Bogumil (Ciphergen Biosystems, Fremont, CA, USA), immunoabsorption and SELDI-MS was applied to verify some of the small-molecular-weight CML-modified proteins detected by the polyclonal CML-antiserum. As indicated in **Figure 4-22**, the monoclonal CML antibody 2F8 was covalently coupled to an aluminium chip (CipherGen ProteinChip®, CipherGen, Fremont, CA, USA) and the Mono Mac 6 cell lysates (same as in **Figure 4-21**, blot **d**) were immunoabsorbed. By SELDI-MS, a newly CML-modified protein (as compared to the 0 h sample) with a mass of 24737 kDa was found, which corresponds to the 25 kDa protein observed on the Western blot. Control measurements were performed on chips coated with unspecific IgG and found to be negative.

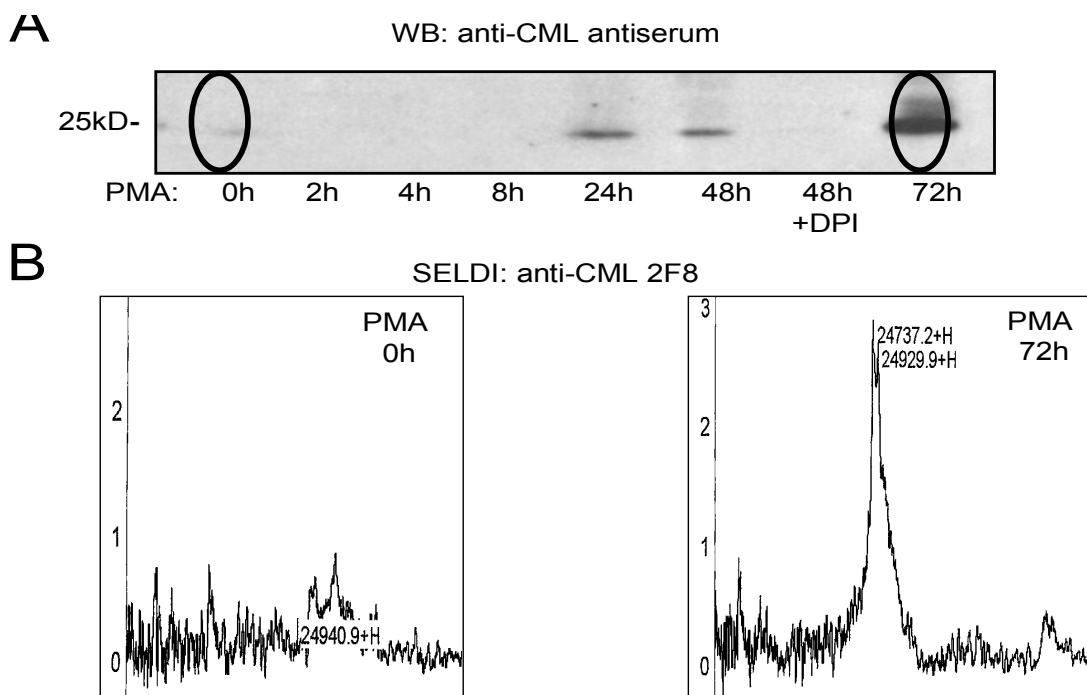


Figure 4-22. Legend see following page.

Figure 4-22. Characterisation of a 25 kD CML-modified protein using two independent anti-CML antibodies for Western blot analysis and SELDI-MS. Pre-differentiated Mono Mac 6 monocytic cells were stimulated by 20 nM PMA for 0 to 72 h without or with the NADPH oxidase inhibitor DPI (100 μ M). Cell lysates from the indicated time points were split and either analysed by anti-CML Western blot analysis (**A**, 7.5% polyacrylamide gel; 30 μ g protein/lane; primary antibody: rabbit anti-CML antiserum (Prof. Schleicher, Tuebingen, Germany), dil. 1:8000, exposure 4 min) or by surface-enhanced laser desorption/ionisation mass spectrometry (SELDI-MS) analysis (**B**). For this technique, 1 μ l of a solution of 0.5 μ g/ μ l of the monoclonal mouse anti-CML antibody 2F8 (NovoNordisk, Bagsvaerd, Denmark) was covalently coupled to an aluminum chip (CipherGen ProteinChip, CipherGen, Fremont, USA). Small-molecular CML-modified proteins from 5 μ l of cell lysate were immunoabsorbed to the chip. The analysis by laser desorption/ionisation mass spectrometry revealed at least two specifically bound proteins with a mass of 24737 and 24929 daltons which were newly CML-modified during PMA-stimulation and which were not present on control chips covered with unspecific mouse IgG (not shown). Abbreviations: WB: Western blot.

Intracellular CML formation is inhibited by DPI, a potent inhibitor of NADPH oxidase and other flavoproteins

As shown in **Figure 4-23**, the intracellular CML formation in stimulated Mono Mac 6 cells can be demonstrated by 3 different anti-CML antibodies, the polyclonal CML antiserum (**Figure 4-23, b**) and the two monoclonals 2F8 and 4G9 (**Figure 4-23, c/d**). Under the conditions used, the antibodies vary in their sensitivity as well as in the pattern of reactive protein bands. The CML formation was inhibited, at least in part, by DPI, an unspecific inhibitor of NADPH oxidase and other flavoproteins.

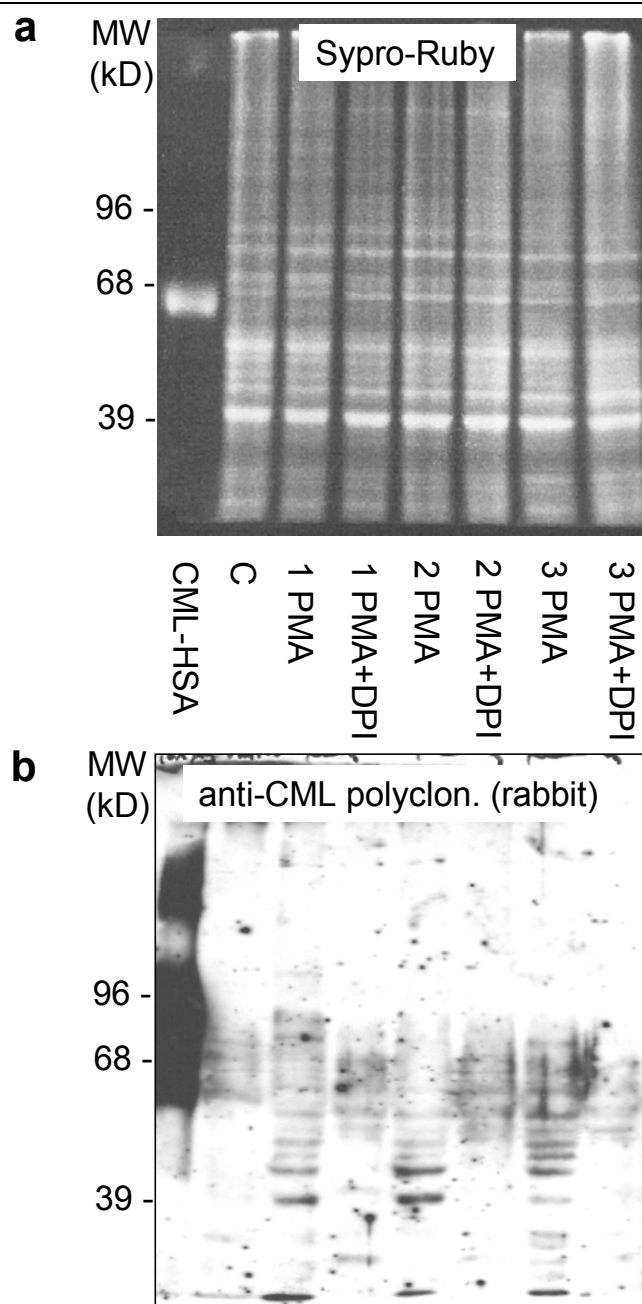


Figure 4-23. Western blot analysis of CML-modified proteins by various anti-CML antibodies. Whole cell lysates from 3 independent experiments (lanes 1, 2, 3) of pre-differentiated Mono Mac 6 cells, grown for 72 h with 20 nM PMA or 20 nM PMA / 100 μ M DPI were separated on parallel gels and stained with Sypro Ruby (a), an unspecific protein stain, or blotted and probed against 3 different anti-CML antibodies (b-d). The CML-modified proteins were visualised by enhanced chemiluminescence detection. Conditions: a: Sypro ruby protein stain (BioRad, Munich, German), excitation: 460 nm, emission 550 nm; (cont.).

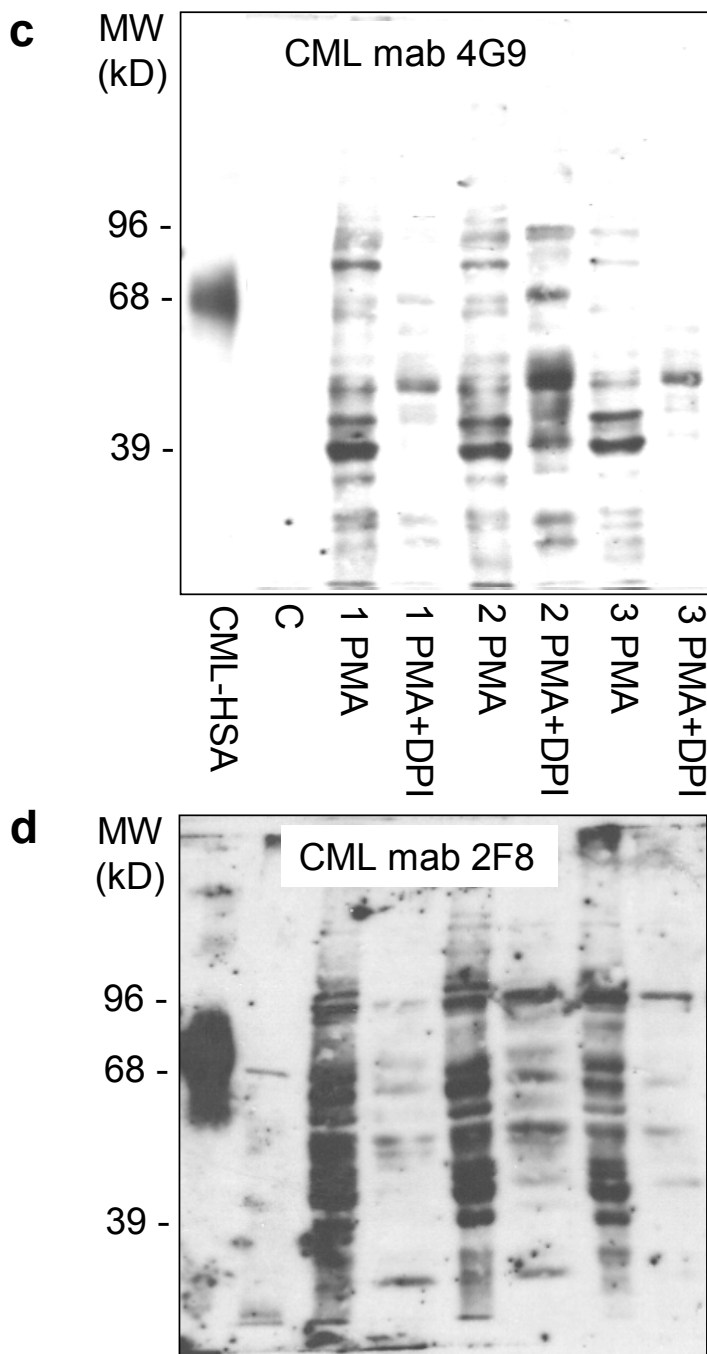


Figure 4-23 (cont.). *b*: rabbit anti-CML antiserum (Prof. Schleicher, Tuebingen, Germany), 1:8000 / anti-rabbit-IgG-HRP conjugate 1:3000; *c*: monoclonal mouse anti-CML 4G9 (Roche, Penzberg, Germany), 1:5000 / anti-mouse-IgG-HRP conjugate 1:3000; *d*: monoclonal mouse anti-CML 2F8 (NovoNordisk, Bagsvaerd, Denmark), 1:5000 / anti-mouse-IgG-HRP conjugate 1:3000. Abbreviations: C: control (unstimulated, pre-differentiated cells); DPI: diphenylene iodonium chloride; PMA: phorbol-12-myristate-13-acetate; MW: molecular weight; kD: kilo Dalton; mab: monoclonal antibody.

Xanthine oxidase or NO synthase do not contribute to CML formation in stimulated Mono Mac 6 monocytic cells

It was tested, whether inhibitors of various cellular ROS sources did influence CML synthesis. As shown in **Figure 4-24**, the CML formation was inhibited by DPI, a potent yet unspecific inhibitor of NADPH oxidase, but not by specific inhibitors of xanthine oxidase (allopurinol 300 μ M) or NO-synthase (L-NAME 100 μ M). Other inhibitors for lipoxygenase (NDG 5 μ M), for cyclooxygenase (indomethacin 500 μ M) or for cytochrome P450 oxidase (17-ODYA 5 μ M) were toxic to the cell system within 24 h and could not be examined further. The concentrations for the inhibitors were chosen according to references [151; 152].

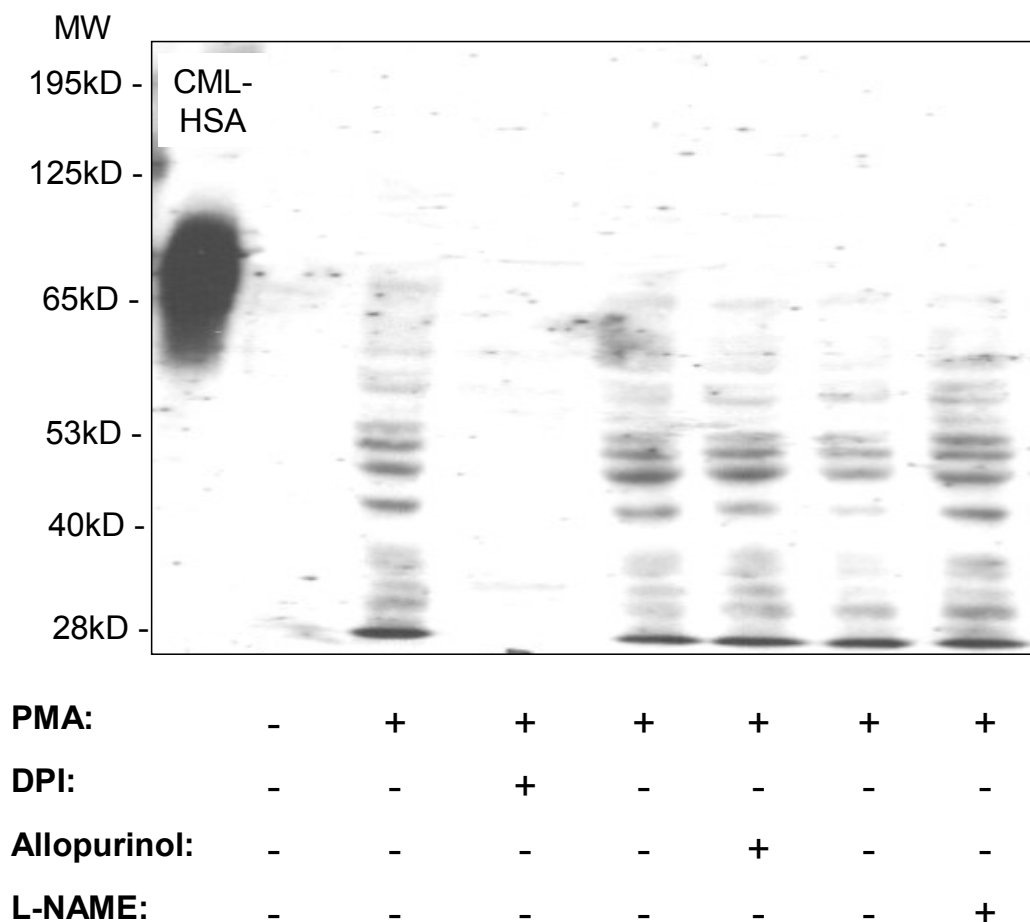


Figure 4-24. Effects of various oxidase inhibitors on the protein carboxymethylation in PMA-stimulated Mono Mac 6 monocytic cells. Pre-differentiated Mono Mac 6 cells were grown for 48 h without or with 20 nM PMA and either 100 μ M DPI (inhibitor for NADPH oxidase) or 300 μ M allopurinol (inhibitor for xanthine oxidase) or 100 μ M L-NAME (inhibitor for NO-synthase). Equal amounts of cell lysates were separated by SDS-PAGE and immunoblotted against a specific rabbit anti-CML antiserum. CML-immunoreactive proteins were visualised by enhanced chemiluminescence detection. For comparison, 0.1 μ g of highly-modified CML-HSA (33.6 mol CML/ mol HSA) was loaded on the left lane. Conditions: 7.5% polyacrylamide gels; 30 μ g protein/lane; primary antibody: rabbit anti-CML antiserum (Prof. Schleicher, Tuebingen, Germany), 1:8000, secondary antibody: anti-rabbit-IgG-HRP conjugate 1:3000; exposure 4 min. Abbreviations: DPI: diphenylene iodonium chloride; PMA: phorbol-12-myristate-13-acetate; MW: molecular weight; kD: kilo Dalton

4.3.3.2 Experiments with pre-differentiated PLB 985 and PLB 985 gp91 Δ 488-497 (NADPH oxidase knock out) monocytic cells

In NADPH oxidase knockout cells, CML formation is not abolished as compared to wild type monocytic cells:

The putative connection between NADPH oxidase activity and protein carboxymethylation was investigated further using the leukemia cell line PLB 985 for which a NADPH oxidase knock out mutant gp91 Δ 488-497 exists [134]. After pre-differentiation with 50 nM 1,25-(OH)₂-vitamin D3 according to the protocol of Perkins et al. [137], the characteristics of monocytic differentiation, such as adherence and change in morphology, became visible. As shown in **Figure 4-25**, a similar time-dependent degree of CML modification of cellular proteins in both, the wild type control and the NADPH oxidase knock out mutant was found under stimulation for 72 h.

Result: The time-dependent carboxymethylation of cellular proteins in stimulated monocytic cells is NADPH oxidase-independent.

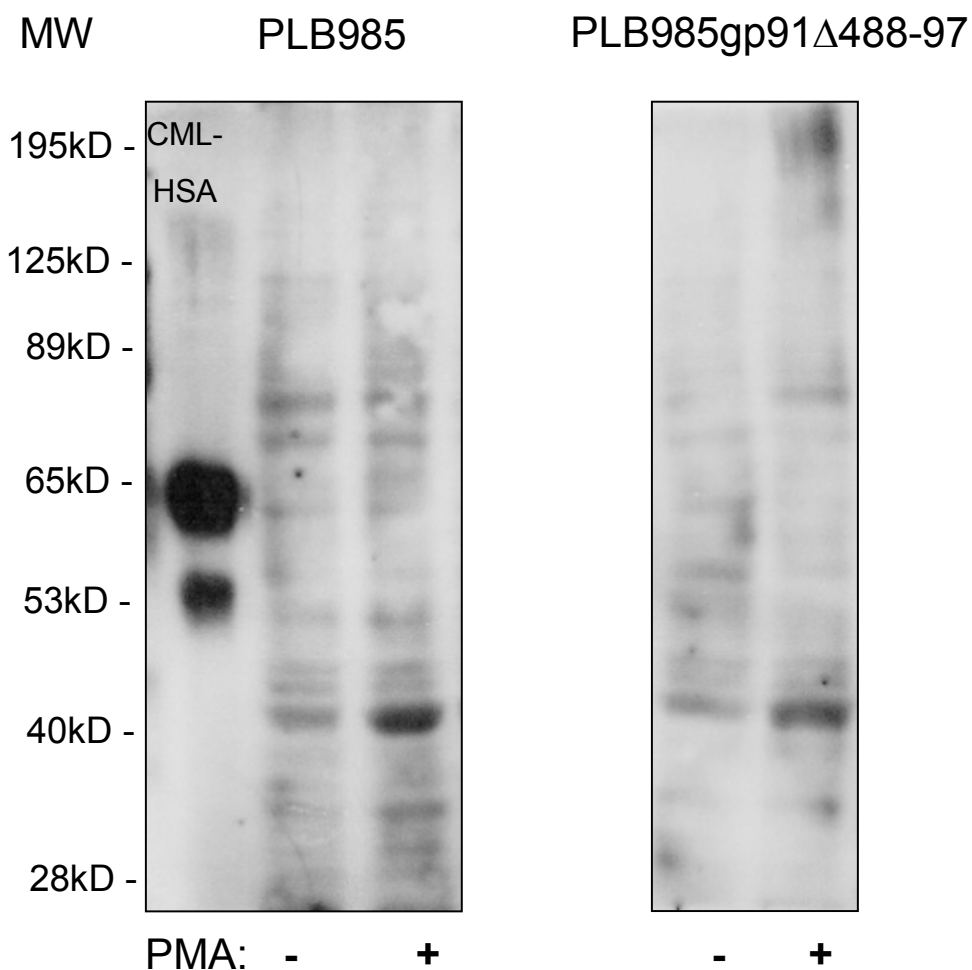


Figure 4-25. Western blot analysis of CML-modified proteins in PLB985 (wild-type) and PLB985 gp91 Δ 488-497 (NADPH oxidase-deficient) monocytic cells. Cells were pre-differentiated with 50 nm 1,25-(OH) $_2$ -vitamin D $_3$ for 3 days to show adherence as a sign of monocytic differentiation. Adherent cells were stimulated with 20 nM PMA for 72 h and harvested. Equal amounts of cell lysates were separated by SDS-PAGE and immunoblotted against a specific rabbit anti-CML antiserum. CML-immunoreactive proteins were visualised by enhanced chemiluminescence. Wild-type PLB985 monocytic cells showed an increased CML-modification of a 40 kD protein within 72 h. This effect was not abolished in the PLB 985gp91 Δ 488-497 mutant (NADPH oxidase-deficient), indicating, that NADPH oxidase is not required for the observed protein carboxymethylation. Conditions: 10 μ g protein/lane; 7.5% polyacrylamide gel; primary antibody: rabbit anti-CML antiserum (Prof. Schleicher, Tuebingen, Germany), 1:8000, secondary antibody: anti-rabbit-IgG-HRP conjugate 1:3000; exposure 15 min.

4.3.4 CML formation in stimulated N11 and N11/6 (NADPH oxidase deficient) microglia cells

The phagocytic form (PHOX) of NADPH oxidase has not only been described in granulocytes and monocytes, but also in microglia cells [153-156]. In the present study, the stimulation of N11 microglia cells by arachidonic acid (100 μ M) for 24 h led to increased CML modification of cell proteins (**Figure 4-26**). Other stimulators of microglial NADPH oxidase, described in the literature [154; 157], were used. But stimulation with PMA (20nM), fMLF (1 μ M), leukotriene B4 (2 μ M), lactosyl ceramide (5 μ M) or opsonised zymosan did not result in increased CML formation (data not shown) as compared to the controls (solvent only). DPI was found to be toxic within 24 h and could not be used in this cell type. Therefore, HMAP (2mM) was used for cell inhibition experiments. These experiments demonstrated that stimulation of N11 microglial cells led to a CML modification of cellular proteins by arachidonic acid which could be inhibited in part by HMAP, an unspecific NADPH oxidase inhibitor. Stimulation of NADPH oxidase deficient cells led to a comparable degree of protein carboxymethylation. Therefore, the CML formation did not depend on NADPH oxidase activity in this cell type.

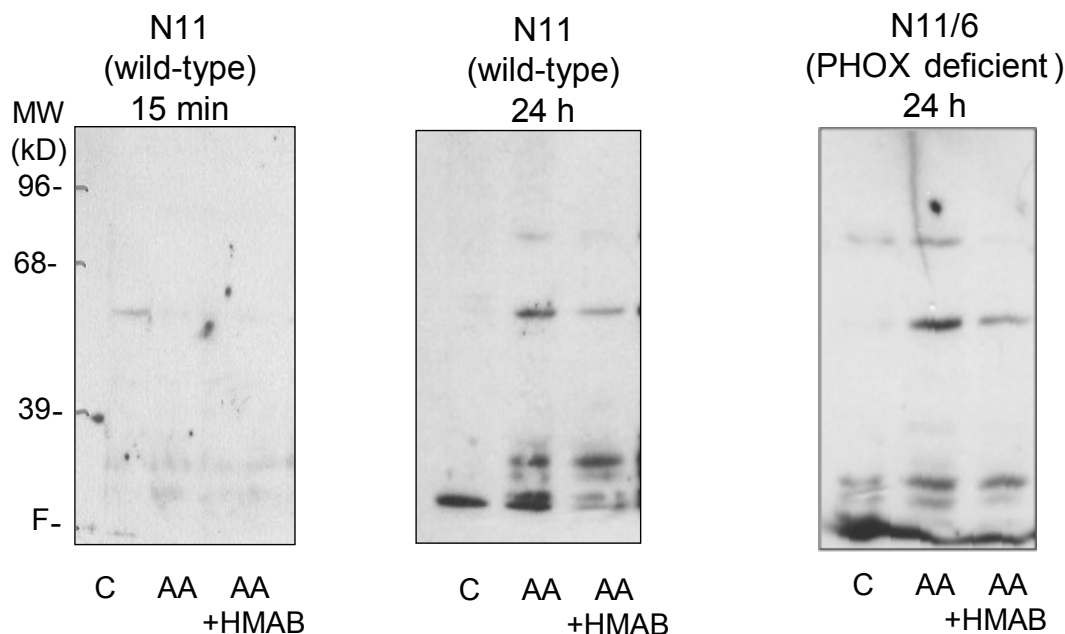
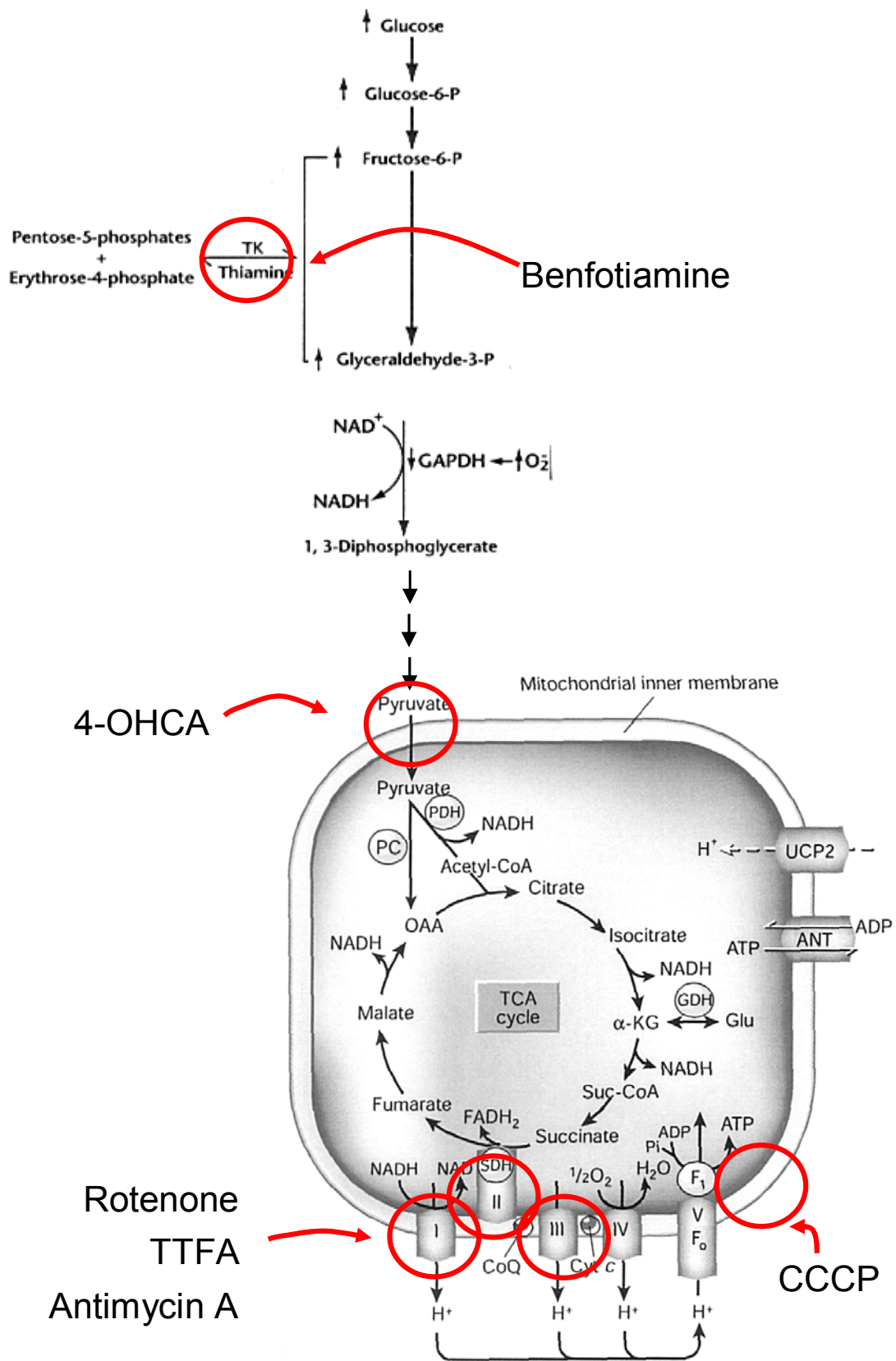


Figure 4-26. Western blot analysis of CML-modified proteins in N11 (wild type) and N11/6 (NADPH oxidase-deficient) murine microglial cells. Cells were stimulated for 15 min and 24 h, respectively, with 100 μ M arachidonic acid (AA) without or with the NADPH oxidase inhibitor HMAP (2mM). Equal amounts of cell lysates were separated by SDS-PAGE and immunoblotted against a specific rabbit anti-CML antiserum. CML-immunoreactive proteins were visualised by enhanced chemiluminescence. In N11 wild-type cells, cellular protein carboxymethylation was found within 24 h. This process is not dependent on phagocytic NADPH oxidase (PHOX) since it is not abolished in the NADPH oxidase-deficient mutant N11/6. Conditions: 10 μ g protein/lane; 7.5% polyacrylamide gel; primary antibody: rabbit anti-CML antiserum (Prof. Schleicher, Tuebingen, Germany), 1:8000, secondary antibody: anti-rabbit-IgG-HRP conjugate 1:3000; exposure 15 min. Abbreviations: AA: arachidonic acid; HMAP: 4-hydroxy-3-methoxy-acetophenon; PMA: phorbol-12-myristate-13-acetate; MW: molecular weight; kD: kilo Dalton; PHOX: NADPH oxidase.

4.3.5 Do inhibitors of the respiratory chain influence CML formation?

It was tested whether the compounds, listed in **Figure 4-27** influence CML formation in the cell culture model of PMA stimulated monocytic cells. As shown in **Figure 4-28**, and discussed in 5.3.3, a reduction of CML formation by 4-OHCA, an inhibitor of pyruvate transport through the mitochondrial membranes, and to some extent also by rotenone, an inhibitor for complex I, was observed but not by generalised uncoupling of the respiratory chain (CCCP) or by specific inhibition of complex II (TTFA) or complex III (antimycin A). This result was obtained by 3 different anti-CML antibodies and by the monoclonal anti-CE_L antibody 1F2A1(Novo Nordisk) which also crossreacts with CML (**Figure 4-28, E**).

Figure 4-27. (Figure see following page). Compounds used in the present study. Benfotiamine has been shown to prevent AGE formation by activating transketolase and diverting glycolytic intermediates to the pentose phosphate pathway. α -cyano-4-hydroxycinnamic acid (4-OHCA) reduces oxidative phosphorylation by inhibiting the pyruvate transport into the mitochondrium. Rotenone, 2-thenoyltrifluoroacetone (TTFA) and Antimycin A are selective inhibitors for the respiratory chain complexes I, II and III, respectively. The administration of carbonyl cyanide 3-chlorophenylhydrazone (CCCP) leads to a breakdown of the proton gradient across the inner mitochondrial membrane and to respiratory chain uncoupling. For all of these compounds an inhibition of ROS production from the respiratory chain and, in part, of cellular AGE formation has been described. Abbreviations: TK: transketolase (Collected from [30; 65; 158]).



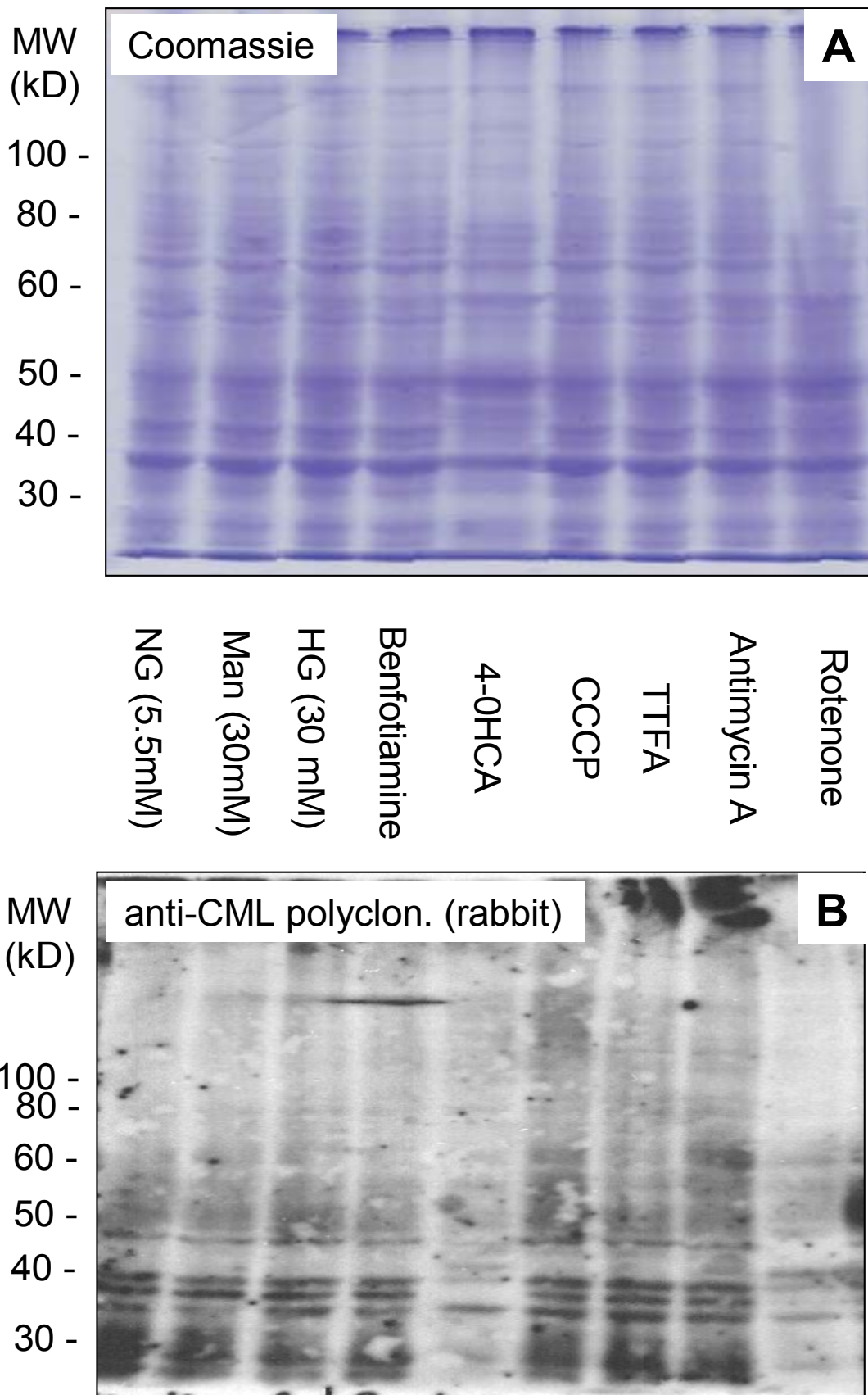


Figure 4-28. Legend see p. 122.

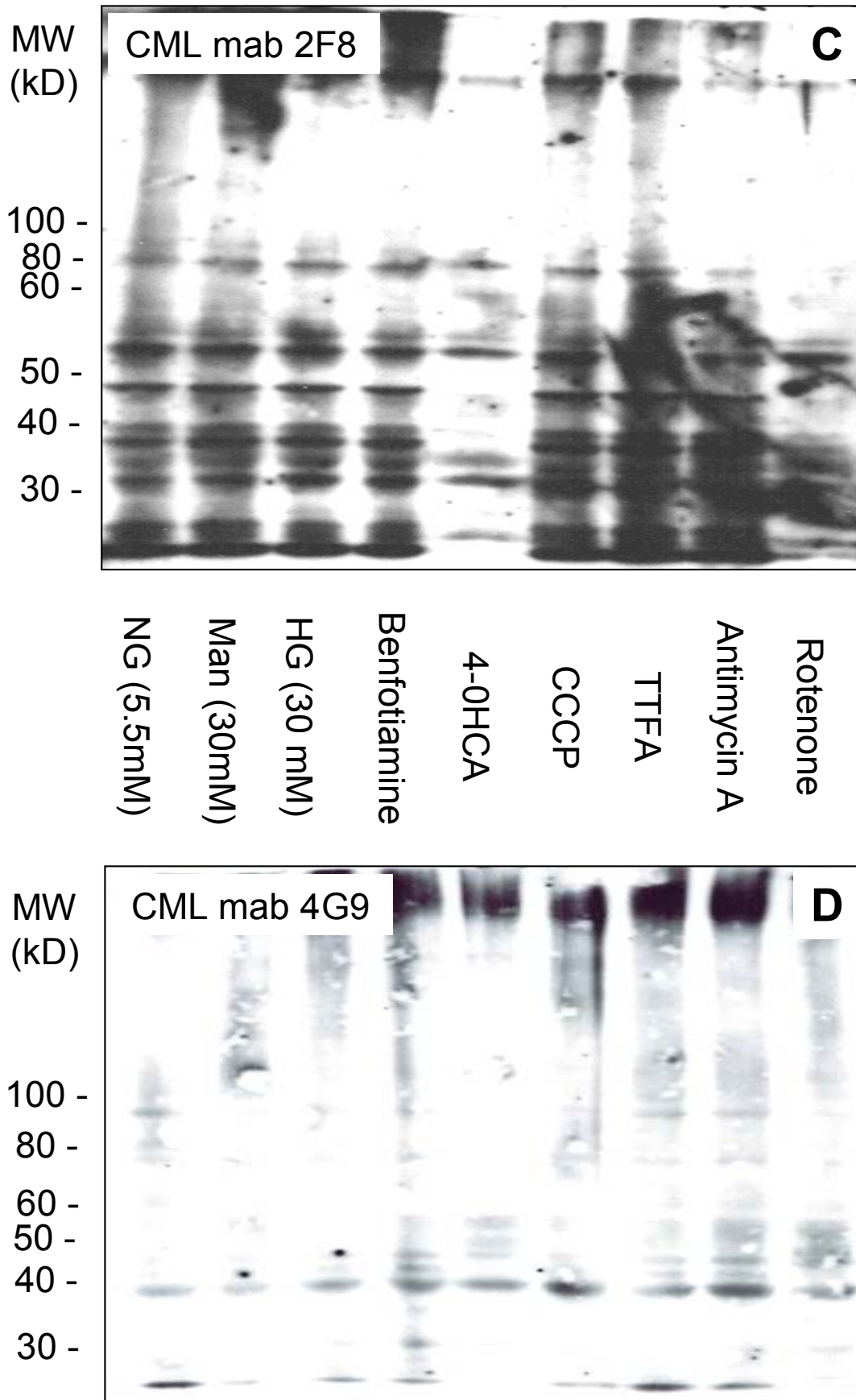


Figure 4-28 (continued). Legend see p. 122.

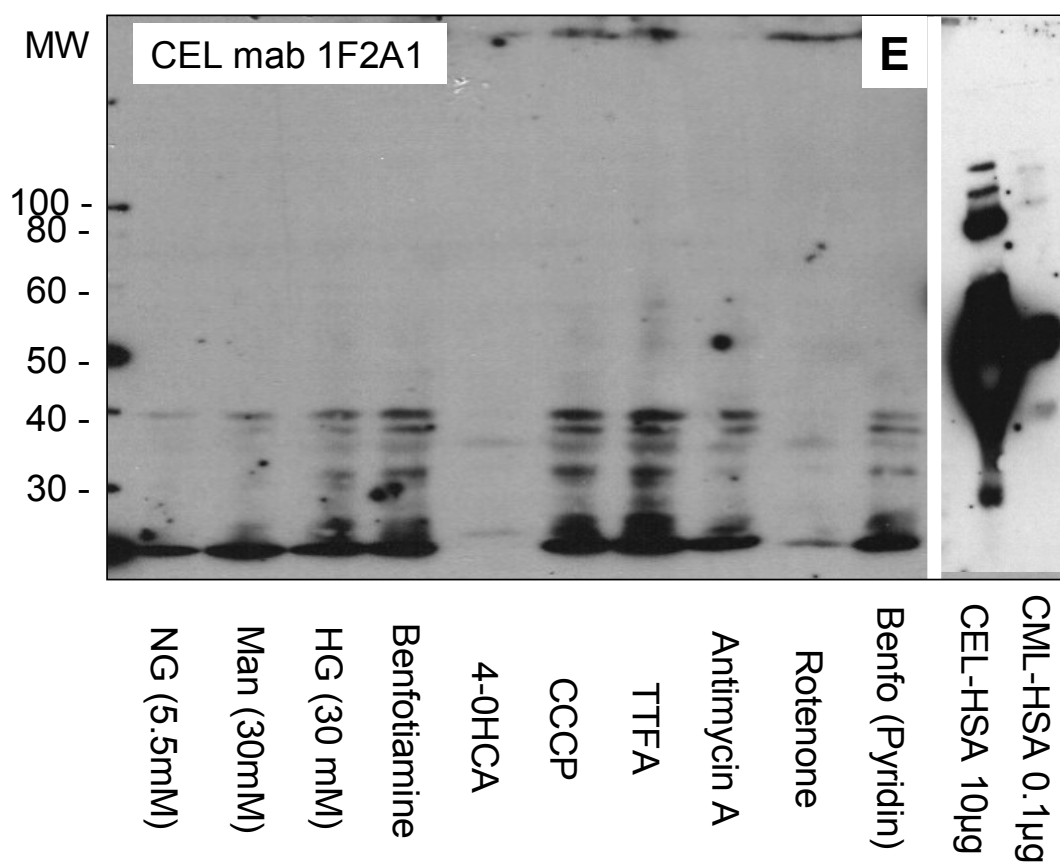


Figure 4-28. Influence of various inhibitors of respiratory chain-mediated ROS production on CML formation. Pre-differentiated Mono Mac 6 monocytic cell were stimulated with 20 nM PMA for 72 h in cell culture medium containing 5.5 mM glucose (normal glucose, NG), 30 mM mannitol (isoosmotic control, Man) or 30 mM glucose (high glucose, HG) without or with inhibitors of cellular ROS formation. Equal amounts of cell lysates were separated by SDS-PAGE on parallel gels and stained with Coomassie brilliant blue (A) or transferred to nitrocellulose membranes and immunoblotted against 3 different anti-CML antibodies (B-D) and an anti-CEL antibody (E) which is crossreactive for CML (E, right lane). (Conditions: benfotiamine 50µM; 4-OHCA 250 µM; CCCP 2.5µM; TTFA 10µM; antimycin A 0.3µM; rotenone 5µM; Western blot: 30 µg/lane; 7.5 % polyacrylamide gels; (B): polyclon. anti-CML 1:8000; (C): anti-CML mab 2F8 1:5000; (D): anti-CML mab 4G9 1:5000; (E): CEL mab 1F2A1 1:1000; exposure 45 min).

4.3.6 Identification of CML-modified proteins

Two different approaches were employed in order to identify some of the CML-modified proteins: (a) Immunoabsorption/immunoprecipitation and (b) 2-D-gel electrophoresis (IPG-DALT/SDS-PAGE) of cell lysates with anti-CML Western blot analysis.

Three different monoclonal CML-antibodies were used:

- (1) monoclonal mouse anti-CML-AK 4G9 (obtained from Roche)
- (2) monoclonal mouse anti-CML-AK 2F8A (obtained from NovoNordisk)
- (3) the monoclonal mouse anti-CML-AK NF1G (obtained from Transgenics)

CML antibodies were absorbed or coupled to (1) NHS-sepharose columns (Amersham Pharmacia Biotech, Freiburg), (2) Protein A- and G-coated magnetic beads (Dynal, Hamburg), (3) anti-IgG-coated magnetic beads (Dynal, Hamburg), (4) Spin-column kits with activated sepharose or with (5) protein A/G-sepharose without or (6) with covalent crosslinking of the CML-antibodies (all from Pierce, Bonn), and (7) classic immuno-precipitation with protein A/G-sepharose. So far, no CML-immunoreactive proteins could be precipitated. Further work will be required to isolate and identify these CML-reactive protein bands.

5 DISCUSSION

5.1 CML excretion in urine

In the present study a specific, reproducible and sensitive HPLC method for the determination of CML excretion in urine has been developed [159]. It has been proposed that the measurement of CML in urine may serve as an integrative biomarker for systemic oxidative stress [160], since its formation requires oxidative chemistry and since CML is the chemically best-defined and most abundant glycoxidation product. Previously, CML in urine has been measured using immunoassays [161]. Several monoclonal and polyclonal antibodies have been raised against CML-modified proteins and peptides and used to measure CML. However, until now, there has been no universally established standard or unit of measurement to compare results from different immunological assays [20; 161]. CML in urine originates from structurally heterogenous compounds which do not share a well defined common epitope, ranging from the free monomer CML to carboxymethylated oligopeptides/polypeptides and proteins [162; 163].

Therefore, the determination of the free modified amino acid CML using chromatographic separation techniques and synthetic CML as a defined standard will provide an advantage. Previously, Knecht et al. have used SIM-GC-MS and ($^2\text{H}_8$)CML as a deuterated internal standard to determine CML in urine [164]. Although this method is specific and very precise, it is not widely available. Drusch et al. [165] had described previously a RP-HPLC method to determine the total CML content of fresh and heat-treated food samples. By adapting this method to urine, a

sensitive and specific assay, using standard equipment, has been developed. A drawback of all methods used, be it GC-MS or HPLC, is the low dynamic range. Excreted urine volumes and analyte concentrations (e.g. of physiological amines and amino acids which are approximately in a 50- to 500-fold excess to CML) vary widely. Therefore, a sample preparation step of evaporation, resuspension and predilution could not be omitted. The values obtained for urinary CML are in good agreement with the few published reports available in the literature. Knecht et al. [164], using SIM-GC-MS in hydrolysed urine, found CML-levels of $1.2 \pm 0.5 \mu\text{g}/\text{mg}$ creatinine (equivalent to $0.67 \pm 0.28 \mu\text{mol}/\text{mmol}$ creatinine) in diabetic subjects. Wagner et al. [166] determined urinary CML in type II diabetic patients and found CML excretion rates of $130 \pm 50 \mu\text{g CML} / \text{mmol creatinine}$ (equivalent to $0.64 \pm 0.25 \mu\text{mol}/\text{mmol crea}$) in diabetic patients with moderate renal impairment.

In diabetic patients, it was found in the present study that the urinary excretion of CML was increased by 30 % compared to young and age-matched non-diabetic controls. This observed increase in total CML excretion in diabetes was due mainly to an increase in protein- and peptide-bound CML (**Figure 4-7**). These data, as well as recent findings from other studies [167], indicate that albuminuria could be the source for the elevated CML excretion observed in diabetes. As shown in **Figure 4-8**, the patients in the present study exhibited an increased albumin excretion. Among the major proteins in serum and urine, albumin is especially prone to carboxymethylation because of, both, its low turnover rate and its high lysine content. Hamelin et al. [167] reported just recently, that CML-albumin is the major excreted

CML-modified protein in rats. In their study, the excretion of CML-albumin was correlated to glycoxidative tissue and kidney damage. In the cohort of diabetic patients examined in the present study, a significant correlation between the degree of proteinuria (most of the excreted protein being albumin) and albuminuria to the urinary excretion of bound CML was found, whereas no such correlation could be observed for the total or free CML excretion (data not shown). A proportion of about 40 % of the excreted CML, which had not been removed by precipitation, was the free amino acid CML. This fraction, originating from protein catabolism or from nutritional sources, was not significantly different between the diabetic and non-diabetic patients.

The observation, that CML-levels in body fluids are not directly correlated to blood glucose control and to HbA1c is in agreement with that of others [45; 168]. Urinary excretion of total CML can not be used as a glycation marker since, both, circulating and excreted CML are known to result from a variety of different metabolic or dietary sources [169]. Koschinsky et al. [170] described that 10% of the ingested AGEs are absorbed into the systemic circulation and that one third of that is excreted within 48 h in the urine in patients with normal renal function. Nevertheless, the results from the present study indicate that the specific determination of CML-modified albumin might be useful as a marker for generalised oxidative stress or glycoxidative kidney damage. The development of assays for CML-albumin, e.g. by mass spectrometric techniques or by antibodies truly specific for CML-modified albumin, are required to clarify this issue further.

5.2 Pathophysiological significance of CML accumulation in diabetes and in chronic inflammatory or chronic degenerative diseases

5.2.1 Over a life time the amount of protein glycation in tissues remains almost constant but the CML content increases in an age-dependent fashion

Protein glycation is an inevitable process even under normal ambient glucose concentrations and it is enhanced in the presence of hyperglycemia. First evidence for posttranslational glucose modifications came from the discovery of the non-enzymatically glycosylated hemoglobin, HbA_{1c}, which was found to carry a glucose Amadori product at its N-terminal valine. Thus, determination of HbA_{1c} became a measure for the amount of Amadori product present in red blood cells. An elevated HbA_{1c} level indicates sustained hyperglycemia in diabetic patients. Subsequently, it was observed that not only hemoglobin but also long-lived proteins of the extracellular matrix and of serum proteins exhibit increased glycation in diabetes. However, there is little evidence that glycation *per se* is a dangerous process (reviewed in [14; 171]). Because of its reversibility and of protein turnover, the extent of protein glycation rarely exceeds 1 % of the lysine residues. The amount of glycation of the extracellular matrix components remains constant over a life time and it is not or only marginally increased in advanced age. This holds particularly true for the matrix of tendons, aorta, coronary arteries, glomerular capillaries and lung [172]. In contrast to glycation, the formation of advanced glycation end-products, i.e. CML, is an irreversible process and CML accumulates naturally in long-lived proteins found in skin or lens tissue at a slow rate under normal glucose conditions, but it is enhanced in the presence of

hyperglycemia and/or when the protein and lipid turnover is prolonged [44].

5.2.2 CML accumulation in extracellular matrix proceeds slowly as an inevitable process over months to years and is increased by hyperglycemia

CML in extracellular matrix is barely detectable at birth and increases linearly with age [42; 43; 173]. In diabetes CML formation occurs at an accelerated rate [44] and elevated age-adjusted levels of CML have been correlated with the severity of diabetic retinopathy and nephropathy [45; 174; 175]. Accumulation of CML in extracellular matrix proceeds slowly and takes months to years.

5.2.3 Under oxidative conditions, CML formation proceeds within hours to days, especially in lesioned tissue and intracellularly

It soon became obvious that CML is formed at a much faster rate when oxidative conditions are present. In *in vitro* studies, using the compound fructose-lysine as a model compound, it could be shown that CML is formed within hours in the presence of oxygen by a free radical mechanism involving superoxide radicals and hydrogen peroxide [92]. Subsequent studies showed rapid intracellular CML formation to occur, within hours to days, in cell culture experiments [45; 88; 109; 131]. Observations from the present study, as well as those from numerous investigations by other authors, indicate that CML formation is a characteristic of lesioned tissue in a variety of diseases in which oxidative stress is implicated in the pathophysiological mechanism. The most widely studied conditions are

- a. Diabetes mellitus and diabetic organ damage,

-
- b. atherosclerosis and vascular disease,
 - c. Alzheimer's disease and neurodegenerative brain disorders,
 - d. degenerative disorders, such as osteoarthritis, and
 - e. inflammatory diseases.

In the following paragraph, the presented observations will be discussed in the context of the current literature.

5.2.3.1 CML accumulation in diabetic organ damage

The results obtained from nerve tissue showed a deposition of CML-modified proteins in the perineum and in vessels of diabetic and vasculitic neuropathy. Western-blotting confirmed the specificity of the CML antiserum. In Western blots, distinct bands were stained which differed from the CML-modified human serum albumin, indicating that the immunohistochemical staining pattern was not caused by plasma proteins. Furthermore, the finding of an increase in CML in the diabetic nerve tissue was confirmed by Western blot analysis. In vasculitic polyneuropathy (PN), CML accumulated in CD4, CD8 or CD68 positive infiltrating mononuclear cells. In contrast, only weak or absent CML was found in demyelating or degenerative PN, where oxidative stress is not considered to be a key pathogenic factor [141].

The presented data on CML localisation confirm the results of Sugimoto et al. [176] concerning the perineurial and vascular CML localisation. However these authors, using a different monoclonal antibody (but one which recognises CML as a major epitope) also found CML-staining in axons and Schwann cells. By immuno electron microscopy and confocal laser scanning microscopy with FITC-labelled secondary antibodies, these

authors demonstrated increased CML immunoreactivity, both, extra- and intracellularly in perineurial and endoneurial tissue, as well as in endoneurial microvessels. CML accumulation was significantly increased in diabetic tissue, but no age dependency was observed [176]. The question was raised as to whether intracellular CML had been taken up by endocytosis. However, when examined on a subcellular level, intracellular CML did not reveal a specific affinity with the lysosomes or cytoplasmatic organelles, but rather distributed itself as electron dense aggregates on the microtubules and neurofilaments. The authors suggested that this distribution would be in accordance with previous findings of excessive glycation of tubulin and neurofilaments in the nerve of diabetic animal models [176].

Until now, the origin of intracellular CML remained a matter of debate, and it is still an open question as to whether the observed CML deposits, such as those observed in diabetes, are the result of hyperglycemia-induced *in situ* accumulation or whether CML is derived from (non-glucose related) secondary products formed by oxidative stress. The present finding of pronounced cytoplasmatic CML staining in perivascular mononuclear cells suggests either an increased intracellular formation of CML-modified proteins or an increased endocytic uptake of CML formed extracellularly in an environment of increased oxidative stress. At least, the accumulation of CML can be taken as a biomarker of oxidative stress in the tissue lesion. Whether CML is a causal factor in the initiation of inflammation or tissue damage or whether CML production in endothelial and perineurial cells is secondary to the elevated free radical production in mononuclear cells remains to be determined. Within the last five years, increased CML deposits

have been found in all tissues prone to diabetic complications. The findings of the present study and the observations of other authors on CML accumulation in diabetic neuropathy, diabetic retinopathy, diabetic nephropathy and diabetic vascular damage are summarised in **Table 5-1**.

Longstanding diabetes mellitus is associated with micro- and macroangiopathic changes. The observation of CML accumulation in diabetic muscle is in good accordance with this general notion. In muscle of diabetic patients, several distinct CML-modified proteins compared to normoglycemic age-matched controls were found in Western blots. More strikingly, the pattern of CML proteins from the diabetic muscle resembles that obtained from a muscle of a patient with severe generalised atherosclerosis caused by heavy smoking. This can be explained by the presented observations on the histological distribution of CML immunoreactivity in diabetic muscle as shown in **Figure 4-13 a**: even in diabetes, CML immunoreactivity was confined to the vasculature. The parenchymal muscle cells and connective tissue were both free from CML. In the current work and in most of the cited studies, CML immunoreactivity has been found in the microvasculature in the organs prone to diabetic late complications. This also holds true in organs which are not the primary target tissue for diabetic end organ damage such as the skeletal muscle (present study) and heart muscle [177]. Therefore, Wautier et al. [178] proposed the determination of CML in blood as a biomarker for microvascular complications in type II diabetic patients.

Table 5-1: Increased CML/AGE depositions in target tissues of diabetic complications (data describing explicitly intracellular CML accumulation are given in bold).

Diabetic complication	References	Antibody	Immunohistochemical localisation of CML/AGE	Species
Diabetic neuropathy	Present study [141]	CML	vessels, perineurium	human
	Sugimoto et al. (1997) [176]	CML	endothel, perineurial, endoneurial cytoplasmatic in axons, Schwann cells, pericytes, endothelial cells (immuno electron microscopy/ confocal fluores. laser scanning microscopy)	human
	Soulis et et al. (1997) [121]	AGEs	nerve	rat, experimental
Diabetic macro/micro-angiopathy	Present study	CML	muscle, small arteries	human
	Schalkwijk et al. (2004) [177]	CML	heart, small vessels	human
	Schleicher et al.(1997) [41]	CML	aortal wall, renal artery, intracellular in macrophages/'foam cells'	human
Diabetic nephropathy	Uesugi et al. (2001) [181]	CML	intracellular in CD68-positive macrophages	human

Diabetic complication	References	Antibody	Immunohistochemical localisation of CML/AGE	Species
	Tanji et al. (2000) [119]	CML	vessels, mesangium, glomerular/tubular basal membrane, colocalisation with RAGE	human
	Miyata et al. (1999) [28]	CML	expanded mesangial matrix, nodular lesions	
	Kushiro et al. (1998) [182]	CML	glomeruli, mesangium	rat, experimental
	Imai et al. (1997) [183]	CML	early: arterial walls, late:glomerular lesions	human
Diabetic retinopathy	Stitt et al. (2002) [180]	CML	retinal pigment epithelium/plexiform layer	rat, experimental
	Endo et al. (2001) [184]	CML	glial cells, capillaries	rat, experimental
	Hammes et al. (1999) [185]	CML	retina (nuclear layer, photoreceptors, glial cells, capillaries) (intra-/extracellular)	rat, experimental human

Further evidence for the potential involvement of CML in the pathogenesis of diabetic microvascular disease and of diabetic organ damage comes from observations in animal models where functionally unrelated inhibitors of the formation of CML and other AGEs partially prevented various functional and structural manifestations of diabetic microvascular disease in blood vessels, retina, kidney and nerve. Soulis et al. [179] observed in an experimental diabetic rat model that the compounds aminoguanidine and 2,3-diaminophenazine inhibited the increased formation of AGEs in the vessels of diabetic animals and prevented the formation of mesenteric vascular hypertrophy. Stitt et al. [180] reported that the AGE inhibitor pyridoxamine reduced the retinal accumulation of CML and protected against the development of diabetic retinopathy in streptozotocin-induced diabetic rats. Most recently, Nakamura et al. reported a reduced CML formation and the retardation of diabetic nephropathy in diabetic OLETF rats in the presence of the AGE inhibitor OPB-9195 [114].

5.2.3.2 CML accumulation in atherosclerosis and vascular disease

As discussed above, the vasculature is the preferred localisation of CML accumulation in diabetic macro- and microangiopathy and also in atherosclerosis associated with other conditions such as in uremia. Since specific CML antibodies have become available, several studies have demonstrated the accumulation and distribution of CML in atheromatous lesions [34; 46; 107; 186; 187] [188]. The current literature is reviewed in **Table 5-2**. In most studies, CML modification of the extracellular matrix was observed in areas of intimal fibrosis and atheromatous plaque

formation, but several authors [34; 46; 186] have made the intriguing observation of a strong cytoplasmatic CML staining within 'foamy macrophages'. Horiuchi et al. [46] described dense intracellular CML deposits in macrophage-derived foam cells (PM-2-K positive cells) in early stages of atherosclerosis (intimal thickening and fatty streak lesions) and strong CML accumulation in macrophage- and SMC-derived foam cells (HHF35-positive cells).

There is ongoing debate about the origin of intracellular CML. On the surface of macrophages and other cells, AGE binding proteins/receptors such as the macrophage scavenger receptor (MSR) and the receptor for AGEs (RAGE) have been characterised [123]. One explanation for CML accumulation may be that macrophages and smooth muscle cells bearing AGE-binding receptors readily take up and degrade CML-modified matrix proteins from the plaques. Horiuchi et al. [46] described that more than 60% of CML-loaded foam cells in atherosclerotic lesions also showed positive reaction to anti-MSR antibodies. However, the unexpectedly high intracellular CML-staining in macrophages may also be explained by intracellular *de novo* formation. At present, there is evidence that both mechanisms can take part in the accumulation of CML: the endocytic uptake of AGE-modified extracellular matrix components [189-191] and the intracellular formation from lipid peroxidation and other oxidative metabolic processes [31; 88; 125; 131]. To clarify this issue of intracellular CML formation, further studies in cell culture systems and the systematic analysis of the CML-modified proteins are required.

Table 5-2: Increased CML/AGE depositions in atherosclerosis (data describing explicitly intracellular CML accumulation are given in bold).

Tissue	References	Antibody	Immunohistochemical localisation of CML/AGE	Source
Aorta/large arteries (atherosclerosis)	Nerlich et al. (1999) [34]	CML	endothel, myofibroblasts/smooth muscle cells, macrophages (occasional)	human
Aorta (atherosclerosis/uremia)	Takayama et al. (1998) [107]	CML	aorta (all layers)	human
Aorta (atherosclerosis)	Sakata et al. (1998) [187]	CML/AGEs	macrophages/foam cells	human
Aorta (atherosclerosis)	Horiuchi et al. (1996) [46]	CML	macrophage-deriv. foam cells (PM-2K-pos.), SMC-derived foam cells (HHK35 pos.)	human
Aorta (atheroclerosis)	Kume et al. 1995 [186]	CML	macrophages, SMC, derived foam cells	human

5.2.3.3 CML formation in Alzheimer's disease and other neurodegenerative conditions

In the current study it has been shown for the first time that intracellular CML formation can be demonstrated in N11 microglial cells under stimulation with arachidonic acid, an agent known to evoke NADPH-dependent intracellular ROS production [192; 193].

CML has been shown to accumulate in aging and at an increased rate in Alzheimer's disease (AD) by various authors [102; 103; 194] and, thus, it has been suggested to play a role in the aging process as well as in the pathogenesis of AD. Recently, Takeda et al. [102] examined brain tissue from patients with AD and described that the increased intracellular CML accumulation seen in glial cells is disease-specific for AD: In this study, electron microscopy was used to examine the subcellular distribution and CML was found intracellularly in the microglial cytoplasm as well as in the cytoplasm of astrocytes and neuronal cells. The glial CML found was generally more prominent in AD brains than in aged brains [102]. As in the case of foam cells in atherosclerosis, the question was raised as to whether the glial CML was derived from the degenerating neurons and had been taken up subsequently by endocytosis. However, the electron microscopic features of glial CML were not those of endocytosomes and the glial CML was also prominent in regions without neuronal loss. Thus, the authors favored the hypothesis that glial CML was primarily synthesised in the glial cytoplasm, especially since recently various oxygen radicals and carbonyl compounds known to promote the formation of CML have been demonstrated in AD brains [195; 196]. This hypothesis is supported by the new finding

from the present study of intracellular CML formation in stimulated N11 microglial cells.

Besides AD, disease-specific CML accumulation has been described in other neurodegenerative disorders such as Pick's disease [197] or amyotrophic lateral sclerosis [198]. The pertinent findings from the literature are summarised in **Table 5-3**.

5.2.3.4 CML formation in degenerative conditions as osteoarthritis

In the present study, it was observed and published for the first time [201] that in osteoarthritis (OA) CML is accumulating intracellularly, namely in chondrocytes of the lesioned cartilage and in subchondral osteocytes (**Figure 4-14**). Drinda et al. [101] have confirmed these findings for OA shortly thereafter and reported an even higher CML accumulation in rheumatoid arthritis (RA), an inflammatory condition of the synovial lining and adjacent structures of the joint. **Table 5-4** summarises the current finding together with pertinent reports from the literature on degenerative conditions, where increased CML formation has been demonstrated intracellularly.

Table 5-3: Increased CML/AGE depositions in neurodegenerative conditions (data describing explicitly intracellular CML accumulation are given in bold).

Tissue	References	Antibody	Immunohistochemical localisation of CML/AGE
Brain (Alzheimer's disease)	Takeda et al (2001) [102]	CML	microglia cells (AD > aging), neurons, astrocytes (electron microscopy)
	Dei et al. (2002) [104]	CML	glial cells (AD >aging), neurons (electron microscopy)
	Munch et al. (1998) [103]	AGEs	neurons, Hirano bodies
	Castellani et al. (2001) [199]	CML	neurons
Brain (Picks's disease)	Kimura et al. (1996) [197]	CML	neurons, Pick's bodies
CNS (Amyotrophic lateral sclerosis)	Kikuchi et al. (2002) [200]	CML	atrophic motor neurons, glial cells

Abbreviations: AD: Alzheimer's disease; CNS: central nervous system

Up to now it has not been clarified whether chondrocytes in osteoarthritis produce CML or whether there is a receptor-mediated uptake of the CML-modified proteins [108]. In Western blot analysis of total tissue protein extracts three distinct CML-modified protein bands were found (see **Figure 4-15**) in the molecular weight range of 39 - 68 kDa which did not react with antibodies specific for major extra-cellular matrix (ECM) components such as osteopontin, collagen II, aggrecan or cartilage oligomeric matrix protein (COMP) [201]. This could indicate that the observed CML-modified proteins have been formed intracellularly. Recently, it has been described that cytokines, in particular tumor necrosis factor alpha ($\text{TNF}\alpha$), induce the formation of AGEs *in vitro* [202] and that $\text{TNF}\alpha$ is enhanced in OA chondrocytes. Hiran et al. [203; 204] described a cellular NADPH oxidase and the NADPH oxidase-dependent production of superoxide anions and other ROS in stimulated porcine articular chondrocytes. To further clarify the origin of intracellular CML in chondrocytes and the role of NADPH oxidase-dependent oxidative stress, the characterisation of some of the CML-modified proteins will be required.

5.2.3.5 CML formation in inflammatory conditions

A prominent finding of the present study is the pronounced intracellular CML accumulation in inflammatory mononuclear cells and the rapid CML modification of cellular proteins in stimulated monocytic (Mono Mac 6) and macrophage-related cells (N11 microglia cells). Using immunohistochemistry, CML depositions have been demonstrated in inflammatory conditions of nerve (vasculitic neuropathy) and muscle (dermatomyositis,

polymyositis). This is in clear contrast to the non-inflammatory polyneuropathies examined: in CDIP, a form of demyelating PN, and in Charcot-Marie-Tooth disease type I (CMT I), a degenerative PN, little to no CML has been found in the tissue.

The observation of CML accumulation in infiltrating macrophages and lymphocytes in the tissue lesions is in line with other reports which have been summarised in **Table 5-5**. Drinda et al. [101] described the presence of CML-loaded macrophages and long-lived T-lymphocytes in the synovial tissue in rheumatoid arthritis (RA) and confirmed the cell's identity by double staining against CD68 and CD45Ro, respectively. In RA, increased CML-staining was also described in the synovial lining and sublining and in the endothelium as compared to healthy control tissue. In a previous report from this laboratory [205], investigating the distribution of CML in normal intestinal mucosa and in chronic inflammatory bowel disease, CML-loaded infiltrating or resident macrophages have been found as a characteristic of inflammatory tissue changes in chronic active and inactive colitis ulcerosa and in M. Crohn. In this report, additional CML staining was observed in apical enterocytes and in interstitial cells, which was significantly increased in inflammatory bowel disease as compared to healthy intestinal tissue.

Table 5-4: Increased CML/AGE depositions in degenerative conditions (data describing explicitly intracellular CML accumulation are given in bold).

Tissue	References	Antibody	Immunohistochemical localisation of CML/AGE
Joints (Osteoarthritis)	Present study [201]	CML	chondrocytes
	Drinda et al. (2002) [101]	CML	vascular endothelial cells, synovial lining, inflammation cells (few)
Retina (Macular degeneration)	Hammes et al. (1999) [124]	CML	CD68 pos. macrophages

Table 5-5: Increased CML/AGE depositions in inflammatory conditions (data describing explicitly intracellular CML accumulation are given in bold).

Tissue	References	Antibody	Immunohistochemical localisation of CML/AGE	Source
Nerve (Vasculitic neuropathy)	Present study [206]	CML	CD4, CD8 pos. lymphocytes, CD68 pos. macrophages in epineural and perivascular infiltrates	Human
Muscle(Polymyositis/ Dermatomyositis)	Present study	CML	Infiltrating mononuclear cells	Human
Joints/Synovia (Rheumatoid arthritis)	Drinda et al. (2002) [101]	CML	CD68 pos. Macrophages CD45Ro pos. lymphocytes	Human
Intestinum (Colitis ulcerosa)	Schleicher et al. (1998) [205]	CML	Macrophages Enterocytes	Human

5.2.4 Is intracellular CML actually formed within the cell?

As shown in the preceding paragraphs, under numerous pathological conditions CML accumulation has been localised intracellularly, especially in infiltrating macrophages and other inflammatory cells. There is ongoing debate, whether the observed depositions represent CML-modified proteins or other macromolecules *actually formed within the cell*, or rather reveal material which has been taken up by endocytosis. To date, there is evidence that both processes occur.

Strong evidence for intracellular *de novo* carboxymethylation of cellular proteins comes from the present data in differentiated monocytic Mono Mac 6 cells. In this cell culture model it was demonstrated for the first time that normal and high glucose conditions, in combination with stimulation by PMA, leads to time-dependent CML modification of distinct cellular proteins. During the experimental conditions great care was taken to ensure that cell pellets were washed thoroughly (resuspended and washed three times in PBS) to remove traces of fetal serum proteins originating from the culture medium. The fetal calf serum itself clearly contains CML-modified proteins, mainly CML albumin, as shown in the experiment using granulocyte suspensions (see paragraph 4.3.2): at the start of the experiment there was already a carboxymethylated protein band at approx. 65 kDa visible in the anti-CML Western blots of culture medium. (see

Figure 4-18). In contrast to this observation, in whole cell lysates from washed cell pellets, no or very little CML immunoreactivity was observed in the early stages (0 – 8 h) of the cell culture experiments using Mono Mac 6 cells. CML formation developed

in a time-dependent fashion at later time points (24 – 72h) indicating that *de novo* CML formation has occurred (see **Figure 4-21 c-f**).

The present findings are in line with observations in various cell types and cell culture models made by other authors. **Table 5-6** reviews recent studies where intracellular *de novo* synthesis has been described in cultured cell lines of epithelial [126], endothelial [31; 125] and neuronal [88; 127] origin. The findings concerning CML-formation in *ex vivo*-isolated circulating blood cells are listed in **Table 5-7**. In the cited reports, oxidative stress was generated either by ROS-generating enzymes, most obviously in granulocytes, where stimulation resulted in an ‘oxidative burst’ from myeloperoxidase and NADPH oxidase [130], or by high glucose-driven superoxide anion production from the respiratory chain [125]. Another mechanism for intracellular CML formation was to diminish antioxidative defense, e.g. by GSH depletion through menadione [45].

Table 5-6. In vitro formation of AGEs in cell lines by stimuli inducing oxidative stress or diminishing antioxidative defense.

Stimuli (References)	Cells	AGE
PMA (Present study)	Human monocytic cells Mono Mac 6	CML, intracell.
Glyoxal (Kasper et al. [126])	Human lung epithelial cells L 132	CML, intracell.
Glyoxal / 3-DG (Niwa et al. [88])	Cultured rat sensory neurons	CML, intracell.
Methylglyoxal / 3-DG (Kikuchi et al. [127])	Cultured cortical neurons	AGEs, intracell.
High glucose/GSH-depletion (Giardino et al [31; 207])	Bovine aortic endothelial cells	AGEs, intracell.
PMA: phorbol 12-myristate 13-acetate, 3-DG: 3-deoxyglucosone, GSH: reduced glutathione		

Table 5-7. Cellular CML formation in ex vivo-isolated circulating leukocytes.

Stimuli (References)	Cells	AGE
Zymosan (Present study)	Human ex vivo granulocytes	CML, extracell.
PMA (Anderson et al. [130])	Human ex vivo granulocytes	CML, extracell.
Diabetes (Present study)	Human ex vivo granulocytes	CML, intracell.
Short term hyperglycemia (Schiekofer et al. [109])	Human ex vivo PBMCs	CML, intracell.
Menadione (Hammes et. al [45])	Human ex vivo lymphocytes	CML, intracell.
PMA: phorbol 12-myristate 13-acetate; PBMC: peripheral blood mononuclear cells		

5.3 Which cellular source of ROS production is involved in CML formation?

In the present study, for the first time, the carboxymethylation of intracellular proteins had been observed in a cell culture model of differentiated monocytic cells. Therefore, the mechanism of cellular CML formation was investigated further. *In vitro* data suggest that protein carboxymethylation is mediated by reactive oxygen species (ROS). If this holds true also in cells, then what would be the oxygen species involved and what would be the cellular source?

5.3.1 Is NADPH oxidase implicated in CML formation?

Among the various cellular ROS-generating systems, NADPH oxidase would be a good candidate for two reasons:

First, NADPH oxidase has been implicated, at least indirectly, in CML/AGE formation:

Up to now there is no good study which proves unequivocally the direct involvement of cellular NADPH oxidase in CML formation. Nevertheless, there was indirect evidence for the contribution of this ROS-generating enzyme to protein carboxymethylation by the report of Anderson et al. [130] who demonstrated that the 'oxidative burst' of stimulated granulocytes led to superoxide anion production and CML formation on proteins. However, in this study the contributions of NADPH oxidase and myeloperoxidase activity have not been separated clearly.

Second, most of the cell types or tissues known to form intracellular CML, have also proven to possess NADPH oxidase or to exert NADPH oxidase activity

In most of the cell types in which CML formation has been described so far, also the presence of NADPH oxidase has been

demonstrated, be it on DNA or RNA level or by demonstrating the presence of NADPH oxidase subunits in Western blots or by functional assays: **Table 5-8** lists the pertinent literature up to the present date. In atherosclerosis, the nonphagocytic/cellular form of NADPH oxidase has been described to be the major source of superoxide anions produced in the vessel wall [208] and in cell lines of cultured vascular smooth muscle cells [144] and endothelial cells [112; 145; 209]. In all of the mentioned vascular components, also CML formation has been observed by other authors (as reviewed in **Table 5-8**). The same holds true for relevant cell types in Alzheimer's disease and rheumatoid arthritis (**Table 5-8**).

Table 5-8: Correlation of CML accumulation and NADPH oxidase expression in different cell types of patients suffering from atherosclerosis, Alzheimer's disease and rheumatoid arthritis.

Disease	CML accumulation in:	NADPH oxidase expression in:
Atherosclerosis	Macrophages Endothel SMC-derived foam cells [34; 46; 107; 188; 210]	Macrophages (Phagocytic NADPH oxidase) Endothelial cells (Nonphagocytic NADPH oxidase) Vasc. smooth muscle cells (Nonphagocytic NADPH oxidase) Fibroblasts (Nonphagocytic NADPH oxidase) [132; 145; 209; 211; 212]
Alzheimer's disease	Neuroglia Neurons [102; 104]	Microglial cells (Phagocytic NADPH oxidase) Neurons [153; 155; 156]
Rheumatoid arthritis	Macrophages Activated T-lymphocytes Synovial lining / sublining) [101]	Synoviocytes (Nonphagocytic NADPH oxidase) Chondrocytes (Nonphagocytic NADPH oxidase) [203; 213; 214]

Abbreviation: SMC: smooth muscle cells

A widely used assay for NADPH oxidase activity is the lucigenin chemiluminescence assay. Although in numerous studies the validity of this assay has been stated [144-146; 215-218], the specificity of this assay is still a matter of debate [148; 149; 219; 220]. In the present study, the protocol of Griending et al. [144] with modifications was applied. A lower concentration of lucigenin was used to eliminate redox cycling of this compound as proposed by Munzel et al. [146]. It is a drawback for the research on NADPH oxidase that there is still no specific cell permeable inhibitor for this enzyme. The most widely used NADPH oxidase inhibitor at present is DPI. Inhibition of superoxide anion production by this compound is accepted in the literature as evidence for NADPH oxidase activity [221-223], but there are emerging data that DPI is not specific for NADPH oxidase, but rather inhibits other NADPH-dependent flavoproteins as well [224-227]. It has been proposed [228; 229] that the inhibitory action occurs by the reaction of DPI with the reduced anionic state of the flavin residue resulting in a phenyl adduct of the flavin group. Besides NADPH oxidase, a DPI-dependent inhibition has been shown for mitochondrial dehydrogenase, for NADPH cytochrome P450 reductase (CPR), for xanthine oxidase, for NO synthase and for sulfite synthase [229].

5.3.2 Is the cellular NADPH oxidase activity crucial for CML formation?

To prove or disprove the results from DPI inhibition experiments, NADPH oxidase knock out mutants of monocytic cells (PLB985 gp91 Δ 488-497) and of microglia cells (N11/6 NADPH oxidase knock outs) were used. In those cell lines, the PHOX subunit had been rendered inactive as characterised previously ([134] and

personal communication from A. Neumann, Würzburg). It was found that the CML formation observed in PLB985 gp91 Δ 488-497 knock out mutants was quantitatively comparable to wild type cells. This result had been corroborated by the findings in microglia cells. In NADPH oxidase deficient N11/6 microglial cells, the CML formation in response to stimulation by arachidonic acid had been observed to the same extent as in N11 wild type cells. From these experiments, clear evidence was obtained that protein carboxymethylation is not dependent on cellular NADPH oxidase.

5.3.3 Is ROS production from the mitochondrial respiratory chain involved in CML formation?

An actual hypothesis links hyperglycemia-dependent increased superoxide anion formation from the respiratory chain to the increased intracellular formation of AGEs [30; 65]. Various compounds, as depicted in **Figure 4-27**, have been shown to reduce respiratory chain-mediated formation of ROS and some of them have been shown to reduce methylglyoxal-derived AGEs [65; 158]. 4-OHCA is known to reduce mitochondrial superoxide anion production by inhibiting the pyruvate transport into the mitochondria and the other compounds are known to interfere with the respiratory chain directly. Either by uncoupling of the oxidative phosphorylation (CCCP) or by interfering with specific mitochondrial redox complexes (rotenone, TTFA, antimycin A) at the working concentrations given in **Table 3-2** and **Figure 4-24**. Benfotiamine has been shown to activate transketolase thereby diverting excess glycolytic intermediates to the pentose phosphate pathway (see **Figure 4-27**). This has been shown to prevent the high glucose-driven formation of methylglyoxal-

derived AGEs without affecting mitochondrial ROS production [158].

It was tested, whether these compounds also influence CML formation in the cell culture model of PMA-stimulated monocytic cells. The results were not entirely conclusive. It was observed that the formation of CML was reduced by 4-OHCA and to some extent by rotenone, a specific inhibitor of complex I, but not by unspecific uncoupling of the respiratory chain (CCCP) or by inhibiting complex II (TTFA) or III (antimycin A). These results are in contrast to Nishikawa et al. [65] who investigated the formation of methylglyoxal-derived AGEs, which are other important AGEs implicated in the pathogenesis of oxidative stress-induced tissue damage. These authors reported a reducing effect of CCCP and TTFA on high glucose-driven ROS generation and on the formation of methylglyoxal-derived AGE formation, but not of rotenone. In summary, the presented results do not indicate that an inhibition of the respiratory chain at various stages does lead to a generalised reduction of CML- or AGE-formation. Further experiments including subcellular fractionation and more specific techniques for the measurement of superoxide anions should be employed to get a clearer picture on the involvement of mitochondrial ROS in CML formation.

6 ZUSAMMENFASSUNG (DEUTSCH)

Zielstellung:

In der vorliegenden Arbeit sollte die Hypothese überprüft werden, daß das ‚advanced glycation end-product (AGE)‘ N^ε-(carboxymethyl)-Lysin (CML)

- (a) intrazellulär in Makrophagen und Granulozyten gebildet wird,
- (b) ein Lipidperoxidationsprodukt darstellt,
- (c) maßgeblich durch den Einfluß reaktiver Sauerstoffspezies (ROS) entsteht, insbesondere durch das Superoxidanion O₂⁻, dem Produkt der zellulären NADPH-Oxidase, und ob somit
- (d) der Nachweis von CML in Geweben und in Körperflüssigkeiten und der Nachweis spezifischer carboxymethylierter Proteine zum Verständnis entzündlicher und degenerativer Prozesse beiträgt.

Vorarbeiten:

In Vorarbeiten wurden Modellproteine chemisch carboxymethyliert und charakterisiert (CML-Albumin, CML-Haemoglobin, CML-Ferritin) und ein CML-Standard synthetisiert und charakterisiert.

Nachweis der *in vivo*-Formation von CML im Urin, in Geweben und in zirkulierenden Entzündungszellen

- Es wurde eine spezifische, reproduzierbare und sensitive HPLC-Methode zur Bestimmung der CML Ausscheidung im Urin entwickelt und veröffentlicht [159]. Diabetiker zeigten eine um 30 % erhöhte Ausscheidung von Gesamt-CML, bedingt durch eine erhöhte Ausscheidung von CML-Albumin. Rund 40% des ausgeschiedenen CML liegen als freie

Aminosäure und 60% als peptid- und proteingebundenes CML vor.

- Mit einem hier erzeugten spezifischen CML-Antiserum und mit monoklonalen CML-Antikörpern wurde immunhistochemisch (IHC) und mittels Western Blot die vermehrte Bildung carboxymethylierter Proteine in Nerven- und Muskelgewebe bei Diabetes mellitus und in Knorpel-, Nerven- und Muskelgewebe bei verschiedenen chronisch-entzündlichen und degenerativen Zuständen gefunden. Diese Arbeiten wurden in Kooperation mit Dr. M. Haslbeck, Erlangen, und Dr. Schwab, Dresden, durchgeführt. Auffällig war die teilweise intrazelluläre Lokalisation (IHC) der CML-Akkumulation in geweberesidenten Zellen und infiltrierenden Entzündungszellen.
- Des Weiteren wurde untersucht, ob eine verstärkte intrazelluläre CML-Bildung auch in zirkulierenden Leukozyten von Diabetikern nachweisbar ist. Dazu wurden Granulozyten, Monozyten und Lymphozyten von Normalpatienten und Diabetikern durch Immunabsorption mit Magnetbeads entsprechend ihrer Oberflächenmarker isoliert. Bei einem Teil der diabetischen Patienten (2 von 8 Patienten) wurden in Granulozyten durch Carboxymethylierung modifizierte zelluläre Proteine gefunden.

Mechanismus der CML Bildung:

- Lipidperoxidation führt zur Proteincarboxymethylierung *in vitro*:
Es wurde untersucht, ob der oxidative Abbau mehrfach ungesättigter Fettsäuren (Lipidperoxidation) *in vitro* zu einer Carboxymethylierung des Modellproteins RNase führt. Des

Weiteren wurde der Einfluß reaktiver Sauerstoffspezies (H_2O_2 , Superoxidanionen) auf die CML-Modifikation von RNase untersucht. Eingesetzt wurden Ölsäure, Linolensäure und Arachidonsäure.

Ergebnis: Es hat sich gezeigt, daß die Carboxymethylierung (a) ein sauerstoffabhängiger Prozess ist, (b) die Reaktionsgeschwindigkeit mit der Anzahl der Doppelbindungen in der Fettsäure steigt und bei Arachidonsäure am höchsten liegt und sich (c) durch H_2O_2 oder ein O_2 -generierendes System nicht steigern läßt.

- Der ‚oxidative burst‘ stimulierter Granulozyten führt zur Carboxymethylierung von Serumproteinen:

Granulozyten zeigen nach Stimulation mit LPS oder opsonisiertem Zymosan eine massive Freisetzung von granulär gespeicherten Effektorenzymen, insbesondere von NADPH-Oxidase und Myeloperoxidase. Dadurch kommt es lokal zu sehr hohen Konzentrationen reaktiver Sauerstoffspezies.

In frisch isolierten Granulozyten führt die Stimulation des ‚oxidativen burst‘ zu einer Zellyse innerhalb von 1-2 Stunden. Dieses System demonstriert den Beitrag der Myeloperoxidase und anderer Effektorenzyme zur CML-Bildung, eignet sich jedoch nicht zur Untersuchung der intrazellulären Protein-Carboxymethylierung.

- Die *in vitro* Stimulation vordifferenzierter Monozyten- und Mikroglia-Zelllinien führt zur zeitabhängigen CML-Modifikation intrazellulärer Proteine. Die CML-Bildung ist unabhängig von der zellulären NADPH-Oxidase und Xanthin-

Oxidase und lässt sich durch Hemmstoffe der mitochondrialen ROS-Produktion nicht durchgängig hemmen:

Die Kinetik der CML-Bildung und der Beitrag der phagozytären (PHOX) Form der NADPH-Oxidase wurde in den monozytären Zelllinien Mono Mac 6, PLB 985 (Wildtyp) und PLB 985gp91 Δ 488-497 (PHOX-defizient) und in der Neuroglia-Zelllinie N11 (Wildtyp) und N11/6 (PHOX-defizient) mittels spezifischer polyklonaler und monoklonaler CML-Antikörper untersucht. Zur Bestimmung der ROS-Produktion und der NADPH-Oxidase Aktivität wurde ein Lucigenin-Chemilumineszenztest entsprechend der Vorschrift von Griending et al. [144] mit Modifikationen verwendet.

In vordifferenzierten und stimulierten (PMA 20nM) Mono Mac 6 Zellen wurde eine zeitabhängige CML-Modifikation intrazellulärer Protein innerhalb von 1 – 3 Tagen beobachtet. Diese konnte durch DPI (100 μ M), einen unspezifischen Inhibitor der NADPH-Oxidase und anderer Flavoproteine, gehemmt werden. Hemmstoffe der Xanthin-Oxidase (Allopurinol 300 μ M) oder der NO-Synthase (L-NAME) reduzieren die CML-Bildung nicht. Hemmstoffe der mitochondrialen ROS-Bildung zeigten keinen einheitlichen Effekt auf die CML-Modifikation zellulärer Proteine. N11 Zellen zeigten CML-Bildung innerhalb von 24 h. In den NADPH-defizienten Mutanten war die CML-Bildung nicht unterdrückt.

Ergebnis: Die beobachtete CML-Modifikation zellulärer Protein ist unabhängig von NADPH-Oxidase oder Xanthin-Oxidase und lässt sich durch Inhibitoren der mitochondrialen ROS-Produktion nicht generell reduzieren. Andere, bislang

ungeklärte Quellen für reaktive Sauerstoffverbindungen oder bislang unbekannte Mechanismen scheinen für die CML-Bildung verantwortlich zu sein.

Zusammenfassung:

Zusammenfassend erscheint es aus den vorgelegten Ergebnissen unwahrscheinlich, daß CML durch einen einzelnen, spezifischen Mechanismus und aus einer einzelnen, definierten Vorläufersubstanz gebildet wird. Durch Untersuchungen mit NADPH-Oxidase defizienten Zelllinien wurde nachgewiesen, daß CML kein spezifischer Marker für die zelluläre NADPH-Oxidaseaktivität ist.

7 SUMMARY (ENGLISH)

Aims of this study:

In the present study, the hypothesis was tested, whether the advanced glycation end product (AGE) N^ε-(carboxymethyl)-lysine (CML) is

- (a) produced intracellularly in macrophages and granulocytes,
- (b) a product of lipid peroxidation,
- (c) formed under the influence of reactive oxygen species (ROS), especially the superoxide anion, produced by cellular NADPH oxidase.

Furthermore, it was studied, whether

- (d) the detection and measurement of CML in tissues and body fluids and the identification of specific CML-modified proteins may add to the understanding of the pathophysiological processes in chronic inflammatory and degenerative diseases.

Preparatory work:

In preparation for this study, test proteins were chemically carboxymethylated and analysed (CML-albumin, CML-hemoglobin, CML-ferritin), and a CML-standard was synthesised and characterised.

Detection of the *in vivo* formation of CML in urine, tissues, and circulating leukocytes:

A specific, sensitive and reproducible HPLC method for the analysis of CML excretion in urine was developed [159]. Diabetic patients exhibited a 30 % increase in the excretion of total CML due to an increase in CML albumin excretion. About 40% CML is excreted as free amino acid, while the remaining 60% is peptide- and protein-bound CML.

By immunohistochemistry (IHC) and Western blot techniques, using a specific CML antiserum and monoclonal CML-antibodies, an increase in the formation of CML-modified proteins in nerve tissue, muscle tissue and cartilage tissue has been found in diabetics and in various chronic inflammatory and degenerative conditions. A common feature concerning these findings was the intracellular localisation (IHC) of CML accumulation in resident and infiltrating inflammatory cells.

Because of this result, it was investigated further as to whether an increased intracellular CML accumulation could be seen in the circulating leukocytes of diabetics. For this purpose, granulocytes, monocytes and lymphocytes from control patients and diabetics were isolated by immunoabsorption with magnetic beads. CML-modified cellular proteins were found in granulocytes from a minor portion of the diabetic patients (2/8).

Potential mechanisms of CML formation

Lipid peroxidation leads to carboxymethylation of proteins *in vitro*

:

It was investigated, whether the oxidative degradation of the polyunsaturated fatty acids (oleic acid, linolenic acid, and arachidonic acid) leads to a carboxymethylation of the model protein RNase. The influence of reactive oxygen species (superoxide anions and H₂O₂) on the CML modification of RNase was also investigated.

It was found that

- (a) carboxymethylation is an oxygen-dependent process,
- (b) the degree of CML modification increases with the number of double bonds in the fatty acids (highest in arachidonic acid),
- (c) the degree of carboxymethylation could not be increased by H₂O₂ or by superoxide anion-generating systems.

The “oxidative burst” of stimulated granulocytes leads to CML modification of serum proteins:

Freshly isolated granulocytes were stimulated by LPS or opsonised zymosan to study the contribution of NADPH oxidase and myeloperoxidase, released during the “oxidative burst”, to the carboxymethylation of serum proteins.

The ‘oxidative burst’ of granulocytes leads to a rapid carboxymethylation of ambient serum proteins and of cellular proteins, set free during cell lysis. This result demonstrates the contribution of myeloperoxidase and other effector enzymes to the formation of CML. However, the technique is not suitable for investigating intracellular carboxymethylation since rapid cell lysis occurs within 60 – 120 min.

The stimulation of differentiated monocytic and microglia cell lines leads to time-dependent CML modification of intracellular proteins *in vitro*:

The kinetics of CML formation and the contribution of the phagocytic (PHOX) form of NADPH oxidase were analysed in the monocytic cell lines Mono Mac 6, PLB 985 (wild type) and PLB 985gp91 Δ 488-497 (PHOX-deficient), and in the neuroglia-cell lines N11 (wild type) and N11/6 (PHOX-deficient), using specific polyclonal and monoclonal antibodies directed against CML. For the analysis of ROS production and the measurement of NADPH oxidase activity, a lucigenin chemiluminescence test was used according to Griending et al. [144]. In pre-differentiated and stimulated (PMA 20nM) Mono Mac 6 cells, a time-dependent CML modification of intracellular proteins was observed within 1-3 days. This effect could be blocked by DPI (100 μ M), an unspecific inhibitor of NADPH oxidase and other flavoproteins. Inhibitors of

xanthine oxidase (allopurinol 300 μ M) or of NO-Synthase (L-NAME) had no effect. The effects of various inhibitors of mitochondrial ROS production were not conclusive.

N11 cells showed CML-formation within 24 h. CML formation was not reduced in NADPH oxidase deficient mutants, neither in monocytic PLB 985gp91 Δ 488-497 nor in microglial N11/6 cells.

The observed CML modification of cellular proteins is independent of NADPH oxidase or xanthine oxidase. The direct or indirect inhibition of mitochondrial ROS production does not lead to a general reduction of CML formation. Other unidentified sources of reactive oxygen species or different mechanisms appear to be responsible for the formation of CML.

In summary, this study has proven that CML is not a specific marker for cellular NADPH oxidase activity. From the presented results it seems not likely that CML is formed by a single mechanism or from a single precursor.

8 REFERENCES

- [1.] Maillard LC. Action des acides amines sur les sucres; formation des melanoidins par voie methodique. C R Acad Sci Ser 1912;154:66-68.
- [2.] Ledl F, Beck J, Sengl M, Osiander H, Estendorfer S, Severin T, Huber B. Chemical pathways of the Maillard reaction. Prog Clin Biol Res 1989;304:23-42.
- [3.] Njoroge FG, Monnier VM. The chemistry of the Maillard reaction under physiological conditions: a review. Prog Clin Biol Res 1989;304:85-107.
- [4.] Brownlee M. Negative consequences of glycation. Metabolism 2000;49:9-13.
- [5.] John WG, Lamb EJ. The Maillard or browning reaction in diabetes. Eye 1993;7:230-237.
- [6.] Thorpe SR, Baynes JW. Role of the Maillard reaction in diabetes mellitus and diseases of aging. Drugs Aging 1996;9:69-77.
- [7.] Vlassara H, Bucala R, Striker L. Pathogenic effects of advanced glycosylation: biochemical, biologic, and clinical implications for diabetes and aging. Lab Invest 1994;70:138-151.
- [8.] Koenig RJ, Blobstein SH, Cerami A. Structure of carbohydrate of hemoglobin Alc. J Biol Chem 1977;252:2992-2997.
- [9.] Makita Z, Vlassara H, Rayfield E, Cartwright K, Friedman E, Rodby R, Cerami A, Bucala R. Hemoglobin-AGE: a circulating marker of advanced glycosylation. Science 1992;258:651-653.
- [10.] Vlassara H, Palace MR. Diabetes and advanced glycation endproducts. J Intern Med 2001;251:87-101.

-
- [11.] Schleicher E. Glykierung von Proteinen: Pathobiochemische und diagnostische Aspekte. *Lab med* 1993;17:381-387.
- [12.] Furth AJ. Glycated proteins in diabetes. *Br J Biomed Sci* 1997;54:192-200.
- [13.] Monnier VM, Sell DR, Nagaraj RH, Miyata S, Grandhee S, Odetti P, Ibrahim SA. Maillard reaction-mediated molecular damage to extracellular matrix and other tissue proteins in diabetes, aging, and uremia. *Diabetes* 1992;41:36-41.
- [14.] Wells-Knecht KJ, Brinkmann E, Wells-Knecht MC, Litchfield JE, Ahmed MU, Reddy S, Zyzak DV, Thorpe SR, Baynes JW. New biomarkers of Maillard reaction damage to proteins. *Nephrol Dial Transplant* 1996;11 Suppl 5:41-47.
- [15.] Brownlee M. The pathological implications of protein glycation. *Clin Invest Med* 1995;18:275-281.
- [16.] Wu JT. Advanced glycosylation end products: a new disease marker for diabetes and aging. *J Clin Lab Anal* 1993;7:252-255.
- [17.] Monnier VM, Nagaraj RH, Portero-Otin M, Glomb M, Elgawish AH, Sell DR, Friedlander MA. Structure of advanced Maillard reaction products and their pathological role. *Nephrol Dial Transplant* 1996;11 Suppl 5:20-26.
- [18.] Thornalley PJ. Cell activation by glycated proteins. AGE receptors, receptor recognition factors and functional classification of AGEs. *Cell Mol Biol (Noisy -le-grand)* 1998;44:1013-1023.
- [19.] Kislinger T, Fu C, Huber B, Qu W, Taguchi A, Du YS, Hofmann M, Yan SF, Pischetsrieder M, Stern D, Schmidt AM. N(epsilon)-(carboxymethyl)lysine adducts of proteins are ligands for receptor for advanced glycation end products that activate cell signaling pathways and

- modulate gene expression. *J Biol Chem* 1999;274:31740-31749.
- [20.] Singh R, Barden A, Mori T, Beilin L. Advanced glycation end-products: a review. *Diabetologia* 2001;44:129-146.
- [21.] Baynes JW, Thorpe SR, Murtiashaw MH. Nonenzymatic glycosylation of lysine residues in albumin. *Methods Enzymol* 1984;106:88-98.
- [22.] Fu MX, Wells-Knecht KJ, Blackledge JA, Lyons TJ, Thorpe SR, Baynes JW. Glycation, glycooxidation, and cross-linking of collagen by glucose. Kinetics, mechanisms, and inhibition of late stages of the Maillard reaction. *Diabetes* 1994;43:676-683.
- [23.] Thornalley PJ, Langborg A, Minhas HS. Formation of glyoxal, methylglyoxal and 3-deoxyglucosone in the glycation of proteins by glucose. *Biochem J* 1999;344:109-116.
- [24.] Degenhardt TP, Thorpe SR, Baynes JW. Chemical modification of proteins by methylglyoxal. *Cell Mol Biol (Noisy -le-grand)* 1998;44:1139-1145.
- [25.] Miyata T, Inagi R, Asahi K, Yamada Y, Horie K, Sakai H, Uchida K, Kurokawa K. Generation of protein carbonyls by glycooxidation and lipoxidation reactions with autoxidation products of ascorbic acid and polyunsaturated fatty acids. *FEBS Lett* 1998;437:24-28.
- [26.] Miyata T, van Ypersele d, Kurokawa K, Baynes JW. Alterations in nonenzymatic biochemistry in uremia: origin and significance of "carbonyl stress" in long-term uremic complications. *Kidney Int* 1999;55:389-399.
- [27.] Miyata T, Fu MX, Kurokawa K, van Ypersele d, Thorpe SR, Baynes JW. Autoxidation products of both carbohydrates and lipids are increased in uremic plasma: is there oxidative stress in uremia? *Kidney Int* 1998;54:1290-1295.

-
- [28.] Miyata T, Sugiyama S, Suzuki D, Inagi R, Kurokawa K. Increased carbonyl modification by lipids and carbohydrates in diabetic nephropathy. *Kidney Int* 1999;71:S54-S56.
- [29.] Suzuki D, Miyata T, Saotome N, Horie K, Inagi R, Yasuda Y, Uchida K, Izuhara Y, Yagame M, Sakai H, Kurokawa K. Immunohistochemical evidence for an increased oxidative stress and carbonyl modification of proteins in diabetic glomerular lesions. *J Am Soc Nephrol* 1999;10:822-832.
- [30.] Brownlee M. Biochemistry and molecular cell biology of diabetic complications. *Nature* 2001;414:813-820.
- [31.] Giardino I, Edelstein D, Brownlee M. Nonenzymatic glycosylation in vitro and in bovine endothelial cells alters basic fibroblast growth factor activity. A model for intracellular glycosylation in diabetes. *J Clin Invest* 1994;94:110-117.
- [32.] Shinohara M, Thornalley PJ, Giardino I, Beisswenger P, Thorpe SR, Onorato J, Brownlee M. Overexpression of glyoxalase-I in bovine endothelial cells inhibits intracellular advanced glycation endproduct formation and prevents hyperglycemia-induced increases in macromolecular endocytosis. *J Clin Invest* 1998;101:1142-1147.
- [33.] Thornalley PJ. The glyoxalase system: new developments towards functional characterization of a metabolic pathway fundamental to biological life. *Biochem J* 1990;269:1-11.
- [34.] Nerlich AG, Schleicher ED. N(epsilon)-(carboxymethyl)lysine in atherosclerotic vascular lesions as a marker for local oxidative stress. *Atherosclerosis* 1999;144:41-47.
- [35.] Thorpe SR, Baynes JW. CML: a brief history. In: Horiuchi S et al., eds. *The Maillard Reaction in Food Chemistry and Medical Science: Update for the Postgenomic Era.*

-
- Elsevier International Congress Series. Volume 1245. Amsterdam: Elsevier, 2002.
- [36.] Shaw JN, Baynes JW, Thorpe SR. N epsilon-(carboxymethyl)lysine (CML) as a biomarker of oxidative stress in long-lived tissue proteins. *Methods Mol Biol* 2002;186:129-137.
- [37.] Ikeda K, Higashi T, Sano H, Jinnouchi Y, Yoshida M, Araki T, Ueda S, Horiuchi S. N (epsilon)-(carboxymethyl)lysine protein adduct is a major immunological epitope in proteins modified with advanced glycation end products of the Maillard reaction. *Biochemistry* 1996;35:8075-8083.
- [38.] Reddy S, Bichler J, Wells-Knecht KJ, Thorpe SR, Baynes JW. N epsilon-(carboxymethyl)lysine is a dominant advanced glycation end product (AGE) antigen in tissue proteins. *Biochemistry* 1995;34:10872-10878.
- [39.] Ahmed MU, Thorpe SR, Baynes JW. Identification of N epsilon-carboxymethyllysine as a degradation product of fructoselysine in glycated protein. *J Biol Chem* 1986;261:4889-4894.
- [40.] Fu MX, Requena JR, Jenkins AJ, Lyons TJ, Baynes JW, Thorpe SR. The advanced glycation end product, Nepsilon-(carboxymethyl)lysine, is a product of both lipid peroxidation and glycoxidation reactions. *J Biol Chem* 1996;271:9982-9986.
- [41.] Schleicher ED, Wagner E, Nerlich AG. Increased accumulation of the glycoxidation product N(epsilon)-(carboxymethyl)lysine in human tissues in diabetes and aging. *J Clin Invest* 1997;99:457-468.
- [42.] Dunn JA, Patrick JS, Thorpe SR, Baynes JW. Oxidation of Glycated Proteins: Age-Dependent Accumulation of N(epsilon)-(Carboxymethyl)lysine in Lens Proteins. *Biochemistry* 1989;28:9464-9468.

-
- [43.] Dunn JA, McCance DR, Thorpe SR, Lyons TJ, Baynes JW. Age-dependent accumulation of N epsilon-(carboxymethyl)lysine and N epsilon-(carboxymethyl)hydroxylysine in human skin collagen. *Biochemistry* 1991;30:1205-1210.
- [44.] Dyer DG, Dunn JA, Thorpe SR, Bailie KE, Lyons TJ, McCance DR, Baynes JW. Accumulation of Maillard reaction products in skin collagen in diabetes and aging. *J Clin Invest* 1993;91:2463-2469.
- [45.] Hammes HP, Brownlee M, Lin J, Schleicher E, Bretzel RG. Diabetic retinopathy risk correlates with intracellular concentrations of the glycoxidation product Nepsilon-(carboxymethyl) lysine independently of glycohaemoglobin concentrations. *Diabetologia* 1999;42:603-607.
- [46.] Horiuchi S, Sano H, Higashi T, Ikeda K, Jinnouchi Y, Nagai R, Takahashi K. Extra- and intracellular localization of advanced glycation end-products in human atherosclerotic lesions. *Nephrol Dial Transplant* 1996;11 Suppl 5:81-86.
- [47.] Ceriello A. Hyperglycaemia: the bridge between non-enzymatic glycation and oxidative stress in the pathogenesis of diabetic complications. *Diabetes Nutr Metab* 1999;12:42-46.
- [48.] Giugliano D, Ceriello A, Paolisso G. Oxidative stress and diabetic vascular complications. *Diabetes Care* 1996;19:257-267.
- [49.] Friedman EA. Advanced glycosylated end products and hyperglycemia in the pathogenesis of diabetic complications. *Diabetes Care* 1999;22 Suppl 2:B65-B71.
- [50.] McCance DR, Dyer DG, Dunn JA, Bailie KE, Thorpe SR, Baynes JW, Lyons TJ. Maillard reaction products and their relation to complications in insulin-dependent diabetes mellitus. *J Clin Invest* 1993;91:2470-2478.

-
- [51.] Koya D, King GL. Protein kinase C activation and the development of diabetic complications. *Diabetes* 1998;47:859-866.
- [52.] Lee AY, Chung SS. Contributions of polyol pathway to oxidative stress in diabetic cataract. *FASEB J* 1999;13:23-30.
- [53.] Veerababu G, Tang J, Hoffman RT, Daniels MC, Hebert LF, Jr., Crook ED, Cooksey RC, McClain DA. Overexpression of glutamine: fructose-6-phosphate amidotransferase in the liver of transgenic mice results in enhanced glycogen storage, hyperlipidemia, obesity, and impaired glucose tolerance. *Diabetes* 2000;49:2070-2078.
- [54.] Nishikawa T, Edelstein D, Du XL, Yamagishi S, Matsumura T, Kaneda Y, Yorek MA, Beebe D, Oates PJ, Hammes HP, Giardino I, Brownlee M. Normalizing mitochondrial superoxide production blocks three pathways of hyperglycaemic damage. *Nature* 2000;404:787-790.
- [55.] Nishikawa T, Edelstein D, Brownlee M. The missing link: a single unifying mechanism for diabetic complications. *Kidney Int* 2000;77:S26-S30.
- [56.] Baynes JW, Thorpe SR. Role of oxidative stress in diabetic complications: a new perspective on an old paradigm. *Diabetes* 1999;48:1-9.
- [57.] Wolff SP, Jiang ZY, Hunt JV. Protein glycation and oxidative stress in diabetes mellitus and ageing. *Free Radic Biol Med* 1991;10:339-352.
- [58.] Wolff SP. Diabetes mellitus and free radicals. Free radicals, transition metals and oxidative stress in the aetiology of diabetes mellitus and complications. *Br Med Bull* 1993;49:642-652.
- [59.] Laaksonen DE, Atalay M, Niskanen L, Uusitupa M, Hanninen O, Sen CK. Increased resting and exercise-

- induced oxidative stress in young IDDM men. *Diabetes Care* 1996;19:569-574.
- [60.] Altomare E, Vendemiale G, Chicco D, Procacci V, Cirelli F. Increased lipid peroxidation in type 2 poorly controlled diabetic patients. *Diabete Metab* 1992;18:264-271.
- [61.] Haffner SM, Agil A, Mykkanen L, Stern MP, Jialal I. Plasma oxidizability in subjects with normal glucose tolerance, impaired glucose tolerance, and NIDDM. *Diabetes Care* 1995;18:646-653.
- [62.] MacRury SM, Gordon D, Wilson R, Bradley H, Gemmell CG, Paterson JR, Rumley AG, MacCuish AC. A comparison of different methods of assessing free radical activity in type 2 diabetes and peripheral vascular disease. *Diabet Med* 1993;10:331-335.
- [63.] Nourooz-Zadeh J, Tajaddini-Sarmadi J, McCarthy S, Betteridge DJ, Wolff SP. Elevated levels of authentic plasma hydroperoxides in NIDDM. *Diabetes* 1995;44:1054-1058.
- [64.] Rosen P, Nawroth PP, King G, Moller W, Tritschler HJ, Packer L. The role of oxidative stress in the onset and progression of diabetes and its complications: a summary of a Congress Series sponsored by UNESCO-MCBN, the American Diabetes Association and the German Diabetes Society. *Diabetes Metab Res Rev* 2001;17:189-212.
- [65.] Nishikawa T, Edelstein D, Du XL, Yamagishi S, Matsumura T, Kaneda Y, Yorek MA, Beebe D, Oates PJ, Hammes HP, Giardino I, Brownlee M. Normalizing mitochondrial superoxide production blocks three pathways of hyperglycaemic damage. *Nature* 2000;404:787-790.
- [66.] Mullarkey CJ, Edelstein D, Brownlee M. Free radical generation by early glycation products: a mechanism for accelerated atherogenesis in diabetes. *Biochem Biophys Res Commun* 1990;173:932-939.

-
- [67.] Yan SD, Schmidt AM, Anderson GM, Zhang J, Brett J, Zou YS, Pinsky D, Stern D. Enhanced cellular oxidant stress by the interaction of advanced glycation end products with their receptors/binding proteins. *J Biol Chem* 1994;269:9889-9897.
- [68.] Noberasco G, Odetti P, Boeri D, Maiello M, Adezati L. Malondialdehyde (MDA) level in diabetic subjects. Relationship with blood glucose and glycosylated hemoglobin. *Biomed Pharmacother* 1991;45:193-196.
- [69.] Packer L, Witt EH, Tritschler HJ. alpha-Lipoic acid as a biological antioxidant. *Free Radic Biol Med* 1995;19:227-250.
- [70.] Suzuki YJ, Tsuchiya M, Packer L. Lipoate prevents glucose-induced protein modifications. *Free Radic Res Commun* 1992;17:211-217.
- [71.] Borcea V, Nourooz-Zadeh J, Wolff SP, Klevesath M, Hofmann M, Urich H, Wahl P, Ziegler R, Tritschler H, Halliwell B, Nawroth PP. alpha-Lipoic acid decreases oxidative stress even in diabetic patients with poor glycemic control and albuminuria. *Free Radic Biol Med* 1999;26:1495-1500.
- [72.] Maxwell SR, Thomason H, Sandler D, LeGuen C, Baxter MA, Thorpe GH, Jones AF, Barnett AH. Poor glycaemic control is associated with reduced serum free radical scavenging (antioxidant) activity in non-insulin-dependent diabetes mellitus. *Ann Clin Biochem* 1997;34:638-644.
- [73.] Sundaram RK, Bhaskar A, Vijayalingam S, Viswanathan M, Mohan R, Shanmugasundaram KR. Antioxidant status and lipid peroxidation in type II diabetes mellitus with and without complications. *Clin Sci (Lond)* 1996;90:255-260.
- [74.] Atalay M, Laaksonen DE, Niskanen L, Uusitupa M, Hanninen O, Sen CK. Altered antioxidant enzyme defences in insulin-dependent diabetic men with increased resting and exercise-induced oxidative stress. *Acta Physiol Scand* 1997;161:195-201.

-
- [75.] Nourooz-Zadeh J, Rahimi A, Tajaddini-Sarmadi J, Tritschler H, Rosen P, Halliwell B, Betteridge DJ. Relationships between plasma measures of oxidative stress and metabolic control in NIDDM. *Diabetologia* 1997;40:647-653.
- [76.] Hofmann MA, Schiekofer S, Isermann B, Kanitz M, Henkels M, Joswig M, Treusch A, Morcos M, Weiss T, Borcea V, Abdel KA, Amiral J, Tritschler H, Ritz E, Wahl P, Ziegler R, Bierhaus A, Nawroth PP. Peripheral blood mononuclear cells isolated from patients with diabetic nephropathy show increased activation of the oxidative-stress sensitive transcription factor NF-kappaB. *Diabetologia* 1999;42:222-232.
- [77.] Bierhaus A, Chevion S, Chevion M, Hofmann M, Quehenberger P, Illmer T, Luther T, Berentshtein E, Tritschler H, Muller M, Wahl P, Ziegler R, Nawroth PP. Advanced glycation end product-induced activation of NF-kappaB is suppressed by alpha-lipoic acid in cultured endothelial cells. *Diabetes* 1997;46:1481-1490.
- [78.] Halliwell B. The role of oxygen radicals in human disease, with particular reference to the vascular system. *Haemostasis* 1993;23 Suppl 1:118-126.
- [79.] Finkel T, Holbrook NJ. Oxidants, oxidative stress and the biology of ageing. *Nature* 2000;408:239-247.
- [80.] Halliwell B, Gutteridge JMC. Free radicals in biology and medicine. 3rd ed. Oxford, UK: Oxford Science Publications, 1998.
- [81.] Halliwell B. Antioxidants in human health and disease. *Annu Rev Nutr* 1996;16:33-50.
- [82.] Sies H. Strategies of antioxidant defense. *Eur J Biochem* 1993;215:213-219.
- [83.] Stahl W, Sies H. Antioxidant defense: vitamins E and C and carotenoids. *Diabetes* 1997;46 Suppl 2:S14-S18.

-
- [84.] Wolff SP, Dean RT. Glucose autoxidation and protein modification. The potential role of 'autoxidative glycosylation' in diabetes. *Biochem J* 1987;245:243-250.
- [85.] Wells-Knecht KJ, Zyzak DV, Litchfield JE, Thorpe SR, Baynes JW. Mechanism of autoxidative glycosylation: identification of glyoxal and arabinose as intermediates in the autoxidative modification of proteins by glucose. *Biochemistry* 1995;34:3702-3709.
- [86.] Dunn JA, Ahmed MU, Murtiashaw MH, Richardson JM, Walla MD, Thorpe SR, Baynes JW. Reaction of ascorbate with lysine and protein under autoxidizing conditions: formation of N epsilon-(carboxymethyl)lysine by reaction between lysine and products of autoxidation of ascorbate. *Biochemistry* 1990;29:10964-10970.
- [87.] Litchfield JE, Thorpe SR, Baynes JW. Oxygen is not required for the browning and crosslinking of protein by pentoses: relevance to Maillard reactions in vivo. *Int J Biochem Cell Biol* 1999;31:1297-1305.
- [88.] Niwa H, Takeda A, Wakai M, Miyata T, Yasuda Y, Mitsuma T, Kurokawa K, Sobue G. Accelerated formation of N epsilon-(carboxymethyl) lysine, an advanced glycation end product, by glyoxal and 3-deoxyglucosone in cultured rat sensory neurons. *Biochem Biophys Res Commun* 1998;248:93-97.
- [89.] Glomb MA, Monnier VM. Mechanism of protein modification by glyoxal and glycolaldehyde, reactive intermediates of the Maillard reaction. *J Biol Chem* 1995;270:10017-10026.
- [90.] Fu S, Fu MX, Baynes JW, Thorpe SR, Dean RT. Presence of dopa and amino acid hydroperoxides in proteins modified with advanced glycation end products (AGEs): amino acid oxidation products as a possible source of oxidative stress induced by AGE proteins. *Biochem J* 1998;330:233-239.

-
- [91.] Hamada Y, Nakamura J, Naruse K, Komori T, Kato K, Kasuya Y, Nagai R, Horiuchi S, Hotta N. Epalrestat, an aldose reductase inhibitor, reduces the levels of Nepsilon-(carboxymethyl)lysine protein adducts and their precursors in erythrocytes from diabetic patients. *Diabetes Care* 2000;23:1539-1544.
- [92.] Smith PR, Thornalley PJ. Mechanism of the degradation of non-enzymatically glycosylated proteins under physiological conditions. Studies with the model fructosamine, N epsilon-(1-deoxy-D-fructos-1-yl)hippuryl-lysine. *Eur J Biochem* 1992;210:729-739.
- [93.] Hunt JV, Dean RT, Wolff SP. Hydroxyl radical production and autoxidative glycosylation. Glucose autoxidation as the cause of protein damage in the experimental glycation model of diabetes mellitus and ageing. *Biochem J* 1988;256:205-212.
- [94.] Hunt JV, Smith CC, Wolff SP. Autoxidative glycosylation and possible involvement of peroxides and free radicals in LDL modification by glucose. *Diabetes* 1990;39:1420-1424.
- [95.] Jiang ZY, Woollard AC, Wolff SP. Hydrogen peroxide production during experimental protein glycation. *FEBS Lett* 1990;268:69-71.
- [96.] Saxena AK, Saxena P, Wu X, Obrenovich M, Weiss MF, Monnier VM. Protein aging by carboxymethylation of lysines generates sites for divalent metal and redox active copper binding: relevance to diseases of glycoxidative stress. *Biochem Biophys Res Commun* 1999;260:332-338.
- [97.] Requena JR, Stadtman ER. Conversion of lysine to N(epsilon)-(carboxymethyl)lysine increases susceptibility of proteins to metal-catalyzed oxidation. *Biochem Biophys Res Commun* 1999;264:207-211.
- [98.] Nagai R, Unno Y, Hayashi MC, Masuda S, Hayase F, Kinae N, Horiuchi S. Peroxynitrite induces formation of N(

- epsilon)-(carboxymethyl) lysine by the cleavage of Amadori product and generation of glucosone and glyoxal from glucose: novel pathways for protein modification by peroxyxynitrite. *Diabetes* 2002;51:2833-2839.
- [99.] Wells-Knecht MC, Thorpe SR, Baynes JW. Pathways of formation of glycoxidation products during glycation of collagen. *Biochemistry* 1995;34:15134-15141.
- [100.] Kennedy AL, Lyons TJ. Glycation, oxidation, and lipoxidation in the development of diabetic complications. *Metabolism* 1997;46:14-21.
- [101.] Drinda S, Franke S, Canet CC, Petrow P, Brauer R, Huttich C, Stein G, Hein G. Identification of the advanced glycation end products N(epsilon)-carboxymethyllysine in the synovial tissue of patients with rheumatoid arthritis. *Ann Rheum Dis* 2002;61:488-492.
- [102.] Takeda A, Wakai M, Niwa H, Dei R, Yamamoto M, Li M, Goto Y, Yasuda T, Nakagomi Y, Watanabe M, Inagaki T, Yasuda Y, Miyata T, Sobue G. Neuronal and glial advanced glycation end product [Nepsilon-(carboxymethyl)lysine] in Alzheimer's disease brains. *Acta Neuropathol (Berl)* 2001;101:27-35.
- [103.] Munch G, Cunningham AM, Riederer P, Braak E. Advanced glycation endproducts are associated with Hirano bodies in Alzheimer's disease. *Brain Res* 1998;796:307-310.
- [104.] Dei R, Takeda A, Niwa H, Li M, Nakagomi Y, Watanabe M, Inagaki T, Washimi Y, Yasuda Y, Horie K, Miyata T, Sobue G. Lipid peroxidation and advanced glycation end products in the brain in normal aging and in Alzheimer's disease. *Acta Neuropathol (Berl)* 2002;104:113-122.
- [105.] Weiss MF, Erhard P, Kader-Attia FA, Wu YC, Deoreo PB, Araki A, Glomb MA, Monnier VM. Mechanisms for the formation of glycoxidation products in end-stage renal disease. *Kidney Int* 2000;57:2571-2585.

-
- [106.] Horie K, Miyata T, Maeda K, Miyata S, Sugiyama S, Sakai H, van Ypersole dS, Monnier VM, Witztum JL, Kurokawa K. Immunohistochemical colocalization of glycoxidation products and lipid peroxidation products in diabetic renal glomerular lesions. Implication for glycoxidative stress in the pathogenesis of diabetic nephropathy. *J Clin Invest* 1997;100:2995-3004.
- [107.] Takayama F, Aoyama I, Tsukushi S, Miyazaki T, Miyazaki S, Morita T, Hirasawa Y, Shimokata K, Niwa T. Immunohistochemical detection of imidazolone and N(epsilon)-(carboxymethyl)lysine in aortas of hemodialysis patients. *Cell Mol Biol (Noisy -le-grand)* 1998;44:1101-1109.
- [108.] Kislinger T, Fu C, Huber B, Qu W, Taguchi A, Du YS, Hofmann M, Yan SF, Pischetsrieder M, Stern D, Schmidt AM. N(epsilon)-(carboxymethyl)lysine adducts of proteins are ligands for receptor for advanced glycation end products that activate cell signaling pathways and modulate gene expression. *J Biol Chem* 1999;274:31740-31749.
- [109.] Schiekofer S, Andrassy M, Chen J, Rudofsky G, Schneider J, Wendt T, Stefan N, Humpert P, Fritsche A, Stumvoll M, Schleicher E, Haring HU, Nawroth PP, Bierhaus A. Acute Hyperglycemia Causes Intracellular Formation of CML and Activation of ras, p42/44 MAPK, and Nuclear Factor kappaB in PBMCs. *Diabetes* 2003;52:621-633.
- [110.] Zill H, Gunther R, Erbersdobler HF, Folsch UR, Faist V. RAGE expression and AGE-induced MAP kinase activation in Caco-2 cells. *Biochem Biophys Res Commun* 2001;288:1108-1111.
- [111.] Borrebaek J, Prydz K, Fjeldstad K, Vuong TT, Berg TJ, Holkov C, Kolset SO. The AGE product N epsilon-(carboxymethyl)lysine serum albumin is a modulator of proteoglycan expression in polarized cultured kidney epithelial cells. *Diabetologia* 2001;44:488-494.

-
- [112.] Wautier MP, Chappey O, Corda S, Stern DM, Schmidt AM, Wautier JL. Activation of NADPH oxidase by AGE links oxidant stress to altered gene expression via RAGE. *Am J Physiol Endocrinol Metab* 2001;280:E685-E694.
- [113.] Nakamura S, Makita Z, Ishikawa S, Yasumura K, Fujii W, Yanagisawa K, Kawata T, Koike T. Progression of nephropathy in spontaneous diabetic rats is prevented by OPB-9195, a novel inhibitor of advanced glycation. *Diabetes* 1997;46:895-899.
- [114.] Nakamura S, Tachikawa T, Tobita K, Aoyama I, Takayama F, Enomoto A, Niwa T. An inhibitor of advanced glycation end product formation reduces N epsilon-(carboxymethyl)lysine accumulation in glomeruli of diabetic rats. *Am J Kidney Dis* 2003;41:S68-S71.
- [115.] Schmidt AM, Hori O, Cao R, Yan SD, Brett J, Wautier JL, Ogawa S, Kuwabara K, Matsumoto M, Stern D. RAGE: a novel cellular receptor for advanced glycation end products. *Diabetes* 1996;45 Suppl 3:S77-S80.
- [116.] Schmidt AM, Yan SD, Yan SF, Stern DM. The biology of the receptor for advanced glycation end products and its ligands. *Biochim Biophys Acta* 2000;1498:99-111.
- [117.] Bierhaus A, Schiekofer S, Schwaninger M, Andrassy M, Humpert PM, Chen J, Hong M, Luther T, Henle T, Kloting I, Morcos M, Hofmann M, Tritschler H, Weigle B, Kasper M, Smith M, Perry G, Schmidt AM, Stern DM, Haring HU, Schleicher E, Nawroth PP. Diabetes-associated sustained activation of the transcription factor nuclear factor-kappaB. *Diabetes* 2001;50:2792-2808.
- [118.] Bierhaus A, Hofmann MA, Ziegler R, Nawroth PP. AGEs and their interaction with AGE-receptors in vascular disease and diabetes mellitus. I. The AGE concept. *Cardiovasc Res* 1998;37:586-600.
- [119.] Tanji N, Markowitz GS, Fu C, Kislinger T, Taguchi A, Pischetsrieder M, Stern D, Schmidt AM, D'Agati VD. Expression of advanced glycation end products and their

- cellular receptor RAGE in diabetic nephropathy and nondiabetic renal disease. *J Am Soc Nephrol* 2000;11:1656-1666.
- [120.] Stitt AW, Li YM, Gardiner TA, Bucala R, Archer DB, Vlassara H. Advanced glycation end products (AGEs) co-localize with AGE receptors in the retinal vasculature of diabetic and of AGE-infused rats. *Am J Pathol* 1997;150:523-531.
- [121.] Soulis T, Thallas V, Youssef S, Gilbert RE, McWilliam BG, Murray-McIntosh RP, Cooper ME. Advanced glycation end products and their receptors co-localise in rat organs susceptible to diabetic microvascular injury. *Diabetologia* 1997;40:619-628.
- [122.] Hori O, Yan SD, Ogawa S, Kuwabara K, Matsumoto M, Stern D, Schmidt AM. The receptor for advanced glycation end-products has a central role in mediating the effects of advanced glycation end-products on the development of vascular disease in diabetes mellitus. *Nephrol Dial Transplant* 1996;11 Suppl 5:13-16.
- [123.] Schmidt AM, Hori O, Brett J, Yan SD, Wautier JL, Stern D. Cellular receptors for advanced glycation end products. Implications for induction of oxidant stress and cellular dysfunction in the pathogenesis of vascular lesions. *Arterioscler Thromb* 1994;14:1521-1528.
- [124.] Hammes HP, Hoerauf H, Alt A, Schleicher E, Clausen JT, Bretzel RG, Laqua H. N(epsilon)(carboxymethyl)lysine and the AGE receptor RAGE colocalize in age-related macular degeneration. *Invest Ophthalmol Vis Sci* 1999;40:1855-1859.
- [125.] Giardino I, Edelstein D, Brownlee M. BCL-2 expression or antioxidants prevent hyperglycemia-induced formation of intracellular advanced glycation endproducts in bovine endothelial cells. *J Clin Invest* 1996;97:1422-1428.
- [126.] Kasper M, Roehlecke C, Witt M, Fehrenbach H, Hofer A, Miyata T, Weigert C, Funk RH, Schleicher ED. Induction

- of apoptosis by glyoxal in human embryonic lung epithelial cell line L132. *Am J Respir Cell Mol Biol* 2000;23:485-491.
- [127.] Kikuchi S, Shinpo K, Moriwaka F, Makita Z, Miyata T, Tashiro K. Neurotoxicity of methylglyoxal and 3-deoxyglucosone on cultured cortical neurons: synergism between glycation and oxidative stress, possibly involved in neurodegenerative diseases. *J Neurosci Res* 1999;57:280-289.
- [128.] Pamplona R, Portero-Otin M, Bellmun MJ, Gredilla R, Barja G. Aging increases Nepsilon-(carboxymethyl)lysine and caloric restriction decreases Nepsilon-(carboxyethyl)lysine and Nepsilon-(malondialdehyde)lysine in rat heart mitochondrial proteins. *Free Radic Res* 2002;36:47-54.
- [129.] Pamplona R, Portero-Otin M, Requena J, Gredilla R, Barja G. Oxidative, glycoxidative and lipoxidative damage to rat heart mitochondrial proteins is lower after 4 months of caloric restriction than in age-matched controls. *Mech Aging Dev* 2002;123:1437-1446.
- [130.] Anderson MM, Requena JR, Crowley JR, Thorpe SR, Heinecke JW. The myeloperoxidase system of human phagocytes generates Nepsilon-(carboxymethyl)lysine on proteins: a mechanism for producing advanced glycation end products at sites of inflammation. *J Clin Invest* 1999;104:103-113.
- [131.] Schleicher E, Nerlich A, Haslbeck M, Heuss D, Kasper M, Bierhaus A, Nawroth PP, Haering HU, Friess U. Formation of N(epsilon)-(carboxymethyl)lysine in inflammatory and noninflammatory conditions of nerve and muscle and in inflammatory cells in vitro. In: Horiuchi S and et.al., eds. *The Maillard Reaction in Food Chemistry and Medical Science: Update for the Postgenomic Era*. Elsevier International Congress Series. Elsevier, Amsterdam, 2002:53-59.

-
- [132.] Griendling KK, Sorescu D, Ushio-Fukai M. NAD(P)H oxidase: role in cardiovascular biology and disease. *Circ Res* 2000;86:494-501.
- [133.] Ziegler-Heitbrock HW, Thiel E, Futterer A, Herzog V, Wirtz A, Riethmuller G. Establishment of a human cell line (Mono Mac 6) with characteristics of mature monocytes. *Int J Cancer* 1988;41:456-461.
- [134.] Yu L, Cross AR, Zhen L, Dinauer MC. Functional analysis of NADPH oxidase in granulocytic cells expressing a delta488-497 gp91(phox) deletion mutant. *Blood* 1999;94:2497-2504.
- [135.] Weber C, Aepfelbacher M, Haag H, Ziegler-Heitbrock HW, Weber PC. Tumor necrosis factor induces enhanced responses to platelet-activating factor and differentiation in human monocytic Mono Mac 6 cells. *Eur J Immunol* 1993;23:852-859.
- [136.] Ziegler-Heitbrock HW, Schraut W, Wendelgaß.P., Ströbel MST, Weber C, Aepfelbacher M, Ehlers M, Schütt C, Haas JG. Distinct patterns of differentiation induced in the monocytic cell line Mono Mac 6. *Journal of Leukocyte Biology* 1994;55:73-80.
- [137.] Perkins SL, Link DC, Kling S, Ley TJ, Teitelbaum SL. 1,25-Dihydroxyvitamin D3 induces monocytic differentiation of the PLB-985 leukemic line and promotes c-fgr mRNA expression. *J Leukoc Biol* 1991;50:427-433.
- [138.] Onorato JM, Jenkins AJ, Thorpe SR, Baynes JW. Pyridoxamine, an inhibitor of advanced glycation reactions, also inhibits advanced lipoxidation reactions. Mechanism of action of pyridoxamine. *J Biol Chem* 2000;275:21177-21184.
- [139.] Liardon R, Weck-Gaudard D, Philipossian G, Finot P. Identification of N(epsilon)-Carboxymethyllysine: A new Maillard Reaction Product, in Rat Urine. *J Agric Food Chem* 1987;35:427-431.

-
- [140.] Gempel KE, Wagner EM, Schleicher ED. Production and Characterization of Antibodies against Carboxymethyllysine-modified Proteins. *Maillard Reactions in Chemistry, Food and Health* 1994;392-396.
- [141.] Haslbeck KM, Schleicher ED, Friess U, Kirchner A, Neundorfer B, Heuss D. N(epsilon)-Carboxymethyllysine in diabetic and non-diabetic polyneuropathies. *Acta Neuropathol (Berl)* 2001;104:45-52.
- [142.] Schwab W, Friess U, Hempel U, Schulze E, Makita Z, Kasper M, Simank HG. Immunohistochemical demonstration of N(epsilon)-carboxymethyllysine protein adduct in normal and osteoarthritic cartilage. *Histochem Cell Biol* 2002;117:541-546.
- [143.] Gerber CE, Kuci S, Zipfel M, Niethammer D, Bruchelt G. Phagocytic activity and oxidative burst of granulocytes in persons with myeloperoxidase deficiency. *Eur J Clin Chem Clin Biochem* 1996;34:901-908.
- [144.] Griending KK, Minieri CA, Ollerenshaw JD, Alexander RW. Angiotensin II stimulates NADH and NADPH oxidase activity in cultured vascular smooth muscle cells. *Circ Res* 1994;74:1141-1148.
- [145.] Christ M, Bauersachs J, Liebetrau C, Heck M, Gunther A, Wehling M. Glucose increases endothelial-dependent superoxide formation in coronary arteries by NAD(P)H oxidase activation: attenuation by the 3-hydroxy-3-methylglutaryl coenzyme A reductase inhibitor atorvastatin. *Diabetes* 2002;51:2648-2652.
- [146.] Munzel T, Afanas'ev IB, Kleschyov AL, Harrison DG. Detection of superoxide in vascular tissue. *Arterioscler Thromb Vasc Biol* 2002;22:1761-1768.
- [147.] Li Y, Zhu H, Kuppusamy P, Roubaud V, Zweier JL, Trush MA. Validation of lucigenin (bis-N-methylacridinium) as a chemiluminescent probe for detecting superoxide anion radical production by enzymatic and cellular systems. *J Biol Chem* 1998;273:2015-2023.

-
- [148.] Janiszewski M, Souza HP, Liu X, Pedro MA, Zweier JL, Laurindo FR. Overestimation of NADH-driven vascular oxidase activity due to lucigenin artifacts. *Free Radic Biol Med* 2002;32:446-453.
- [149.] Spasojevic I, Liochev SI, Fridovich I. Lucigenin: redox potential in aqueous media and redox cycling with O₂ production. *Arch Biochem Biophys* 2000;373:447-450.
- [150.] Nerlich AG, Schleicher ED, Boos N. 1997 Volvo Award winner in basic science studies. Immunohistologic markers for age-related changes of human lumbar intervertebral discs. *Spine* 1997;22:2781-2795.
- [151.] Behl C, Davis JB, Lesley R, Schubert D. Hydrogen peroxide mediates amyloid beta protein toxicity. *Cell* 1994;77:817-827.
- [152.] Souza HP, Laurindo FR, Ziegelstein RC, Berlowitz CO, Zweier JL. Vascular NAD(P)H oxidase is distinct from the phagocytic enzyme and modulates vascular reactivity control. *Am J Physiol Heart Circ Physiol* 2001;280:H658-H667.
- [153.] Shimohama S, Tanino H, Kawakami N, Okamura N, Kodama H, Yamaguchi T, Hayakawa T, Nunomura A, Chiba S, Perry G, Smith MA, Fujimoto S. Activation of NADPH oxidase in Alzheimer's disease brains. *Biochem Biophys Res Commun* 2000;273:5-9.
- [154.] Sankarapandi S, Zweier JL, Mukherjee G, Quinn MT, Huso DL. Measurement and characterization of superoxide generation in microglial cells: evidence for an NADPH oxidase-dependent pathway. *Arch Biochem Biophys* 1998;353:312-321.
- [155.] Tammariello SP, Quinn MT, Estus S. NADPH oxidase contributes directly to oxidative stress and apoptosis in nerve growth factor-deprived sympathetic neurons. *J Neurosci* 2000;20:RC53.

-
- [156.] Bianca VD, Dusi S, Bianchini E, Dal P, I, Rossi F. beta-amyloid activates the O-2 forming NADPH oxidase in microglia, monocytes, and neutrophils. A possible inflammatory mechanism of neuronal damage in Alzheimer's disease. *J Biol Chem* 1999;274:15493-15499.
- [157.] Meier B, Radeke HH, Selle S, Habermehl GG, Resch K, Sies H. Human fibroblasts release low amounts of reactive oxygen species in response to the potent phagocyte stimulants, serum-treated zymosan, N-formyl-methionyl-leucyl-phenylalanine, leukotriene B4 or 12-O-tetradecanoylphorbol 13-acetate. *Biol Chem Hoppe Seyler* 1990;371:1021-1025.
- [158.] Hammes HP, Du X, Edelstein D, Taguchi T, Matsumura T, Ju Q, Lin J, Bierhaus A, Nawroth P, Hannak D, Neumaier M, Bergfeld R, Giardino I, Brownlee M. Benfotiamine blocks three major pathways of hyperglycemic damage and prevents experimental diabetic retinopathy. *Nat Med* 2003;9:294-299.
- [159.] Friess U, Waldner M, Wahl HG, Lehmann R, Haering HU, Voelter W, Schleicher E. HPLC-based determination of urinary free and total N(epsilon)-(carboxymethyl)lysine excretion in normal and diabetic subjects. *J Chromatogr B Analyt Technol Biomed Life Sci* 2003;794:273-280.
- [160.] Miyata T, Wada Y, Cai Z, Iida Y, Horie K, Yasuda Y, Maeda K, Kurokawa K, van Ypersele dS. Implication of an increased oxidative stress in the formation of advanced glycation end products in patients with end-stage renal failure. *Kidney Int* 1997;51:1170-1181.
- [161.] Mitsuhashi T, Vlassara H, Founds HW, Li YM. Standardizing the immunological measurement of advanced glycation endproducts using normal human serum. *J Immunol Methods* 1997;207:79-88.
- [162.] Buongiorno AM, Sagratella E, Morelli S, Di Virgilio A, Sensi M. Advanced glycosylation end product quantification: differently produced polyclonal antisera do

- not share the recognition of epitopes of different nature. *Ann Ist Super Sanita* 2002;38:393-399.
- [163.] Henle T, Deppisch R, Beck W, Hergesell O, Hansch GM, Ritz E. Advanced glycated end-products (AGE) during haemodialysis treatment: discrepant results with different methodologies reflecting the heterogeneity of AGE compounds. *Nephrol Dial Transplant* 1999;14:1968-1975.
- [164.] Knecht KJ, Dunn JA, McFarland KF, McCance DR, Lyons TJ, Thorpe SR, Baynes JW. Effect of diabetes and aging on carboxymethyllysine levels in human urine. *Diabetes* 1991;40:190-196.
- [165.] Drusch S, Faist V, Erbersdobler HF. Determination of N- ϵ -carboxymethyllysine in milk products by a modified reversed-phase HPLC method. *Food Chemistry* 1999;65:547-553.
- [166.] Wagner Z, Wittmann I, Mazak I, Schinzel R, Heidland A, Kientsch-Engel R, Nagy J. N(epsilon)-(carboxymethyl)lysine levels in patients with type 2 diabetes: role of renal function. *Am J Kidney Dis* 2001;38:785-791.
- [167.] Hamelin M, Borot-Laloi C, Friguet B, Bakala H. Increased level of glycoxidation product N(varepsilon)-(carboxymethyl)lysine in rat serum and urine proteins with aging: link with glycoxidative damage accumulation in kidney. *Arch Biochem Biophys* 2003;411:215-222.
- [168.] Takeuchi M, Makita Z, Yanagisawa K, Kameda Y, Koike T. Detection of noncarboxymethyllysine and carboxymethyllysine advanced glycation end products (AGE) in serum of diabetic patients. *Mol Med* 1999;5:393-405.
- [169.] Henle T. AGEs in foods: Do they play a role in uremia? *Kidney Int Suppl* 2003;84:S145-S147.
- [170.] Koschinsky T, He CJ, Mitsuhashi T, Bucala R, Liu C, Buenting C, Heitmann K, Vlassara H. Orally absorbed

-
- reactive glycation products (glycotoxins): an environmental risk factor in diabetic nephropathy. *Proc Natl Acad Sci U S A* 1997;94:6474-6479.
- [171.] Kennedy L, Baynes JW. Non-enzymatic glycosylation and the chronic complications of diabetes: an overview. *Diabetologia* 1984;26:93-98.
- [172.] Schleicher E, Wieland OH. Kinetic analysis of glycation as a tool for assessing the half-life of proteins. *Biochim Biophys Acta* 1986;884:199-205.
- [173.] Ling X, Nagai R, Sakashita N, Takeya M, Horiuchi S, Takahashi K. Immunohistochemical distribution and quantitative biochemical detection of advanced glycation end products in fetal to adult rats and in rats with streptozotocin-induced diabetes. *Lab Invest* 2001;81:845-861.
- [174.] Meng J, Sakata N, Imanaga Y, Takebayashi S, Nagai R, Horiuchi S. Carboxymethyllysine in dermal tissues of diabetic and nondiabetic patients with chronic renal failure: relevance to glycoxidation damage. *Nephron* 2001;88:30-35.
- [175.] Monnier VM, Bautista O, Kenny D, Sell DR, Fogarty J, Dahms W, Cleary PA, Lachin J, Genuth S. Skin collagen glycation, glycoxidation, and crosslinking are lower in subjects with long-term intensive versus conventional therapy of type 1 diabetes: relevance of glycated collagen products versus HbA1c as markers of diabetic complications. DCCT Skin Collagen Ancillary Study Group. *Diabetes Control and Complications Trial. Diabetes* 1999;48:870-880.
- [176.] Sugimoto K, Nishizawa Y, Horiuchi S, Yagihashi S. Localization in human diabetic peripheral nerve of N(epsilon)-carboxymethyllysine-protein adducts, an advanced glycation endproduct. *Diabetologia* 1997;40:1380-1387.

-
- [177.] Schalkwijk CG, . Increased accumulation of the glycooxidation product N(epsilon)-(carboxymethyl)lysine in hearts of diabetic patients. *Diabetologia*. 2004 (in press).
- [178.] Wautier M, Massin P, Guillausseau P, Huijberts M, Levy B, Boulanger E, Laloi-Michelin M, Wautier J. N(carboxymethyl)lysine as a biomarker for microvascular complications in type 2 diabetic patients. *Diabetes Metab* 2003;29:44-52.
- [179.] Soulis T, Sastra S, Thallas V, Mortensen SB, Wilken M, Clausen JT, Bjerrum OJ, Petersen H, Lau J, Jerums G, Boel E, Cooper ME. A novel inhibitor of advanced glycation end-product formation inhibits mesenteric vascular hypertrophy in experimental diabetes. *Diabetologia* 1999;42:472-479.
- [180.] Stitt A, Gardiner TA, Alderson NL, Canning P, Frizzell N, Duffy N, Boyle C, Januszewski AS, Chachich M, Baynes JW, Thorpe SR, Anderson NL. The AGE inhibitor pyridoxamine inhibits development of retinopathy in experimental diabetes. *Diabetes* 2002 Sep ;51(9):2826 - 32 2002;51:2826-2832.
- [181.] Uesugi N, Sakata N, Horiuchi S, Nagai R, Takeya M, Meng J, Saito T, Takebayashi S. Glycooxidation-modified macrophages and lipid peroxidation products are associated with the progression of human diabetic nephropathy. *Am J Kidney Dis* 2001;38:1016-1025.
- [182.] Kushiro M, Shikata K, Sugimoto H, Ikeda K, Horiuchi S, Makino H. Accumulation of Nsigma-(carboxymethyl)lysine and changes in glomerular extracellular matrix components in Otsuka Long-Evans Tokushima fatty rat: a model of spontaneous NIDDM. *Nephron* 1998;79:458-468.
- [183.] Imai N, Nishi S, Suzuki Y, Karasawa R, Ueno M, Shimada H, Kawashima S, Nakamaru T, Miyakawa Y, Araki N, Horiuchi S, Gejyo F, Arakawa M. Histological localization of advanced glycosylation end products in the

-
- progression of diabetic nephropathy. *Nephron* 1997;76:153-160.
- [184.] Endo M, Yanagisawa K, Tsuchida K, Okamoto T, Matsushita T, Higuchi M, Matsuda A, Takeuchi M, Makita Z, Koike T. Increased levels of vascular endothelial growth factor and advanced glycation end products in aqueous humor of patients with diabetic retinopathy. *Horm Metab Res* 2001;33:317-322.
- [185.] Hammes HP, Alt A, Niwa T, Clausen JT, Bretzel RG, Brownlee M, Schleicher ED. Differential accumulation of advanced glycation end products in the course of diabetic retinopathy. *Diabetologia* 1999;42:728-736.
- [186.] Kume S, Takeya M, Mori T, Araki N, Suzuki H, Horiuchi S, Kodama T, Miyauchi Y, Takahashi K. Immunohistochemical and ultrastructural detection of advanced glycation end products in atherosclerotic lesions of human aorta with a novel specific monoclonal antibody. *Am J Pathol* 1995;147:654-667.
- [187.] Sakata N, Imanaga Y, Meng J, Tachikawa Y, Takebayashi S, Nagai R, Horiuchi S, Itabe H, Takano T. Immunohistochemical localization of different epitopes of advanced glycation end products in human atherosclerotic lesions. *Atherosclerosis* 1998;141:61-75.
- [188.] Sakata N, Imanaga Y, Meng J, Tachikawa Y, Takebayashi S, Nagai R, Horiuchi S. Increased advanced glycation end products in atherosclerotic lesions of patients with end-stage renal disease. *Atherosclerosis* 1999;142:67-77.
- [189.] Dobrian A, Lazar V, Tirziu D, Simionescu M. Increased macrophage uptake of irreversibly glycosylated albumin modified-low density lipoproteins of normal and diabetic subjects is mediated by non-saturable mechanisms. *Biochim Biophys Acta* 1996;1317:5-14.
- [190.] Westwood ME, McLellan AC, Thornalley PJ. Receptor-mediated endocytic uptake of methylglyoxal-modified

- serum albumin. Competition with advanced glycation end product-modified serum albumin at the advanced glycation end product receptor. *J Biol Chem* 1994;269:32293-32298.
- [191.] Takata K, Horiuchi S, Araki N, Shiga M, Saitoh M, Morino Y. Scavenger receptor of human monocytic leukemia cell line (THP-1) and murine macrophages for nonenzymatically glycosylated proteins. *Biochim Biophys Acta* 1989;986:18-26.
- [192.] Henderson LM, Thomas S, Banting G, Chappell JB. The arachidonate-activatable, NADPH oxidase-associated H⁺ channel is contained within the multi-membrane-spanning N-terminal region of gp91-phox. *Biochem J* 1997;325:701-705.
- [193.] Doussiere J, Bouzidi F, Poinas A, Gaillard J, Vignais PV. Kinetic study of the activation of the neutrophil NADPH oxidase by arachidonic acid. Antagonistic effects of arachidonic acid and phenylarsine oxide. *Biochemistry* 1999;38:16394-16406.
- [194.] Castellani RJ, Harris PL, Sayre LM, Fujii J, Taniguchi N, Vitek MP, Founds H, Atwood CS, Perry G, Smith MA. Active glycation in neurofibrillary pathology of Alzheimer disease: N(epsilon)-(carboxymethyl) lysine and hexitol-lysine. *Free Radic Biol Med* 2001;31:175-180.
- [195.] Good PF, Werner P, Hsu A, Olanow CW, Perl DP. Evidence of neuronal oxidative damage in Alzheimer's disease. *Am J Pathol* 1996;149:21-28.
- [196.] Smith MA, Perry G, Richey PL, Sayre LM, Anderson VE, Beal MF, Kowall N. Oxidative damage in Alzheimer's. *Nature* 1996;382:120-121.
- [197.] Kimura T, Ikeda K, Takamatsu J, Miyata T, Sobue G, Miyakawa T, Horiuchi S. Identification of advanced glycation end products of the Maillard reaction in Pick's disease. *Neurosci Lett* 1996;219:95-98.

-
- [198.] Kikuchi S, Shinpo K, Ogata A, Tsuji S, Takeuchi M, Makita Z, Tashiro K. Detection of N epsilon-(carboxymethyl)lysine (CML) and non-CML advanced glycation end-products in the anterior horn of amyotrophic lateral sclerosis spinal cord. *Amyotroph Lateral Scler Other Motor Neuron Disord* 2002;3:63-68.
- [199.] Castellani RJ, Harris PL, Sayre LM, Fujii J, Taniguchi N, Vitek MP, Founds H, Atwood CS, Perry G, Smith MA. Active glycation in neurofibrillary pathology of Alzheimer disease: N(epsilon)-(carboxymethyl) lysine and hexitol-lysine. *Free Radic Biol Med* 2001;31:175-180.
- [200.] Kikuchi S, Shinpo K, Ogata A, Tsuji S, Takeuchi M, Makita Z, Tashiro K. Detection of N epsilon-(carboxymethyl)lysine (CML) and non-CML advanced glycation end-products in the anterior horn of amyotrophic lateral sclerosis spinal cord. *Amyotroph Lateral Scler Other Motor Neuron Disord* 2002;3:63-68.
- [201.] Schwab W, Friess U, Hempel U, Schulze E, Makita Z, Kasper M, Simank HG. Immunohistochemical demonstration of -(carboxymethyl)lysine protein adducts in normal and osteoarthritic cartilage. *Histochem Cell Biol* 2002;117:541-546.
- [202.] Van Herreweghe F, Mao J, Chaplen FW, Grooten J, Gevaert K, Vandekerckhove J, Vancompernelle K. Tumor necrosis factor-induced modulation of glyoxalase I activities through phosphorylation by PKA results in cell death and is accompanied by the formation of a specific methylglyoxal-derived AGE. *Proc Natl Acad Sci U S A* 2002;99:949-954.
- [203.] Hiran TS, Moulton PJ, Hancock JT. Detection of superoxide and NADPH oxidase in porcine articular chondrocytes. *Free Radic Biol Med* 1997;23:736-743.
- [204.] Hiran TS, Moulton PJ, Hancock JT. In situ detection of superoxide anions within porcine articular cartilage. *Br J Biomed Sci* 1998;55:199-203.

-
- [205.] Schleicher ED, Gempel KE, Wagner E, Nerlich AG. Immunolocalization of the Glycooxidation Product N(epsilon)-(carboxymethyl)Lysine in Normal and Inflamed Human Intestinal Tissues. In: O'Brian JO, Nursten H, Crabbe MJC, and Ames JM, eds. Cambridge, UK: The Royal Society of Chemistry, 1998:316-321.
- [206.] Haslbeck KM, Schleicher ED, Friess U, Kirchner A, Neundorfer B, Heuss D. N(epsilon)-Carboxymethyllysine in diabetic and non-diabetic polyneuropathies. *Acta Neuropathol (Berl)* 2002;104:45-52.
- [207.] Giardino I, Edelstein D, Brownlee M. BCL-2 expression or antioxidants prevent hyperglycemia-induced formation of intracellular advanced glycation endproducts in bovine endothelial cells. *J Clin Invest* 1996;97:1422-1428.
- [208.] Griendling KK, Ushio-Fukai M. Redox control of vascular smooth muscle proliferation. *J Lab Clin Med* 1998;132:9-15.
- [209.] Gorlach A, Brandes RP, Nguyen K, Amidi M, Dehghani F, Busse R. A gp91phox containing NADPH oxidase selectively expressed in endothelial cells is a major source of oxygen radical generation in the arterial wall. *Circ Res* 2000;87:26-32.
- [210.] Schleicher E, Nerlich A. Atherosclerosis as a diabetic complication. In: Colaco C, ed. *The Glycation Hypothesis of Atherosclerosis*. 1997:151-168.
- [211.] Gorlach A, Brandes RP, Bassus S, Kronemann N, Kirchmaier CM, Busse R, Schini-Kerth VB. Oxidative stress and expression of p22phox are involved in the up-regulation of tissue factor in vascular smooth muscle cells in response to activated platelets. *FASEB J* 2000;14:1518-1528.
- [212.] Sorescu D, Weiss D, Lassegue B, Clempus RE, Szocs K, Sorescu GP, Valppu L, Quinn MT, Lambeth JD, Vega JD, Taylor WR, Griendling KK. Superoxide production and

- expression of nox family proteins in human atherosclerosis. *Circulation* 2002;105:1429-1435.
- [213.] Moulton PJ, Hiran TS, Goldring MB, Hancock JT. Detection of protein and mRNA of various components of the NADPH oxidase complex in an immortalized human chondrocyte line. *Br J Rheumatol* 1997;36:522-529.
- [214.] Tanabe T, Otani H, Mishima K, Ogawa R, Inagaki C. Phorbol 12-myristate 13-acetate (PMA)-induced oxyradical production in rheumatoid synovial cells. *Jpn J Pharmacol* 1997;73:347-351.
- [215.] Warnholtz A, Nickenig G, Schulz E, Macharzina R, Brasen JH, Skatchkov M, Heitzer T, Stasch JP, Griendling KK, Harrison DG, Bohm M, Meinertz T, Munzel T. Increased NADH-oxidase-mediated superoxide production in the early stages of atherosclerosis: evidence for involvement of the renin-angiotensin system. *Circulation* 1999;99:2027-2033.
- [216.] Munzel T, Kurz S, Rajagopalan S, Thoenes M, Berrington WR, Thompson JA, Freeman BA, Harrison DG. Hydralazine prevents nitroglycerin tolerance by inhibiting activation of a membrane-bound NADH oxidase. A new action for an old drug. *J Clin Invest* 1996;98:1465-1470.
- [217.] Munzel T, Mollnau H, Hartmann M, Geiger C, Oelze M, Warnholtz A, Yehia AH, Forstermann U, Meinertz T. Effects of a nitrate-free interval on tolerance, vasoconstrictor sensitivity and vascular superoxide production. *J Am Coll Cardiol* 2000;36:628-634.
- [218.] Rajagopalan S, Kurz S, Munzel T, Tarpey M, Freeman BA, Griendling KK, Harrison DG. Angiotensin II-mediated hypertension in the rat increases vascular superoxide production via membrane NADH/NADPH oxidase activation. Contribution to alterations of vasomotor tone. *J Clin Invest* 1996;97:1916-1923.

-
- [219.] Liochev SI, Fridovich I. Lucigenin as mediator of superoxide production: revisited. *Free Radic Biol Med* 1998;25:926-928.
- [220.] Rost M, Karge E, Klinger W. What do we measure with luminol-, lucigenin- and penicillin-amplified chemiluminescence? 1. Investigations with hydrogen peroxide and sodium hypochlorite. *J Biolumin Chemilumin* 1998;13:355-363.
- [221.] Morre DJ. Preferential inhibition of the plasma membrane NADH oxidase (NOX) activity by diphenyleneiodonium chloride with NADPH as donor. *Antioxid Redox Signal* 2002;4:207-212.
- [222.] Kono H, Rusyn I, Uesugi T, Yamashina S, Connor HD, Dikalova A, Mason RP, Thurman RG. Diphenyleneiodonium sulfate, an NADPH oxidase inhibitor, prevents early alcohol-induced liver injury in the rat. *Am J Physiol Gastrointest Liver Physiol* 2001;280:G1005-G1012.
- [223.] Jones RD, Thompson JS, Morice AH. The NADPH oxidase inhibitors iodonium diphenyl and cadmium sulphate inhibit hypoxic pulmonary vasoconstriction in isolated rat pulmonary arteries. *Physiol Res* 2000;49:587-596.
- [224.] Li Y, Trush MA. Diphenyleneiodonium, an NAD(P)H oxidase inhibitor, also potently inhibits mitochondrial reactive oxygen species production. *Biochem Biophys Res Commun* 1998;253:295-299.
- [225.] Li Y, Zhu H, Trush MA. Detection of mitochondria-derived reactive oxygen species production by the chemilumigenic probes lucigenin and luminol. *Biochim Biophys Acta* 1999;1428:1-12.
- [226.] Rembish SJ, Trush MA. Further evidence that lucigenin-derived chemiluminescence monitors mitochondrial superoxide generation in rat alveolar macrophages. *Free Radic Biol Med* 1994;17:117-126.

-
- [227.] Tsukamoto M, Tampo Y, Yonaha M. Lucigenin reduction by NADPH-cytochrome P450 reductase and the effect of phospholipids and albumin on chemiluminescence. *Biochem Mol Biol Int* 1998;45:115-123.
- [228.] O'Donnell BV, Tew DG, Jones OT, England PJ. Studies on the inhibitory mechanism of iodonium compounds with special reference to neutrophil NADPH oxidase. *Biochem J* 1993;290:41-49.
- [229.] Chakraborty S, Massey V. Reaction of reduced flavins and flavoproteins with diphenyliodonium chloride. *J Biol Chem* 2002;277:41507-41516.

9 APPENDIX

Meine akademischen Lehrer waren:

Herr Prof. Dr. I. B. Autenrieth

Herr Prof. Dr. H. Bisswanger

Herr Prof. Dr. K. W. Bock

Herr Prof. Dr. P. Bohley

Frau Prof. Dr. Dr. U. Breyer-Pfaff

Herr PD Dr. R. Dringen

Herr Prof. Dr. M. Duszenko

Herr Prof. Dr. K. Eisele

Herr Prof. Dr. K.-U. Fröhlich

Herr Prof. Dr. G. Gauglitz

Herr Prof. Dr. Dr. h.c. M. Hanack

Herr Prof. Dr. G. Häfelinger

Herr Prof. Dr. H. Hagenmaier, Ph. D.

Herr Prof. Dr. B. Hamprecht

Herr Prof. Dr. H.-U. Häring

Herr Prof. Dr. G. Jung

Herr Prof. Dr. H. Liebich

Herr Prof. Dr. E. Lindner

Herr Prof. Dr. D. Mecke

Herr Prof. Dr. W. Nakel

Herr Prof. Dr. H. Oberhammer

Herr Prof. Dr. W. Pfeiffer

Herr Prof. Dr. H. Probst

Herr Prof. Dr. H.-G. Rammensee

Herr Prof. Dr. E. Schleicher

Herr Prof. Dr. R.-M. Schmülling

Herr Prof. Dr. Dr. h.c. J. Strähle

Herr Prof. Dr. Dr. h.c. W. Voelter

Herr Prof. Dr. U. Weser

Curriculum Vitae:	Dr. med Dipl. Biochem. Ulrich Friess geb. 14.06.61 in Tübingen verheiratet, 3 Kinder
<u>Vorbildung:</u>	1967 - 1980 Grundschule und Gymnasium in Tübingen Zivildienst im Krankenpflagedienst
<u>Studium Medizin:</u>	1981 - 1989 Medizinstudium in Heidelberg und Tübingen, PJ in GB und USA, FMGEMS und FLEX abgelegt
<u>Studium Biochemie:</u>	1994 - 1998 Studium zum Diplom-Biochemiker Universität Tübingen
<u>Ärztliche Prüfung:</u>	5/1989 Med. Staatsexamen: Med. Univ.- Klinik Tübingen, Note: 'sehr gut'
<u>Diplomprüfung:</u>	10/1998 Diplomprüfung Biochemie, Note: sehr gut
<u>Diplomarbeit:</u>	5/1999 Med. Univ.-Klinik Tübingen, Zentrallabor, Note: sehr gut (Betreuer Prof. E. Schleicher/ Prof. W. Voelter)
<u>Promotion:</u>	5/1989: Universität Heidelberg (Med. Klinik, Prof. Ritz/Prof. Gross)

<u>Berufserfahrung:</u>	6/1989 - 7/1990	Paul-Lechler-Krankenhaus Tübingen (Innere/Tropenmedizin)
	8/1990 - 9/1991	Städt. Krankenhaus Pforzheim, II. Med. Klinik (Prof. Sanwald, Gastroenterologie)
	2/1992 - 7/1992	Kreiskrankenhaus Kirchheim/Teck, Innere Abt. (CA Dr. Rapp, Allg. Innere Medizin)
	1/1993-12/1993	Kreiskrankenhaus Herrenberg, Anaesthesieabt. (Anaesthesie, Intensivmedizin, ca. 200 Notarzteinsätze)
	seit 1988	Mitarbeit im elterlichen Unternehmen (Eltern 1976/1988 verstorben)
<u>Derzeit:</u>	ab 6/99	Wiss. Angestellter im Zentrallabor (Med. IV) des Universitäts- Klinikums Tübingen (AG Prof. Erwin Schleicher, Ärztl. Direktor: Prof. H.U. Haering)
<u>Vorraussichtl.:</u>	2/2005	Facharztprüfung zum FA für Laboratoriumsmedizin
	3/2005	Anerkennung als Klinischer Chemiker

